

**PROCESS SELECTION AND DESIGN FOR THE  
MICROBIAL BIOTRANSFORMATION OF  
POORLY WATER-SOLUBLE NITRILE  
COMPOUNDS**

**By Stephen Geoffrey Cull**

A thesis submitted to the  
University of London  
for the degree of  
Doctor of Philosophy

Department of Biochemical Engineering  
University College London  
2001

ProQuest Number: 10014327

All rights reserved

INFORMATION TO ALL USERS

The quality of this reproduction is dependent upon the quality of the copy submitted.

In the unlikely event that the author did not send a complete manuscript and there are missing pages, these will be noted. Also, if material had to be removed, a note will indicate the deletion.



ProQuest 10014327

Published by ProQuest LLC(2016). Copyright of the Dissertation is held by the Author.

All rights reserved.

This work is protected against unauthorized copying under Title 17, United States Code.  
Microform Edition © ProQuest LLC.

ProQuest LLC  
789 East Eisenhower Parkway  
P.O. Box 1346  
Ann Arbor, MI 48106-1346

## **Acknowledgements**

I am grateful for the guidance and supervision of Dr Gary Lye, particularly for his encouragement and enthusiasm throughout this work. I would also like to thank Dr Panagiota Angeli and Dr John Woodley for their advice, experience and many useful discussions. Thanks must also go to those at UCL; the technical and administrative staff and everyone in Foster Court. I would also like to acknowledge the financial support of the BBSRC. Finally I would like to thank my friends and family for their constant encouragement and support throughout this project. Special thanks and love to Sarah.

## Abstract

The biotransformation of poorly water-soluble aromatic dinitriles is of scientific and industrial interest. Although processes do exist for the transformation of water-soluble compounds, such as acrylonitrile, no description of a process suitable for the large scale biotransformation of poorly water soluble nitriles currently appears in the literature. This work investigates the systematic design and optimisation of a process for the production of 3-cyanobenzamide from the poorly water soluble 1,3-dicyanobenzene (1,3-DCB) and defines criteria for successful scale-up of the process to 75 L scale. A two-liquid phase process was initially designed at the laboratory scale (10 mL) which utilised the nitrile hydratase (NHase) activity of a whole cell *Rhodococcus* R312 biocatalyst. Toluene was selected as the carrier solvent and the process was optimised for amide production. This allowed the definition of a suitable operating window where the maximum space-time yield of amide formation could be obtained.

The use of a room temperature ionic liquid, 1-butyl-3-methylimidazolium hexafluorophosphate [bmim][PF<sub>6</sub>], was also investigated for the first time as a potential replacement for organic solvents in such multiphase bioconversion processes. Transformations carried out in aqueous-ionic liquid systems showed similar kinetic profiles for amide and acid production and enhanced stability of the whole cell biocatalysts.

Scale-down studies on the hydrodynamics of the bioconversion process at 3 L and 75 L scales in geometrically similar vessels were performed. On-line measurements of droplet size distribution were used to investigate the dynamic variation of droplet size distributions as a function of dispersed phase volume fraction and agitation rate. This allowed the definition of constant power input per unit volume as a scale-up basis for the maintenance of mean droplet size at each scale. Based on this understanding of the reactor hydrodynamics the reliable scale-up of 1,3-DCB bioconversion from the 3 L to 75 L scales was finally demonstrated.

# CONTENTS

<b>Title Page</b>	1
<b>Acknowledgements</b>	2
<b>Abstract</b>	3
<b>Contents</b>	4
<b>Index of Figures</b>	12
<b>Index of Tables</b>	16
<b>Nomenclature</b>	17
<b>1 INTRODUCTION</b>	<b>19</b>
<b>1.1 The industrial importance of nitriles</b>	<b>19</b>
<b>1.2 Nitrile conversions</b>	<b>19</b>
1.2.1 The importance of nitrile hydratase	19
1.2.2 The nitrile metabolism pathway	20
1.2.3 The characteristics of nitrile hydratase (NHase)	21
1.2.4 Regioselective two-step hydrolysis	23
1.2.5 Amidase selectivity	27
1.2.6 Nitrilase selectivity	27
<b>1.3 <i>Rhodococcus R312</i></b>	<b>27</b>
<b>1.4 Two-phase biotransformations</b>	<b>29</b>
1.4.1 Catalyst form	29
1.4.1 Immobilisation of the biocatalyst	31
<b>1.5 Selection of an organic solvent phase</b>	<b>32</b>
1.5.1 Solvent characteristics	32
1.5.2 Solvent biocompatibility	33
1.5.3 Solvent selection strategy	34
1.5.4 Phase ratio	34
<b>1.6 Bioreactor design and optimisation</b>	<b>36</b>
1.6.1 Reaction location	37
1.6.2 Reaction kinetics	37

1.6.3	Mass transfer	38
1.6.4	Windows of operation	40
<b>1.7</b>	<b>Scale-up of two-liquid-phase bioreactors</b>	<b>40</b>
1.7.1	Mixing	41
1.7.2	Scale-up	42
<b>1.8</b>	<b>Drop size measurements in agitated two-phase systems</b>	<b>45</b>
<b>1.9</b>	<b>Aims and objectives of the project</b>	<b>46</b>
<b>2</b>	<b>MATERIALS AND METHODS</b>	<b>48</b>
<b>2.1</b>	<b>Chemicals and microorganism</b>	<b>48</b>
2.1.1	Main chemicals	48
2.1.2	Synthesis and purification of [bmim][PF <sub>6</sub> ]	48
2.1.2.1	1-Butyl-3-methylimidazolium chloride, [bmim]Cl	48
2.1.2.2	1-Butyl-3-methylimidazolium hexafluorophosphate, [bmim][PF <sub>6</sub> ]	48
2.1.3	Organism source	49
2.1.4	Culture storage (short term)	49
2.1.5	Culture storage (long term)	50
2.1.5.1	Agar slopes	50
2.1.5.2	Glycerol stocks	50
<b>2.2</b>	<b>Media composition and conditions for growth</b>	<b>50</b>
2.2.1	Rich growth medium (RGM)	50
2.2.2	Tryptic soy broth (TSB) medium	51
<b>2.3</b>	<b>Fermentation conditions and biomass harvesting</b>	<b>51</b>
2.3.1	Shake flask fermentations	51
2.3.2	Stirred tank fermentations	51
2.3.2.1	7 L Fermentation	52
2.3.2.2	20 L Fermentation	52
2.3.2.3	450 L Fermentation	53
<b>2.4</b>	<b>Cell preparation</b>	<b>53</b>
2.4.1	Small Scale	53

2.4.2	Large scale	54
<b>2.5</b>	<b>NHase and amidase activity assays</b>	<b>54</b>
<b>2.6</b>	<b>Biotransformation of 1,3-DCB by <i>Rhodococcus</i> R312</b>	<b>55</b>
2.6.1	Shake flask biotransformations	55
2.6.1.1	Single-phase biotransformations	55
2.6.1.1.1	Amidase inhibition study	55
2.6.1.1.2	Stability of <i>Rhodococcus</i> R312 NHase activity with variable pH and temperature	55
2.6.1.2	Two-phase biotransformations	56
2.6.1.2.1	Solvent selection and partition coefficients	56
2.6.1.2.2	NHase and amidase activity of <i>Rhodococcus</i> R312 in a aqueous-toluene system	57
2.6.1.2.3	Biotransformation with variable biomass concentrations	57
2.6.1.2.4	Biotransformations with variable phase volume ratios	58
2.6.1.2.5	Biotransformation activity with variable initial substrate concentrations	58
2.6.1.2.6	25 mL shake flask two- phase biotransformations of 1,3-DCB by <i>Rhodococcus</i> R312	58

2.6.1.2.7	Comparative two-phase biotransformations of 1,3-DCB using aqueous-toluene and aqueous-[bmim][PF <sub>6</sub> ] systems	59
2.6.1.2.8	Activity of <i>Rhodococcus</i> R312 cells after exposure to a second phase	59
2.6.2	Stirred tank biotransformations	60
2.6.2.1	Stirred tank geometry and operation	60
2.6.2.2	Two-phase biotransformations of 1,3-DCB (3 L scale)	61
2.6.2.3	Two-phase biotransformations of 1,3-DCB using an aqueous-toluene system (75 L scale)	61
2.6.2.4	On-line measurement of droplet size distributions	62
2.6.2.5	Droplet size measurement	63
2.6.2.6	Power consumption and phase continuity	63
<b>2.7</b>	<b>Analytical techniques and physical measurements</b>	<b>64</b>
2.7.1	Off-line fermentation growth measurements: optical density, wet weight and dry cell weight	64
2.7.2	Density	65
2.7.3	Viscosity	65
2.7.4	Surface tension and interfacial tension	66
2.7.5	Quantitative HPLC assay	67
<b>3</b>	<b>BIOCATALYST SELECTION AND PRODUCTION</b>	<b>69</b>
3.1	Introduction	69
3.1.1	Objectives	69
<b>3.2</b>	<b>Materials and methods</b>	<b>70</b>
3.2.1	Chemicals and microorganism	70

3.2.2	Experimental methods	70
<b>3.3</b>	<b>Results and discussion</b>	<b>71</b>
3.3.1	Biocatalyst selection and form	71
3.3.2	Shake flask fermentations	73
3.3.2.1	Growth of <i>Rhodococcus</i> R312 on RGM	73
3.3.2.2	Growth of <i>Rhodococcus</i> R312 on TSB	73
3.3.3	Scale-up of stirred tank reactor (STR) fermentations	74
3.3.3.1	7 L Stirred tank reactor fermentation	74
3.3.3.2	20 L and 450 L Stirred tank reactor fermentations	75
3.3.4	Biocatalyst recovery and separation	79
<b>3.4</b>	<b>Conclusions</b>	<b>79</b>
<b>4</b>	<b>PROCESS SELECTION AND OPTIMISATION FOR AROMATIC NITRILE HYDRATION</b>	<b>81</b>
<b>4.1</b>	<b>Introduction</b>	<b>81</b>
4.1.1.	The importance of nitrile hydration	81
4.1.2	Objectives	82
<b>4.2</b>	<b>Materials and methods</b>	<b>83</b>
4.2.1	Chemicals and microorganism	83
4.2.2	Experimental methods	84
<b>4.3</b>	<b>Results and discussion</b>	<b>84</b>
4.3.1	Single-phase biotransformation of 1,3-DCB	84
4.3.2	Two-phase biotransformation of 1,3-DCB	85
4.3.2.1	Solvent selection	87
4.3.2.2	Operating parameters for the two-phase process	88
4.3.3	Biotransformation process design and operating conditions	94
<b>4.4</b>	<b>Conclusions</b>	<b>97</b>

<b>5</b>	<b>USE OF ROOM TEMPERATURE IONIC LIQUIDS AS ORGANIC SOLVENT REPLACEMENTS</b>	<b>99</b>
<b>5.1</b>	<b>Introduction</b>	<b>99</b>
5.1.1	Can ionic liquids replace organic solvents in two-phase bioprocesses?	99
5.1.2	Objectives	101
<b>5.2</b>	<b>Materials and methods</b>	<b>101</b>
5.2.1	Chemicals and microorganism	101
5.2.2	Experimental methods	101
<b>5.3</b>	<b>Results and discussion</b>	<b>103</b>
5.3.1	Ionic liquid selection and physical properties	103
5.3.2	Two-phase biotransformation of 1,3-DCB	104
<b>5.4</b>	<b>Conclusions</b>	<b>108</b>
<b>6</b>	<b>TWO-PHASE REACTOR HYDRODYNAMICS AND SCALE-UP</b>	<b>109</b>
<b>6.1</b>	<b>Introduction</b>	<b>109</b>
6.1.1	The hydrodynamics of two-phase bioreactors	109
6.1.2	Current scale-up methodologies	112
6.1.3	Objectives	112
<b>6.2</b>	<b>Materials and methods</b>	<b>113</b>
6.2.1	Chemicals and microorganism	113
6.2.2	Experimental methods	113
<b>6.3</b>	<b>Results and discussion</b>	<b>114</b>
6.3.1	Phase physical properties	114
6.3.2	Power curves for agitated liquid-liquid systems (3 L scale)	115
6.3.3	Effect of agitation rate and phase composition on drop size distribution (3 L scale)	119
6.3.3.1	Prediction of sauter mean drop diameter (3 L scale)	120

6.3.4	Criteria for reactor scale-up to 75 L scale	122
6.4	<b>Conclusions</b>	<b>128</b>
<b>7</b>	<b>SCALE-UP OF TWO-PHASE AROMATIC NITRILE HYDRATION</b>	<b>129</b>
7.1	<b>Introduction</b>	<b>129</b>
7.1.1	Objectives	129
7.2	<b>Materials and methods</b>	<b>130</b>
7.2.1	Chemical and microorganism	130
7.2.2	Experimental methods	130
7.3	<b>Results and discussion</b>	<b>130</b>
7.3.1	Selection of agitation rates for scale-up studies	130
7.3.2	Biomass production and processing	133
7.3.3	3 L scale biotransformation experiments	133
7.3.4	75 L scale biotransformation experiments	133
7.4	<b>Conclusions</b>	<b>137</b>
<b>8</b>	<b>GENERAL DISCUSSION AND CONCLUSIONS</b>	<b>138</b>
8.1	<b>General discussion</b>	<b>138</b>
8.1.1	<b>Biocatalyst production</b>	<b>138</b>
8.1.2	<b>Bioconversion process design and optimisation</b>	<b>139</b>
8.1.3	<b>Use of ionic liquids</b>	<b>141</b>
8.1.4	<b>Two-phase bioreactor hydrodynamics</b>	<b>142</b>
8.1.5	<b>Two-phase bioconversion scale-up</b>	<b>143</b>
8.2	<b>Conclusions</b>	<b>144</b>
8.3	<b>Future work</b>	<b>145</b>
	<b>REFERENCES</b>	<b>147</b>
	<b>APPENDICES</b>	<b>164</b>
A1	<b>75 L Reactor guide SOP</b>	<b>164</b>

*Contents*

A1.1	Operating procedure for toluene/aqueous mixing studies in the 75 L reactor	164
A1.2	Operating procedure for toluene/aqueous biotransformation and mixing studies in the 75 L reactor	165
A2	<b>Calculation of modified weber number</b>	<b>166</b>

# INDEX OF FIGURES

1.1	Two pathways for nitrile metabolism	20
1.2	The proposed mechanism of NHase (Asano <i>et al.</i> , 1982)	21
1.3	The three-dimensional structure of NHase from <i>Rhodococcus</i> R312 at a resolution of 2.65 Å	22
1.4	Hydrolysis of dinitriles by SP361 (Cohen <i>et al.</i> (1990)	25
2.1	Scale diagrams of the 3 L and 75 L vessels	60
2.2	(a) 1,3-DCB and (b) 3-cyanobenzoic acid calibration curves as measured by HPLC	68
3.1	Shake flask fermentation profile for growth of <i>Rhodococcus</i> R312 on RGM	72
3.2	Off-line measurements for 7 L fermentation profile for growth of <i>Rhodococcus</i> R312 on TSB	76
3.3	On-line fermentation data for a 7 L TSB fermentation	77
3.4	On-line fermentation data for a 450 L TSB fermentation	78
4.1	Mass transfer and reaction steps in the two-phase biotransformation of 1,3-DCB using the two-step nitrile degradation pathway of <i>Rhodococcus</i> R312	82
4.2	Single-phase <i>Rhodococcus</i> R312 biotransformation kinetics	86
4.3	Single-phase NHase and amidase activities as a function of temperature	86
4.4	Single-phase NHase and amidase activities as a function of pH	87
4.5	Two-phase <i>Rhodococcus</i> R312 biotransformation for a mass transfer limited system	90
4.6	Initial rates of amide and acid production as a function of biocatalyst concentration in an aqueous-toluene two- phase system	92

4.7	Initial rates of amide and acid production as a function of phase volume ratio	92
4.8	Initial rates of amide and acid production as a function of initial substrate concentration in the toluene phase	93
4.9	Operating window for the <i>Rhodococcus</i> R312 catalysed transformation of 1,3-DCB in an aqueous-toluene two-phase system at pH7 and 30°C	95
4.10	Two-phase <i>Rhodococcus</i> R312 biotransformation kinetics for final optimised conditions	96
5.1	Chemical structure of [bmim][PF <sub>6</sub> ] and examples of cations and anions commonly used in the creation of ionic liquids (from Roberts and Lye, 2001)	102
5.2	<i>Rhodococcus</i> R312 catalysed transformation of 1,3-DCB in an aqueous-toluene two-phase system	106
5.3	<i>Rhodococcus</i> R312 catalysed transformation of 1,3-DCB in an aqueous-[bmim][PF <sub>6</sub> ] two-phase system	106
5.4	Retention of <i>Rhodococcus</i> R312 nitrile hydratase activity in aqueous-toluene and aqueous-[bmim][PF <sub>6</sub> ] two-phase systems	107
6.1	Power curves for a variety of agitated two-liquids phase systems	116
6.2	Droplet size frequency distribution by volume as a function of agitation rate for a 20 % v/v aqueous-toluene system in the 3 L reactor in the absence of substrate and biomass	117
6.3	Droplet size frequency distribution by volume for a 20 % v/v aqueous-toluene system agitated at 600 rpm in the 3 L reactor	117
6.4	Droplet size frequency distribution by volume for a 20 % v/v aqueous-toluene system agitated at 700 rpm in the 3 L reactor	118
6.5	Droplet size frequency distribution by volume for a 20 % v/v aqueous-toluene system agitated at 800 rpm in	118

	the 3 L reactor	
6.6	Sauter mean diameter ( $d_{32}$ ) against agitation rate in 20% v/v toluene-aqueous systems in the 3 L reactor	122
6.7	Sauter mean diameter ( $d_{32}$ ) for a 20 % v/v toluene-aqueous system in the 3 L scale-down reactor and the 75 L pilot scale reactor for scale-up under constant P/V and constant tip speed criteria	124
6.8	Droplet size frequency distribution by volume for a 20 % v/v toluene-aqueous system in the absence of substrate or biomass: 600 rpm	125
6.9	Droplet size frequency distribution by volume for a 20 % v/v toluene-aqueous system in the absence of substrate or biomass: 700 rpm	125
6.10	Droplet size frequency distribution by volume for a 20 % v/v toluene-aqueous system in the absence of substrate or biomass: 800 rpm	126
6.11	Droplet size frequency distribution by volume for a 20 % v/v toluene-aqueous system in the absence of substrate or biomass: 900 rpm	126
6.12	Sauter mean diameter ( $d_{32}$ ) against agitation rate in 20% v/v toluene-aqueous systems in the 75 L reactor	127
7.1	Kinetics of 3-cyanobenzamide production over a range of agitation rates in the 3 L bioreactor	132
7.2	Two-phase <i>Rhodococcus</i> R312 biotransformation kinetics at an agitation rate of 600 rpm in a 3 L bioreactor	132
7.3	Two-phase <i>Rhodococcus</i> R312 biotransformation kinetics at an agitation rate of 700 rpm in a 3 L bioreactor	135
7.4	Two-phase <i>Rhodococcus</i> R312 biotransformation kinetics at an agitation rate of 218 rpm in a 75 L bioreactor	135
7.5	Two-phase <i>Rhodococcus</i> R312 biotransformation	136

	kinetics at an agitation rate of 305 rpm in a 75 L bioreactor	
7.6	Two-phase <i>Rhodococcus</i> R312 biotransformation kinetics at an agitation rate of 357 rpm in a 75 L bioreactor	136
8.1	Operating window for operation at $[1,3\text{-DCB}]_{\text{org}} = 25$ $\text{g.L}^{-1}$ showing further constraints imposed by downstream processing considerations	141

# INDEX OF TABLES

1.1	Characteristics of nitrile hydratase purified from a selection of nitrile metabolising microorganisms	24
1.2	Desired characteristics of solvents for use in two-phase biotransformations. From Bruce and Daugulis (1991)	32
2.1	Buffer comparison and pH range used in biotransformation experiments	56
3.1	STR fermentation tip speed scale-up data	74
3.2	Fermentation process comparison data	80
4.1	Log P values and 1,3-DCB saturation concentrations of the solvents screened for use in a two-phase biotransformation process.	88
4.2	Process constraints table for the hydration of 1,3-DCB by the whole cell NHase of <i>Rhodococcus</i> R312	89
5.1	Physicochemical properties of ionic liquids (from Roberts and Lye, 2001)	100
5.2	Physical and equilibrium properties of toluene and [bmim][PF <sub>6</sub> ] systems	104
6.1	Literature correlations for the prediction of Sauter mean drop diameter in agitated liquid-liquid systems (compiled from Zhou and Kresta (1998))	111
6.2	Experimentally determined phase physical properties	114
6.3	Reactor agitation rates at 3 L and 75 L scales for scale-up using constant power input per unit volume and constant tip speed criteria	123

# NOMENCLATURE

[bmim][PF <sub>6</sub> ]	1-butyl-3-methylimidazolium hexafluorophosphate
1,3-DCB	1,3-dicyanobenzene
1,3-DCB	1,3-dicyanobenzene
3-CA	3-cyanobenzoic acid
3-CB	3-cyanobenzamide
A	interfacial area
C	concentration (g.L <sup>-1</sup> )
$c_1, c_2, \dots$	constant (dimensionless)
$d_{32}$	sauter mean drop diameter (μm)
$D_i$	impeller diameter (m)
$d_{max}$	maximum drop diameter (μm)
E	enzyme concentration in aqueous phase (g.L <sup>-1</sup> )
H	tank height (m)
H	liquid height (m)
K	substrate partition coefficient ( $K = C_{aq}/C_{org}$ , or $C_{aq}/C_{il}$ )
$k_I$	enzyme activity reaction rate constant (mmol.g <sup>-1</sup> .min <sup>-1</sup> )
$k_{MI}$	enzyme michaelis-menton constant (mmol.L <sup>-1</sup> )
$k_s$	substrate mass transfer coefficient (mg.L <sup>-1</sup> )
$m_s$	equilibrium partition coefficient ( $S_w^*/S_w^*$ ) (dimensionless)
N	rotational speed of the impeller (s <sup>-1</sup> )
P	power (W)
$Po$	power number: $Po = P/\rho N^3 D_i^5$ (dimensionless)
P/V	power input per unit volume (kW.m <sup>-3</sup> )
Re	reynolds number: $Re = \rho N D_i^2 / \mu$ (dimensionless)
S	substrate concentration (mmol.L <sup>-1</sup> )
SRR	substrate reaction rate (mmol. L <sup>-1</sup> .min <sup>-1</sup> )
STR	substrate transfer rate (mmol. L <sup>-1</sup> .min <sup>-1</sup> )
STR	stirred tank reactor
T	tank diameter (m)
V	volume (m <sup>3</sup> )
$Vi$	viscosity group: $Vi = \mu_d \sqrt{(\rho_d \sigma_d)}$ (dimensionless)
$V_r$	volume ratio, $V_r = V_{org}/V_{aq}$
$We_{e,T}$	weber number: $We_{e,T} = \rho_c N^2 D_i^3 / \sigma$ (dimensionless)

## Greek symbols

$\gamma$	shear rate (s <sup>-1</sup> )
$\phi$	volume fraction of dispersed phase: $\phi = V_d/V_{total}$ (dimensionless)
$\rho$	density (kg.m <sup>-3</sup> )
$\sigma$	interfacial tension (kg.s <sup>-2</sup> )
$\mu$	dynamic viscosity (Pa.s)
$\tau$	shear stress (Nm <sup>-2</sup> )

## Subscripts

aq	aqueous
bio	biomass
c	continuous phase
d	dispersed phase
dcw	dry cell weight
ex	experimental
il	ionic liquid
lit	literature
m	mixture
o	solvent
org	organic
sat	saturation
tol	toluene
w	water
ww	wet weight

# 1. INTRODUCTION

## 1.1 THE INDUSTRIAL IMPORTANCE OF NITRILES

The biotransformation of nitriles is of interest because a number of economically important organic compounds are currently produced from nitrile starting materials (Jallageas *et al.*, 1980). A biological method of production offers a greener, more selective process and in one case, that of acrylamide production, the yield and purity is better than the original chemical method (Yamada and Kobayashi, 1996). Nitrile hydratase (NHase) is the enzyme of greatest interest for the hydrolysis of nitriles to amides. Consequently over the past decade several processes have been developed for the production of commodity chemicals including acrylamide and nicotinamide and for the treatment of waste (Yamada and Kobayashi, 1996; Kobayashi and Shimizu, 1998). The most significant to date is the Nitto process which utilises NHase for the production of acrylamide, one of the most important commodity chemicals (Yamada and Kobayashi, 1996). NHase catalysed production of acrylamide currently yields 30,000 tonnes of product per annum. The application of NHase for the production of acrylamide removed the use of a toxic copper catalyst in the Nitto process and simplified the process due to a reduction in the number of reaction steps and waste material. Due to the success of the Nitto process NHase is of intense scientific interest both for its application in process biotransformations and its novel biochemistry (Kobayashi and Shimizu, 2000; Endo *et al.*, 2001). Currently the process options for the biotransformation of poorly water soluble nitriles have not been thoroughly investigated.

## 1.2 NITRILE CONVERSIONS

### 1.2.1 The importance of nitrile hydratase

Nitrile metabolising enzymes, in particular nitrile hydratase (NHase) are of great interest to the chemical and waste water treatment industries as they can

potentially perform nitrile hydrolysis reactions more precisely and more efficiently than chemical catalysts and are considered to be a 'green' technology.

### 1.2.2 The nitrile metabolism pathway

The ability to metabolise substrates with nitrile side-groups is possessed by plants and microorganisms. The nitrile metabolism pathway consists of two enzymes. The enzymes are nitrile hydratase (NHase) which hydrolyses the nitrile to its corresponding amide and an amidase which hydrolyses the amide to a carboxylic acid and ammonia. A second similar pathway catalysed by the enzyme nitrilase is also found in microorganisms but transforms the nitrile substrate into a carboxylic acid in one step. The two-step NHase pathway and nitrilase pathways are shown in Figure 1.1.

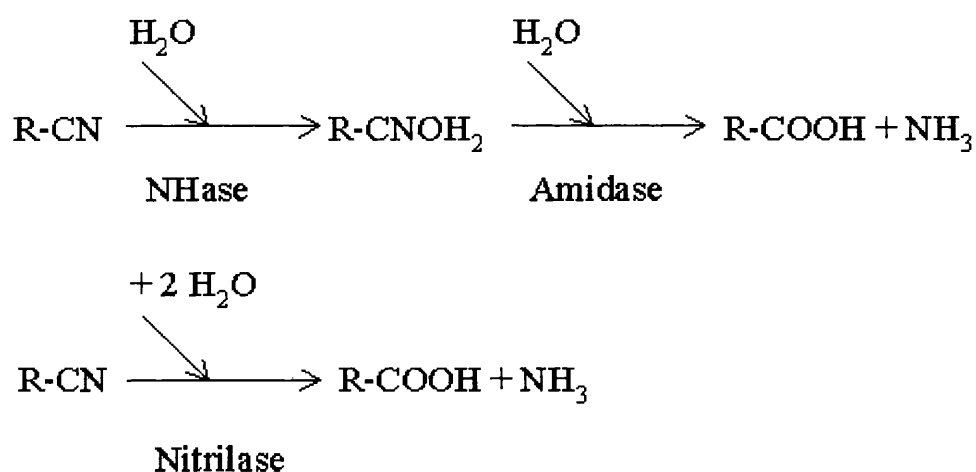


**Figure 1.1** Two pathways for nitrile metabolism: the two-step nitrile hydratase pathway initially produces an amide intermediate which is then further metabolised to acid and ammonia. The nitrilase enzyme achieves this in a specific reaction step.

The mechanism for two-step hydrolysis was first suggested by Asano and co-workers in the early eighties using *Arthrobacter* sp. J1 as the model system for nitrile hydratase (Asano *et al.*, 1982). They found that the enzyme would act on acetonitrile to form acetamide.

Figure 1.2 shows the mechanism proposed by Asano *et al.*, 1982. Nucleophilic attack by a reactive sulfhydryl group of the enzyme forms an enzyme-bound imine, which is hydrated to form a tetrahedral amide intermediate [I]. An acyl-enzyme is formed from the intermediate [I], with the enzyme as a leaving group.

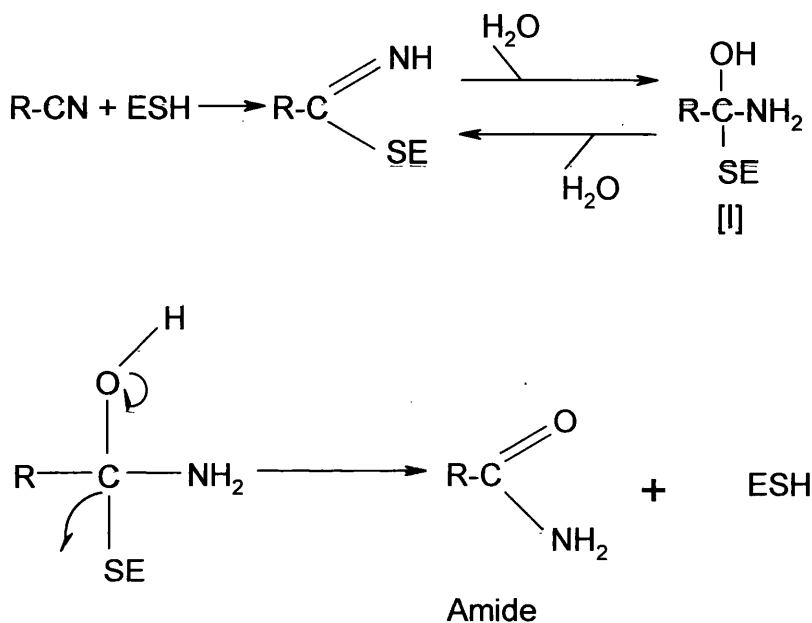


**Figure 1.2** The proposed reaction mechanism of NHase (Asano *et al.*, 1982).

### 1.2.3 The characteristics of nitrile hydratase (NHase)

Nitrile hydratases are metalloenzymes that catalyse the hydration of nitriles to their corresponding amides. Some NHase have been shown to be photosensitive and the enzyme activity is lost if incubated in the dark. However, activity is rapidly restored when irradiated with light (Nagamune *et al.*, 1990). NHases are formed from equal numbers of  $\alpha$  and  $\beta$  sub-units which differ in structure and molecular weight. They incorporate non-heme iron or non-corrinoid cobalt (Payne *et al.*, 1997) ions and it has been claimed that some have a pyrroloquinoline phenylhydrazone (PQQ) prosthetic group as a redox cofactor although this is currently in doubt (Brennan *et al.*, 1994). Non-heme NHases are characterised by low-spin ferric ions (Sugiura *et al.*, 1987) whereas cobalt containing NHases are

characterised by non-corrin low-spin Co (Payne *et al.*, 1997). The three-dimensional structure of NHase was first determined for *Rhodococcus* R312 and is shown in Figure 1.3. It consists of  $\alpha$  and  $\beta$  sub-units which each incorporate a non-heme iron ion.

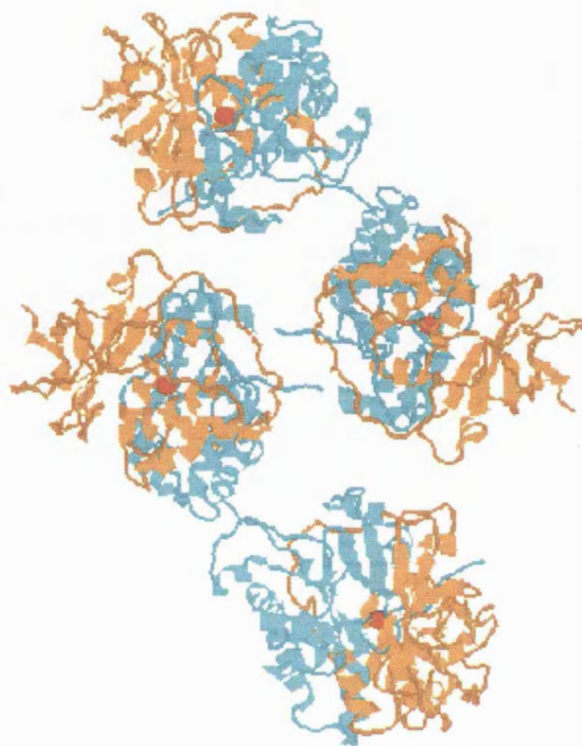


**Figure 1.3** The three-dimensional structure of NHase from *Rhodococcus* R312 at a resolution of 2.65 Å. Four copies of the  $\alpha\beta$  dimer are shown. The dimer enzyme consists of an  $\alpha$  (cyan) and  $\beta$  (orange) with an iron centre (red) which also corresponds to the location of the active site (Huang *et al.*, 1997).

The first extensive study of the enzymes of the 2-step pathway was undertaken on *Brevibacterium* R312. This has recently been reclassified as *Rhodococcus* R312 (Briand *et al.*, 1994) and is one of the most well-characterised of the nitrile hydratase microorganisms discovered so far (Briand *et al.*, 1994). However, due to the strong interest in NHase enzymes the properties and structure of the enzyme has been studied in many other microorganisms and a search of the literature produced over a dozen nitrile hydratase containing microorganisms examples of which are listed in Table 1.1.

### 1.2.4 Regioselective two-step hydrolysis

An often cited advantage for using biotransformations to perform reactions is the ability of the biocatalyst to significantly increase the yield of product or manipulate a specific area of a substrate due to the selective properties of the enzyme. Enzyme selectivity is usually due to: the chemoselectivity, stereoselectivity or regioselectivity of the enzyme. Initially it was thought that nitrilases hydrolysed only aromatic nitriles and nitrile hydratase only hydrolysed aliphatic nitriles. However, it has since been shown that both enzymes catalyse all nitrile forms (Kerridge, 1995).

Regiospecificity towards aromatic dinitriles was first demonstrated by Cohen *et al.* (1990) using a commercially available immobilised enzyme system SP361 (prepared from *Rhodococcus* CH5) from Novo Industries which contained a nitrile hydratase and amidase. Studies on SP361 showed a distinct trend indicated that *meta*- and *para*- substituted dinitriles were hydrolysed to cyanobenzoic acids while *ortho*- substituted dinitriles were hydrolysed to diacids (see Figure 1.4). As can be seen in Figure 1.4 hydrolysis of 1,3-dicyanobenzene and 1,4-dicyanobenzene leads to cyano-acid whereas the hydrolysis of 1,2-dicyanobenzene leads to the diacid. Regioselectivity was extremely prevalent in the hydrolysis of symmetrical dinitriles, however, regioselectivity of unsymmetrical dinitriles was poor. Thus, it seems that for regioselective monohydrolysis the symmetry of the molecule and the position of the disubstituted nitrile group is of importance.

However, during the hydrolysis of nitriles to acids by SP361 negligible (<5%) amide could be detected indicating that nitrile hydratase was present with a fast acting amidase. Therefore to test the regioselectivity 1,3-dibenzamide was used as substrate from which diacid was formed. This implied that the NHase was the regioselective enzyme.

Organism	<i>Rhodococcus</i> R312	<i>Pseudomonas chlororaphis</i> B23	<i>Rhodococcus rhodochrous</i> J1	<i>Corynebacter. pseudodiphtheriticum</i>
<b>Substrates</b>	Aliphatic & aromatic	Aliphatic	Aliphatic & aromatic	Aliphatic
<b>Enzyme</b>	Constitutive	Induced	Induced	Induced
<b>Molec. Mass (kDa)</b>	90	100	500-530	80
<b>No of Sub-units</b>	2: $\alpha$ and 2 $\beta$	4	10 $\alpha$ and 10 $\beta$	-
<b>Sub-unit Mass (kDa)</b>	$\alpha=26, \beta=27$	25	$\alpha=26, \beta=29$	$\alpha=25, \beta=28$
<b>Metal Ions</b>	4 Fe	4 Fe	11 Co	Fe
<b>Opt. Temp. (°C)</b>	25	20	35	25
<b>Heat Stability (°C)</b>	20	20	50	20-50
<b>Opt. PH</b>	7.8	7.5	6.6	7.5
<b>pH Stability</b>	6.5-8.5	6.0-7.5	6.0-8.5	6.5-8.0
<b>Activated by Light</b>	-	-	-	-
<b>Reference</b>	1,2	1,2	1,2,3	7
<b>Organism</b>	<i>Rhodococcus</i> sp. N-774	<i>Rhodococcus</i> sp. N-771	<i>Klebsiella pneumoniae</i>	<i>Bacillus pallidus</i> Dac521
<b>Substrates</b>	-	-	Aliphatic & Aromatic	Aliphatic & Aromatic
<b>Enzyme</b>	-	-	Constitutive	Constitutive
<b>Molec. Mass (kDa)</b>	70	60	-	-
<b>No of Sub-units</b>	2:	2	-	-
<b>Sub-unit Mass (kDa)</b>	$\alpha=28.5, \beta=29$	$\alpha=27.5, \beta=28$	-	-
<b>Metal Ions</b>	Fe	2 Fe	-	-
<b>Opt. Temp. (°C)</b>	<30	-	30	50
<b>Heat Stability (°C)</b>	-	-	-	30-65
<b>Opt. PH</b>	7.7	-	8	7.5
<b>pH Stability</b>	-	-	-	-
<b>Activated by Light</b>	+	+	-	-
<b>Reference</b>	1,3	3,4	5	6

**Table 1.1** Characteristics of nitrile hydratases purified from a selection of nitrile metabolising microorganisms. References: 1. Finnegan *et al.* (1992); 2. Yamada *et al.* (1996); 3. Warhurst and Fewson. (1994); 4. Nagamune *et al.* (1991); 5. Nawaz *et al.* (1992), 6. Cramp *et al.* (1997); 7. Li *et al.* (1992).

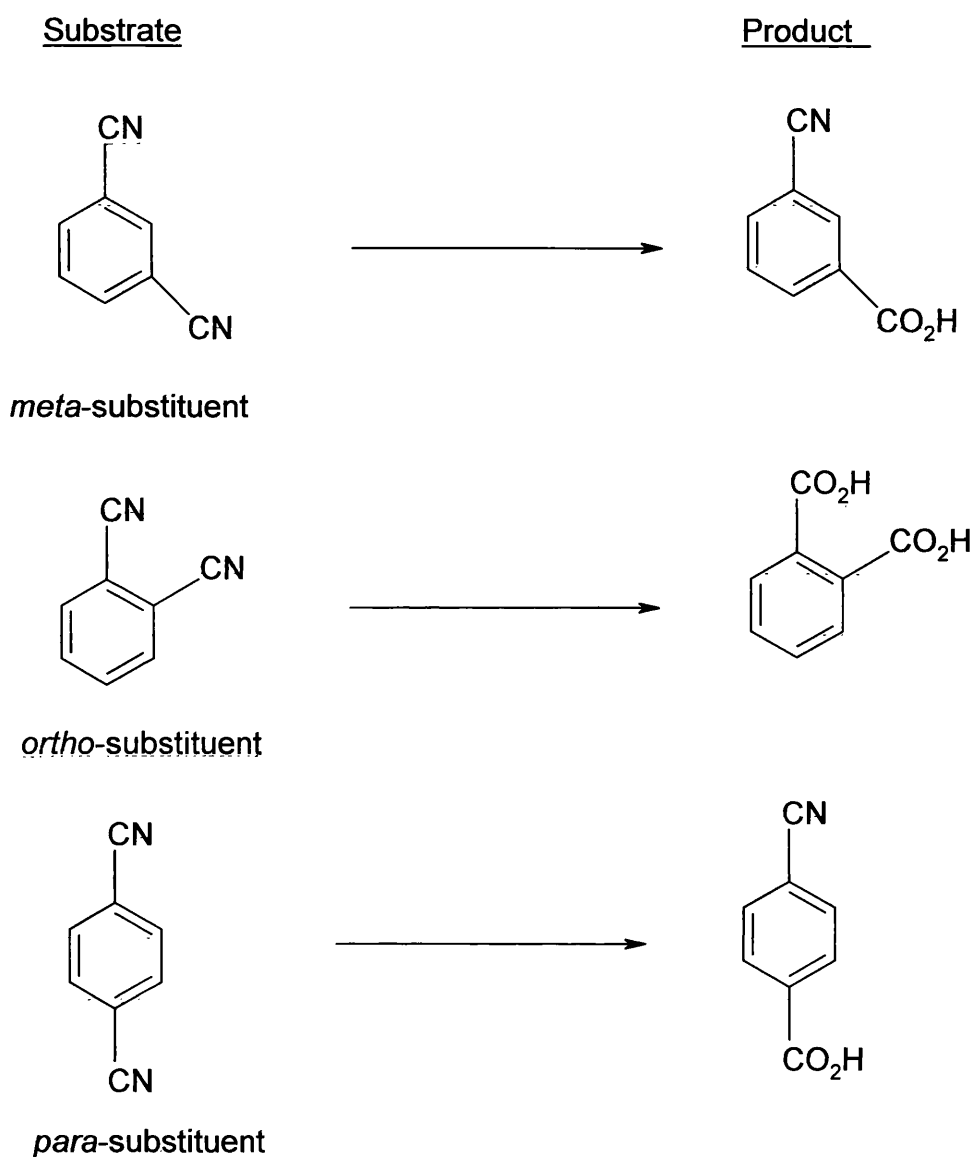


**Figure 1.4** Hydrolysis of dinitriles by SP361 (Cohen *et al.* (1990).

Further analysis of regioselectivity by Crosby *et al.* (1994) revealed that SP361 would only hydrolyse the second nitrile group of 1,3-dicyanobenzene after esterification of the carboxyl group of the cyano-acid to a methyl ester. As before the use of 1,3-dibenzamide as substrate indicated no selectivity as the dibenzamide was converted to diacid. The selection of dinitriles with additional chemical groups appeared to have an effect on hydrolysis. Fluorinated dinitriles were found to depress the rate of hydrolysis of a second nitrile group thus allowing cyano

amides to be isolated in higher yields. A yield of 11% cyano-amide was obtained after 49 hours hydrolysis of 1,3-dicyanobenzene compared to a yield of 40% fluoro-cyano-amide after 21 hours hydrolysis of fluoro-1,3-dicyanobenzene. The addition of an amino group was also investigated. Selective hydrolysis of the nitrile group *ortho* to the amine was found to take place indicating that both steric and electronic factors influence regioselectivity (Crosby *et al.*, 1994).

Investigation of regioselectivity in *Rhodococcus equi* A4 (Martinkova *et al.*, 1995) reconfirmed the regiospecificity of NHase for mono nitrile hydrolysis. However, unlike the SP361 system the NHase is regioselective for the *ortho*-substituted dinitrile. The *R. equi* cells were significantly faster catalysts achieving 65% conversion to cyanoamides of 1,3-dicyanobenzene after 1 hour compared to 11% yield conversion after 49 hours with the SP361 system (Crosby *et al.*, 1994). This is due to *R. equi* possessing a NHase activity 10-20 times higher than its amidase.

In the *R. equi* system product yield decreased with increasing proximity of the two side groups. Thus after 1 hour product yield with 1,4-dicyanobenzene was 81%, 1,3-dicyanobenzene product yield was 65% and after 5 hours 1,2-dicyanobenzene product yield was 48%. This trend is approximately consistent with the findings of Crosby *et al.*, (1994) and Cohen *et al.*, (1990).

Indications that hydrolysis of dinitriles is not always regioselective have emerged from recent studies on *Rhodococcus* AJ270 (Blakey *et al.*, 1995; Meth-Cohn *et al.*, 1995; Meth-Cohn *et al.*, 1997a; Meth-Cohn *et al.*, 1997b). Blakey *et al.*, 1995 demonstrated that there appears to be no regioselectivity in the AJ270 system for 1,2-dicyanobenzene and 1,3-dicyanobenzene. Further analysis of the AJ270 system led Meth-Cohn *et al.*, 1995 to the conclusion that the presence of an adjacent substituent (an *ortho*-substituent or an adjacent ring heteroatom) allows conversion of aromatic and heteroaromatic nitriles into amides instead of the rapid hydrolysis to acid associated with non-adjacently substituted nitriles. Thus the amidase activity is significantly faster with 'non-adjacent compounds'.

More recent analysis of *Rhodococcus* AJ270 indicates that for effective hydrolysis, a molecular diameter of the substrate of no more than 7 Å appears to be a limit to rapid conversion (Meth-Cohn *et al.*, 1997a). Thus slower rates of conversion are observed with molecules that exceed this diameter. However, Meth-Cohn *et al.* (1997b) also observed that regioselective hydrolysis of aliphatic dinitriles is dependent upon the position of the heteroatom and not overall chain length which appears to contradict their earlier work.

### 1.2.5 Amidase selectivity

Regioselectivity in two-step nitrile hydrolysis occurs at the nitrile hydratase level as described in section 1.2.4. Regioselectivity by an amidase has so far not been observed. However, Mayaux *et al.*, (1991) discovered an enantiomer-selective amidase.

### 1.2.6 Nitrilase selectivity

Regioselective and enantioselective selectivity have been observed in nitrilases. Both types of selectivity were found to occur in *Rhodococcus rhodochrous* NCIMB 11216. The nitrilase regioselectively converted 1,3-dicyanobenzene to 3-cyanobenzoic acid (Bengis-Garber and Gutman, 1989) as well as the asymmetric hydrolysis of enantiomers (Gradley and Knowles, 1994a; Gradley *et al.*, 1994b).

## 1.3 *Rhodococcus* R312

Recently reclassified as a *Rhodococcus* instead of a *Brevibacterium* (Briand *et al.*, 1994), R312 has been well characterised (Briand *et al.*, 1994; Kerridge, 1995). *Rhodococcus* R312 is an excellent microorganism for an investigation into regioselective aromatic amide production and was recently recommended by the Commission on Biotechnology (Faber, 1997b). *Rhodococcus* R312 possesses a constitutive (Bui *et al.*, 1984b) wide substrate spectrum (Bui *et al.*, 1984a) NHase, a wide-spectrum amidase and an enantiomer-selective amidase (Mayaux *et al.*, 1991) which are located intracellularly (Miller *et al.*, 1984). However, the

organism does not have a nitrilase (Kerridge, 1995) which is a further advantage for an investigation into amide production. A summary of the general features of *Rhodococcus* R312 is shown below:

- *General features.* It is aerobic, non-motile, gram positive (tends to gram negative with ageing) soil microorganism. Colonies tend to be 'salmon pink'. The degree of this pinkness appears to be linked to the concentration of NHase in the microorganism. It has a thiamine vitamin requirement and is considered a Hazard Group 1 microorganism.
- *Enzyme synthesis and regulation.* The ferrous NHase is constitutive and non-inducible. Therefore while no inducement is required, ferric ions are required for NHase synthesis. NHase has been shown to be inhibited by an excess of nitrile substrate and is known to be competitively inhibited by amide products (Bui *et al.*, 1984b; Maestracci *et al.*, 1988). The amidase is substrate induced by amide (Touneix *et al.*, 1986) and has been shown to be inhibited by aromatic amide substrates (Fournaud *et al.*, 1998). A model developed by Tourniex *et al.*, (1986) suggests that NHase and amidase biosynthesis is controlled by a single repressor gene and that amide represses NHase biosynthesis and induces amidase biosynthesis. For propionitrile hydrolysis both enzymes were found to have a pH optimum of 7 but NHase maintains a significant activity between pH 3-11 whereas the amidase has a more narrow profile of pH 5-8. However, NHase has a temperature optimum of 30°C whereas the amidase had a temperature optimum of 50°C which rapidly declined above 60°C.
- *Molecular Biology.* The chromosome of R312 is approximately 6.44 Mb in size (Bigey *et al.*, 1995). Its NHase and amidase demonstrate a high level of conservation with other species (Duran *et al.*, 1992; Mayaux *et al.*, 1991).

## 1.4 TWO-PHASE BIOTRANSFORMATIONS

The utilisation of a biological catalyst to selectively transform a substrate molecule to a product is established in the literature from early fermentation processes such as the modern manufacture of antibiotics and other fine chemicals. However, many potential substrate/product molecules are poorly water soluble or are toxic to the biocatalyst. Thus a process for the conversion of these substrates is inefficient and problematic (Lilly and Woodley, 1985). A potential solution to overcome poor aqueous solubility and/or toxicity is to dissolve the substrate in an organic solvent as a second phase in the reactor. This enables a constant supply of substrate to be made available to the biocatalyst and also enables a degree of control over the delivery of toxic substrate into the vicinity of the biocatalyst.

The use of an organic solvent as a substrate and product reservoir for two-liquid phase biotransformation was first reported in the 1930s (Halling and Kvittingen, 1999). However, the potential of this technology was not fully realised at the time. In the early 1970s the technology was 'rediscovered', being initially used in the biotransformation of poorly water soluble steroids (Cremonesi *et al.*, 1975), and it was rapidly adapted for use with other poorly water soluble molecules (Buckland *et al.*, 1975; Klibanov *et al.*, 1975).

The use of organic solvents in bioreactors has been reviewed extensively e.g. Cabral *et al.*, 1997; Eggers *et al.*, 1989; Fernandes *et al.*, 1995; Woodley *et al.*, 1991; Lye and Woodley, 2001. There are several major advantages to their application in a two-liquid phase system:

- Increased solubility of substrate and product. If a substrate/product is poorly water soluble dissolving it in solvent can make a process economically viable. Due to an increase in the availability of the substrate for the biocatalyst or extraction of the product i.e. use of organic solvent enabled dehydrogenation of the water-insoluble 6- $\alpha$ -methyl-hydro-cortisone-21-acetate by *Arthrobacter simplex* cells (Fernandes *et al.*, 1995).
- Alteration of enzyme selectivity. Placing an enzyme in nearly anhydrous media can change the selectivity of the enzyme (Carrea *et al.*, 1995).

- Reduce product inhibition. Inhibition of a biocatalyst can be reduced by the extraction of the product from the aqueous phase.
- Shift reaction equilibria. Transfer of products to the organic phase can shift the apparent reaction equilibria.
- Product recovery. As the solvent may contain a higher product concentration and different physical properties compared to water this can facilitate improved product recovery by separation of the two phases and distillation of the product containing phase.

A measure of a solute affinity for a particular solvent is the distribution coefficient. This is defined as the ratio of the solute concentration in the solvent to the solute concentration in the aqueous medium at equilibrium (Bruce and Daugulis, 1991). Therefore, it follows that as the distribution coefficient increases, the greater the affinity of the substrate/product molecule for the solvent. Using the distribution coefficient workers can therefore determine whether a particular solvent will be useful for delivering substrate to the aqueous phase or whether it will be useful in extracting product from the aqueous phase.

The use of organic solvents can also have potential disadvantages within a two-phase bioreactor such as inhibition or inactivation of the biocatalyst due to interfacial effects and molecular toxicity of the solvent. In extractive fermentations, unintentional formation of emulsions and protein stripping can also occur (Van Sonsbeek *et al.*, 1993). Therefore, an important consideration in the design of a two-liquid phase biotransformation is the relationship between the solvent and biocatalyst. This depends on the choice of solvent and the form of the catalyst.

#### 1.4.1 Catalyst form

For a given two-phase biotransformation a biocatalyst can be applied in several forms, either as a whole cell, a free/immobilised isolated enzyme or as a homogenous cell extract. The choice of biocatalyst form depends on many factors such as the scale of the reaction, whether or not cofactor recycling is required for

the enzyme, whether or not the enzyme can be isolated, the type of reaction and the reaction conditions e.g. T °C (Faber, 1997a).

Generally whole cell catalysts are easy to prepare from a fermentation and can therefore be produced rapidly and cheaply. Whole cell catalysts tend to be more stable than isolated enzymes due to the presence of a cell membrane/wall (Woodley *et al.*, 1990). However, side reactions on the substrate may occur inside the cell (Tramper, 1996) and larger substrates will not be easily transported across the cells membrane. Also, the physiology of the cell can lead to further process issues such as surfactant release (schmid *et al.*, 1998) and increased viscosity of the aqueous phase. Enzymes are more expensive to prepare but are unlikely to produce side reactions and are able to interact with larger substrates. They can also be used in near anhydrous conditions where reactions can be reversed such as dehydration instead of hydrolysis (Westcott and Klibanov, 1994; Carrea *et al.*, 1995; Layh and Willetts, 1998).

#### **1.4.2 Immobilisation of the biocatalyst**

The stability and recovery of the different forms of biocatalyst, particularly for isolated enzymes, can be improved by immobilisation. Immobilisation protects the enzyme/cell by making it more difficult to unfold or disrupt by fixing it to a support usually a polymer. The various methods of immobilisation have been extensively reviewed and will not be described here (Ballesteros *et al.*, 1994).

Other advantages of immobilisation include an increase in productivity. As well as facilitated recovery of the biocatalyst immobilisation can also protect the biocatalyst against damage from the reactor itself, such as shearing effects and reduce aggregation of biomass at the liquid-liquid interface (Brink and Tramper, 1985; Van Sonsbeek *et al.*, 1993). However, Brink and Tramper also observed that this did not reduce solvent molecular toxicity effects on the catalyst.

## 1.5 SELECTION OF AN ORGANIC SOLVENT PHASE

### 1.5.1 Solvent characteristics

Selection of an appropriate solvent for two-liquid phase biocatalysis will depend on the properties of the solvent and its interaction with the biocatalyst, the substrate and product. The desirable characteristics for such a solvent have been compiled by Bruce and Daugulis (1991) and are shown in Table 1.2.

Solvents that do not tend to form emulsions increase the ease of phase separation. Recovery of the solvent phase is further affected by density, viscosity and boiling point of the phases. The solvent should also be non-biodegradable so it is not utilised by the organism. In addition to the above characteristics the solvent must perform optimally for both the reaction and product recovery steps (Bruce and Daugulis, 1991).

<b>Desirable solvent characteristics</b>
Favourable distribution coefficient for product
High selectivity
Low emulsion-forming tendency
Low aqueous solubility
Chemical and thermal stability
Favourable properties for product recovery
Non-biodegradability
Non-hazardous
Inexpensive
Available in bulk quantities
Biocompatibility

**Table 1.2** Desired characteristics of solvents for use in two-phase biotransformations. From Bruce and Daugulis (1991).

### 1.5.2 Solvent biocompatibility

Of great importance is the biocompatibility of the solvent. A positive correlation is found between the hydrophobicity of the solvent and a decrease in toxicity to the

biocatalyst. Hydrophilic solvents cause the membrane of biocatalyst cells to become more fluid and this has the effect of reducing enzyme activity (Osborne *et al.*, 1990). A parameter Log P is usually used to indicate the relative polarity of a solvent. It is defined as the logarithm of the partition coefficient of a solvent in a water-octanol two-phase system (Laane *et al.*, 1987) and is given by:

$$\text{Log P} = \text{Log} \left( \frac{[\text{solute}]_{\text{octanol}}}{[\text{solute}]_{\text{water}}} \right) \quad (1.1)$$

The more hydrophobic the solvent is (i.e. the greater proportion in the octanol phase) the higher the Log P value. Below are the three types of solvent as defined by Laane *et al.*, (1987) relative to their Log P values:

1. Solvents having a Log P < 2. These are hydrophilic and are least suitable in biocatalytic systems as they rapidly result in a loss of activity.
2. Solvents having a Log P between 2 and 4. For some applications these solvents might be suitable, but harmful effects to the biocatalyst should be anticipated.
3. Solvents having a Log P > 4. These solvents are hydrophobic and are unlikely to damage the biocatalyst. They are the most applicable to biocatalytic processes.

These are only general rules. Further investigation has revealed that the Log P above which solvents are non-toxic is different for each homologous series of solvent. Also solvent tolerance is slightly higher in gram negative cells than in gram positive ones (Vermuë *et al.*, 1993) and recent studies have shown that some bacteria are especially solvent tolerant possessing membrane pumps for the active removal of solvent or solvent impermeable membranes (de Bont, 1998).

### 1.5.3 Solvent selection strategy

Strategies for the selection of an appropriate solvent have been developed by Bruce and Daugulis (1991). To aid in solvent selection they demonstrated methods to predict the biocompatibility and extractive capability of solvents. Biocompatibility is predicted by using heuristic data or the correlation between bioactivity and the Log P value of the solvent or the concentration of solvent in the cell membrane. To predict the behaviour of a product in an aqueous/solvent system a computer program ESP (extractant screening program) was developed. They further demonstrated that a biocompatible yet poor solvent can be mixed with a toxic solvent that has better extractant properties to yield a mixture that is still biocompatible yet has improved extractant properties. As has already been mentioned solvents disrupt the membrane of cells. However how much of an effect they have on the biocatalyst is relative to their concentration in the aqueous phase and also in the solvent phase. Bruce and Daugulis have derived an equation (1.2) that indicates whether or not a solvent will show dissolved toxicity in the aqueous phase. This is a further aid in selection of a suitable solvent:

$$[\text{Solvent}_{\text{memb}}] = X P_{\text{octanol}}^Y [\text{Solvent}_{\text{aq}}] \quad (1.2)$$

If the aqueous solubility of a solvent is known and its Log P value can be calculated the above equation can be used to determine the maximum concentration the solvent can reach in the cell membrane (Bruce and Daugulis, 1991). Therefore if the critical concentration cannot be attained then the solvent will not show dissolved toxicity.

### 1.5.4 Phase ratio

The ratio of the volumes of two liquid phases has an effect on the mass transfer of reactants and products between the two phases (Westgate *et al.*, 1995), on the activity and stability of the catalysts and the subsequent recovery of catalyst and products (Lilly *et al.*, 1990). Selection of phase ratio must therefore be an

informed decision that will maximise the yield of the desired reaction and minimise toxic and interfacial effects on the catalyst.

In a two-liquid phase system an interface occurs between the two phases across which the transfer of reactants and products may occur (Lilly *et al*, 1990). The two-phase ratio ( $\phi$ ) as defined as ‘the fraction of the total reaction volume occupied by the organic phase’ and can be determined using Equation 1.3.

$$\phi = \frac{V_d}{V_{total}} \quad (1.3)$$

Lilly *et al*, (1990) suggested that three major constraints should be considered when selecting a phase ratio these are operational constraints, mass transfer, and product recovery:

- Operational constraints. The biocatalyst toxicity and inhibition may limit the choice of phase ratio, therefore the characteristics of the reaction must be considered. For example any reaction that results in the removal or addition of hydrogen ions will result in a change in pH. A buffer may be used to control this if reactant amount is small compared to aqueous volume and it does not interfere with subsequent product recovery. Alternatively the addition of acid or base may be used but this will change phase ratio. Regions of high and low pH will be created by the addition of acid/base therefore it is preferable to have an aqueous phase as the continuous phase as this will disperse acid/base in the reactor.
- Mass transfer. The rate of mass transfer of reactant between phases is a function of the interfacial area per unit volume of aqueous phase and organic and aqueous film mass transfer coefficients. In the continuous phase the interfacial area rises with the phase ratio. However, a point is reached where phase inversion occurs and the organic phase becomes the continuous phase. This depends on the properties of the two phases and the catalyst. Increments of the phase ratio beyond the point of inversion reduce the interfacial area and

consequently the rate of mass transfer is reduced. Thus maximum interfacial area is attained below the phase ratio for inversion, normally in the range, 0.4 - 0.7. However, other factors such as agitation rate influence the interfacial area at particular phase ratios e.g. the interfacial area is reduced when the interfacial tension and phase density differences are high.

- Product recovery. Phase ratio affects ease of phase separation and product recovery. At extreme values of phase ratio ( $\phi < 0.1$ ;  $\phi > 0.9$ ) phase separation is poor. Intermediate phase ratio values give better recovery from the continuous phase whether this is aqueous or organic. However, improved recovery is counterbalanced by lower product concentration obtained as the volume of the phase in which it is dissolved increases; this is known as the dilution effect (Chae and Yoo, 1997).

Recovery is also influenced by the Log P value of the product. At high ( $P > 20$ ) and low values ( $P < 0.05$ ) it is sensible to recover product only from the organic or aqueous phases respectively. However for intermediate Log P values it will be necessary to recover product from both phases. Alternatively, product can be recovered from one phase with minimal loss in the other by choosing a phase ratio in favour of the recovery phase. Selection of this phase ratio involves the consideration of the amount of product recovered and its concentration in the phase which will be processed further. The properties of the liquid phases should also be taken into consideration (Lilly *et al.*, 1990).

## 1.6 BIOREACTOR DESIGN AND OPTIMISATION

The design and optimisation of an aqueous two-phase reactor requires the consideration of several important factors. These include: reaction kinetics, location of the reaction, mass transfer, solvent biocompatibility and downstream processing (Woodley and Lilly, 1992; Van Sonsbeek *et al.*, 1993). Once these are known the process can be optimised with heuristics and design tools such as windows of operation (Woodley and Titchener-Hooker, 1996).

The most common reactor selected for two-liquid phase biocatalysis is the stirred tank reactor. Other reactors employed in the study of two-liquid phase catalysis have included an immobilised cell fluidised-bed reactor, column-type bioreactors, liquid-impelled loop reactors and membrane reactors (Van Sonsbeek *et al.*, 1993; Doig *et al.*, 1998).

### 1.6.1 Reaction location

The location of the region where the reaction occurs in the reactor has a direct effect on the kinetics of the overall reaction. Knowing the location of catalysis enables the process to be optimised in that area. This was first demonstrated with the hydrolysis of benzyl acetate by pig liver esterase and toluene oxidation by a strain of *Pseudomonas putida*. In both instances catalysis was found to occur throughout the bulk of the aqueous phase (Woodley *et al.*, 1991). To determine the reaction location three parameters are required (Woodley, 1990): the saturation concentration of reactant within the aqueous phase,  $[S_a^*]$ , the biocatalytic reaction rate as a function of the aqueous phase reactant concentration (this is dependent on the catalyst concentration,  $[Ba]$ ) and finally, the reactant transfer rate from organic to aqueous phase as a function of the aqueous phase reactant concentration. This is dependent on the saturation concentration of reactant within the aqueous phase  $[S_a^*]$ , and the reactant mass transfer coefficient,  $K_L a$ .

These parameters will yield information about the location of catalysis within the reaction medium. This location can then be categorized into one of three reaction zones (Woodley, 1990): conversion of reactant non-uniformly to product in the majority of the aqueous phase solution, exclusively at the liquid-liquid interface or in the bulk of the aqueous phase.

### 1.6.2 Reaction kinetics

A thorough understanding of the kinetics of the biocatalyst used is necessary to decide what concentration of catalyst is required to achieve an optimum rate of reaction. This can then be incorporated with the rate of mass transfer to give an

overall rate of reaction. Chae and Yoo (Chae and Yoo, 1997) refer to the rate of reaction as the substrate rate of reaction (SRR). The SRR is defined as shown in Equation 1.4 assuming that the reaction obeys Michaelis-Menton kinetics and does not occur at the interface.

$$SRR = \frac{k_1 ES_w}{K_{M1} + S_w} \quad (1.4)$$

Where  $k_1$  is the enzyme activity reaction rate constant ( $\text{mmol.g}^{-1}.\text{min}^{-1}$ ),  $k_{M1}$  is the enzyme michaelis-menton constant ( $\text{mmol.L}^{-1}$ ) E is the enzyme concentration in aqueous phase ( $\text{g.L}^{-1}$ ) and S is the substrate concentration ( $\text{mmol.L}^{-1}$ ). So when designing the bioprocess the intrinsic kinetic values of the enzyme, its relative concentration and the concentration of the substrate all need to be considered.

### 1.6.3 Mass transfer

Mass transfer of substrate and product between the two phases has a direct effect on the overall rate of reaction and on the toxicity and the potential change in pH caused by an increase/decrease in substrate/product concentration. The transfer of mass across the liquid-liquid interface is affected by the size of the interfacial area (A), the viscosity of the two liquids and the relative concentration of the substrate/product in either phase.

The mass transfer of solutes in two-phase systems is most commonly described by the ‘Whitman two film theory’ model (Woodley and Lilly, 1990). This model assumes a well mixed system consisting of an aqueous phase, an organic phase and interface. Either side of the interface is a theoretical stagnant liquid film area where no reaction is assumed to take place. Thus a substrate molecule passes from the organic phase, through the organic phase stagnant area, through the interface, through the aqueous stagnant area into aqueous bulk phase where it reacts with the biocatalyst.

When a substrate containing solvent phase is brought into contact with a biocatalyst containing aqueous phase, substrate in the solvent partitions into the aqueous phase until an equilibrium is reached between the substrate concentration in the aqueous phase ( $S_w^*$ ) and in the solvent phase ( $S_o^*$ ). This is defined as the equilibrium partition coefficient ( $m_s$ ) which is shown in Equation 1.5:

$$m_s = \frac{S_o^*}{S_w^*} \quad (1.5)$$

At equilibrium the net mass transfer rate is zero. However, as there is a biocatalyst in the aqueous phase equilibrium is never reached. Two reaction specific mathematical models have been developed to simulate the overall rate of reaction incorporating both mass transfer and reaction kinetics in an two-liquid phase system. Although both use different nomenclature they are almost identical in structure and prediction of reaction behaviour. The two models were developed for the tyrosinase catalysed hydroxylation of phenol (Chae and Yoo, 1997) and the kinetic resolution of  $\alpha$ -methylbenzylamine with  $\omega$ -transaminase (Shin and Kim, 1999).

Chae and Yoo refer to the rate of mass transfer as the substrate transfer rate (STR) which is defined in Equation 1.6:

$$STR = \frac{k_s A}{V_w} (S_o - m_s S_w) \quad (1.6)$$

Where  $k_s A$  is the substrate mass transfer coefficient through the liquid-liquid interface and  $V_w$  is the aqueous phase volume. Thus interfacial area ( $A$ ) and aqueous phase volume have a significant affect on the Substrate transfer rate. So increasing the agitation of the liquids in a two-phase reactor increases ( $A$ ) and increasing the solvent ratio reduces  $V_w$  leading to a higher rate of STR. Combining the STR (Equation 1.6) and SRR (Equation 1.4) terms gives an overall rate of change of substrate concentration in the aqueous phase as described by:

$$\frac{dS_w}{dt} = \frac{k_s A}{V_w} (S_o - m_s S_w) - \frac{k_1 E S_w}{K_{M1} + S_w} \quad (1.7)$$

The rate of product formation and partitioning into the solvent phase can also be described in a similar manner.

The Chae and Yoo (1997) model were found to fit the data well and the conversion of substrate was found to depend strongly on initial substrate and enzyme concentrations and phase volume ratio as well as the size of the interfacial area which correlates with other observations in the literature (Westgate *et al.*, 1995; Collins *et al.*, 1995).

#### 1.6.4 Windows of operation

Optimising a two-phase biotransformation involves the consideration of key quantitative parameters. Often these are the ‘bottle-neck’ or rate limiting steps of the biotransformation and extremes of these parameters will result in an inefficient reaction. Graphical representation of relevant constraints enables the identification of an area of the graph or a ‘window’ through which yield can be maximised or a process optimised. This concept is a ‘window of operation’ (Woodley and Titchener-Hooker, 1996). As the process scale is increased further bounds are introduced these reduce the size of the operating window (Woodley, 1990).

### 1.7 SCALE-UP OF TWO-LIQUID-PHASE BIOREACTORS

Reliable and consistent scale-up of two-phase bioreactors is currently poorly characterised although constant power per unit volume (P/V) has been partially investigated as a scaleable parameter (Woodley, 1990). Inaccurate scale-up requires process re-optimisation which at large scale is expensive and time consuming. Therefore there is a need for a series of concise rules and models that will aid in the accurate scale-up of stirred tank, two-phase bioreactors.

### 1.7.1 Mixing

For effective mixing in a two-liquid-phase bioreactor there must be turbulent conditions in the fluids (Doran, 1997). This is created by agitation of the two phases by an impeller. The most common impeller design used is the 6-flat-blade disc-turbine or Rushton turbine because it can be operated in a broad range of viscous liquids. However, other designs such as the propeller, anchor and helical screw are also available. The application of impeller type is generally governed by the viscosity range of the impeller.

The standard parameter used to measure fluid turbulence in stirred tank bioreactors is the impeller Reynolds number,  $Re_i$  (Equation 1.8).

$$Re_i = \frac{N_i D_i^2 \rho}{\mu} \quad (1.8)$$

Where  $N_i$  is the stirrer speed,  $D_i$  is the impeller diameter,  $\rho$  is the fluid density and  $\mu$  is fluid viscosity. Thus there is a corresponding decrease in  $Re_i$  with increasing fluid viscosity.

As mixing of the two phases is the major function of such a bioreactor this should be the most important characteristic when considering scale-up (Doran, 1997). Increasing the size of the interfacial area through mixing will improve the rate of mass transfer and hence the rate of reaction. Shin and Kim (Shin and Kim, 1999) found that in the two-liquid-phase resolution of  $\alpha$ -methylbenzylamine that at agitation speeds below dispersion conditions the rate of mass transfer increases gradually in response to an increase in convection. However, in the dispersed state the interfacial area changed according to agitation speed. As well as increased interfacial area the turbulence increased the convective mixing. Therefore for a homogenous system with optimal mass transfer a well mixed dispersion is ideal.

### 1.7.2 Scale-up

Transport phenomena such as mass transfer which is one of the most important functions of two-liquid-phase mixing are scale dependent (Atkinson and Mavituna, 1991). As an example the volume of fluid mixing in a stirred tank reactor can be considered. If the reactor is scaled up geometrically the volume also increases as does the length of path of the fluid for bulk circulation. Therefore to keep the mixing time identical the velocity must be increased by increasing agitation. However, power per unit volume is proportional to the fluid velocity squared (Equation 1.9). Thus maintenance of fluid velocity becomes expensive with increasing scale. This method of scale-up is inefficient therefore a practical 'rule of thumb' is to scale-up on the basis of constant power input per unit volume (P/V). This maintains the original parameters of the small scale reactor but the mixing time (due to reduced fluid velocity) will now increase with increasing scale.

$$\frac{P}{V} \propto v^2 \quad (1.9)$$

In theory, complete similarity between bioreactors of different scale can only be achieved by preserving the geometric, kinetic, dynamic, biochemical and chemical properties of the system. However, this is rarely possible. Therefore basic rules of thumb have to be applied. The two most common criteria for scale-up of mixing systems are equal power per unit volume and equal impeller tip speed. Equal power per unit volume can be applied to a variety of mixing processes including those involving mass transfer and dispersion (Okufi *et al.*, 1990). For turbulent systems possessing the same physical properties in geometrically similar tanks the scale-up under a power per unit volume regime (P/V) is related to Equation 1.10 which in turn is related to the power Equation in 1.11.

$$N^3 D_i^2 = \text{Constant} \quad (1.10)$$

$$P = P_o \rho N^3 D_i^2 = \text{Constant} \quad (1.11)$$

Thus the power number represents the ratio of power to inertia forces and is constant at large Reynolds numbers. Therefore, this criterion of equal power input per unit volume represents dynamic similarity under conditions of negligible viscous forces. The relationship for scale-up under a tip speed regime is expressed in Equation 1.12.

$$ND_i = \text{Constant} \quad (1.12)$$

Therefore it is apparent that scale-up under a power per unit volume regime will lead to higher impeller speeds in the bioreactor compared to scale-up under a tip speed regime. This may be more beneficial for the biotransformation than tip speed because of the increased interfacial area associated with a higher impeller speed. Conversely the increase in speed could harm the biocatalyst in which case the slower speed under a tip speed regime would be a more appropriate selection. P/V and tip speed are the most common scale-up criteria other criteria that can be considered are constant mixing time and constant shear rate (relevant where the organism is shear sensitive or the liquid exhibits non-newtonian rheology) (Ju and Chase, 1992).

Many authors indicate the need to maintain geometric similarity during scale-up of a bioreactor (Hempel, 1988; Ju and Chase, 1992; Woodley, 1990; Diaz and Acevedo, 1998). Maintenance of geometric similarity is essential because it reduces the variables of scale-up and has a direct impact on other scaleable parameters such as tip speed (Equation 1.1.3) (Wernesson and Trägårdh, 1999):

$$V_{\text{Tip}} = \pi ND \quad (1.13)$$

Previous texts have observed the  $k_{L,a}$  of oxygen transfer as a single parameter for scale-up on the basis that it is the limiting factor in many fermentations (Diaz and Acevedo, 1999). However Diaz and Acevedo rationalised that it is not so much the  $k_{L,a}$  but the oxygen transfer rate (OTR) (Ju and Chase, 1999; Diaz and Acevedo,

1999). The OTR is a measure of the oxygen mass transfer potential which is analogous to the STR (Equation 1.6) (Chae and Yoo, 1997) mentioned in section 1.6.3. The STR like the OTR is affected by both the physical constraint of interfacial area and the biological constraint of the rate of reaction. Therefore if STR is to be used as a scale-up parameter then SRR should be optimised i.e. the most efficient concentration of biocatalyst in relation to the substrate concentration and phase ratio.

Very little work has been done on the most suitable criteria for the scale-up of two-phase bioreactors apart from one study. An investigation into the power input considerations for scale-up of a two-liquid phase bioreactor which hydrolysed menthyl acetate to menthol by pig liver esterase revealed that optimum activity was observed at 0.3 and 1.5  $\text{W.L}^{-1}$  in two different reactors at an enzyme concentration of 0.1  $\text{g.L}^{-1}$  (Woodley, 1990). The reactors had an identical phase ratio, liquid volume, impeller/reactor diameter ratio and catalyst concentration. However, they differed in diameter (T) and consequently liquid height (h). The wider reactor had an h/T ratio of 0.76 and obtained peak productivity at 0.3  $\text{W.L}^{-1}$  power input whereas the thinner reactor had an h/T ratio of 1.79 and required a power input of 1.5  $\text{W.L}^{-1}$ . Thus from these results it can be seen that consideration of vessel dimensions and relative position of the impeller in the liquor have an effect on power input. Relative position of the impeller in the liquid has also been observed in other reactors to have an effect on power input (Schluter and Deckwar, 1993). However, Woodley (Woodley, 1990) also observed that power input would also have to be increased if the biocatalyst concentration was increased as this would require greater mass transfer. Further issues of increasing biocatalyst concentration are increasing viscosity and increasing non-newtonian rheological properties all requiring greater power input. In addition it was observed in another *Pseudomonas putida* UV4 two-phase biotransformation that increasing the phase ratio necessitates further power input (Collins and Woodley, 1993). Thus any two-phase biotransformation that is scaled-up will first need to be optimised on the basis of reducing liquor viscosity and non-Newtonian behaviour.

## 1.8 DROP SIZE MEASUREMENTS IN AGITATED TWO-PHASE SYSTEMS

To analyse the relative success of a given scale-up regime it will be necessary to measure the interfacial area of liquid-liquid dispersions at different scales. The rationale for this is that if mixing conditions appear to be the same in geometrically similar reactors of different scale then it should be possible to recreate the reaction conditions at different scales without the need for re-optimisation or fresh experiments.

When two immiscible liquids are agitated, a dispersion is formed in which continuous break-up and coalescence of drops occurs. Drop break-up is caused by turbulent fluctuations near the surface of the drop and coalescence occurs occasionally when drops collide. Eventually a dynamic equilibrium is created and this leads to a range of drop sizes in the mixture. The average drop size in this range will depend on the physical properties of the two liquids and any other components in the reactor as well as the level of agitation in the reactor.

The most common term used for expressing drop size and distributions is the Sauter mean diameter ( $d_{32}$ ), defined in Equation 1.14.

$$d_{32} = \frac{\sum_{i=1}^n d_i^3}{\sum_{i=1}^n d_i^2} \quad (1.14)$$

Where  $d_i$  is drop diameter and  $n$  is the number of drops in the distribution. If Sauter mean diameter can be measured in a system then the mixing can be related to different scales for geometrically similar reactors. Knowledge of the properties of a reactor also allow predictions of drop size to be made. A number of correlation equations exist in the literature and take the form shown in Equation 1.15 where  $a$  and  $b$  are constants.

$$\frac{d_{32}}{D_i} = a(1+b\phi)(N_{we})^{-0.6} \quad (1.15)$$

## 1.9 AIMS AND OBJECTIVES OF THE PROJECT

The biotransformation of poorly water-soluble aromatic dinitriles is of scientific and industrial interest. Although processes do exist for the transformation of water-soluble compounds, such as acrylonitrile, no description of a process suitable for the large scale biotransformation of poorly water soluble nitriles currently appears in the literature. This work will attempt to investigate the systematic design and optimisation of a process for the production of 3-cyanobenzamide from the poorly water soluble substrate 1,3-dicyanobenzene (1,3-DCB) and also to define the criteria for successful scale-up of the process to the 75 L scale. The production of 3-cyanobenzamide is of interest as this molecule is not commercially available and is not manufactured industrially by a chemical catalyst.

The biotransformation of 1,3-DCB by *Rhodococcus* R312 was chosen because the microorganism has been extensively studied in the literature and the production of 3-cyanobenzamide from 1,3-dicyanobenzene has previously been shown in a closely related species (Martinkova *et al.*, 1995). *Rhodococcus* R312 is also known to possess only a regio-selective NHase and Amidase (Kerridge, 1995) so no nitrilase is present which may convert the substrate directly into the acid product. Due to the poor water solubility of 1,3-DCB the selection of a two-phase reactor is the most obvious process step to increase the supply of substrate. Use of an organic solvent may harm the biocatalyst but fortunately *Rhodococcus* R312 is known to be a tough and durable biocatalyst.

As part of the process design there will also be an investigation into a potential new type of solvent known as an ionic liquid. These materials are specially prepared room temperature salts that have been researched for the past twenty years in academia but have never been previously applied to a bioprocess. If a two-

phase biotransformation can be demonstrated using an ionic liquid this will be an indicator of further novel applications for 'green' ionic liquid technology.

Having chosen the components for the bioprocess the next stage will be to optimise the process conditions to maximise the production of 3-cyanobenzamide. This can be achieved by using a combination of experimental design, heuristics and process design tools such as windows of operation (Woodley and Titchener-Hooker, 1996).

Assuming that the optimisation stage is successful and biomass can be produced in sufficient quantity the next stage of the project will be an investigation into the most appropriate scale-up regime for the biotransformation. Scale-up criteria of constant P/V and tip speed will be tested. The result of Sauter mean diameter studies and biotransformations will determine which is the better regime for scale-up of two-phase bioreactors on the basis of maintenance of constant interfacial area.

The specific aims of the project are therefore:

- A) To maximise the fermentation production of the biocatalyst *Rhodococcus* R312 to supply biomass for the 75 L bioprocess.
- B) Evaluate the use of a second liquid phase as a process option for making greater concentrations of the poorly water soluble 1,3-DCB available to the biocatalyst. Investigate, define and optimise the conditions of the biotransformation to achieve the maximum space-time yield of the 3-cyanobenzamide from the poorly water soluble substrate, 1,3-DCB.
- C) Investigate the use and application of novel ionic liquids as potential replacements for organic solvents.
- D) Define a reliable basis for scale-up of reactor hydrodynamics.
- E) Assess the effect of agitation and the two scale-up criteria on the profile of the biotransformation and determine which is the most suitable.

## 2. MATERIALS AND METHODS

### 2.1 CHEMICALS AND MICROORGANISM

#### 2.1.1 Main chemicals

The organic solvent toluene and other solvents used in this work were purchased from Sigma-Aldrich Chemical Co. (Dorset, UK) and were of the highest purity available. The reaction substrate 1,3-dicyanobenzene, buffer salts  $\text{KH}_2\text{PO}_4$  and  $\text{K}_2\text{HPO}_4$ , other chemicals and medium components used were also purchased from Sigma-Aldrich Chemical Co. (Dorset, UK) except Oxid agar No.1 which was purchased from Oxoid (Basingstoke, UK).

#### 2.1.2 Synthesis and purification of ionic liquid [bmim][PF<sub>6</sub>]

The ionic liquid [bmim][PF<sub>6</sub>] was synthesised by J.D. Holbrey of the QUILL centre, Queen's University of Belfast, Northern Ireland using the following protocol.

##### 2.1.2.1 1-Butyl-3-methylimidazolium chloride, [bmim]Cl

An autoclave (3 L) was charged with 1-methylimidazole (1030 g, 12.54 mol, 1000 mL, freshly distilled from  $\text{CaH}_2$ ) and 1-chlorobutane (1205 g, 13.02 mol, 1360 mL) and heated at 75 °C for 48 hours under 3 bar pressure of dinitrogen. The reactor contents were transferred to a round-bottomed flask and the excess chlorobutane was removed under reduced pressure with heating. The pale yellow molten product was transferred to a dry-box and poured into a shallow tray, where it crystallised on cooling as an off-white solid (yield 2200 g, 99%).

### 2.1.2.2 1-Butyl-3-methylimidazolium hexafluorophosphate, [bmim][PF<sub>6</sub>]

A stirred solution of [bmim]Cl (313 g, 1.764 mol) (Section 2.1.2.1) in H<sub>2</sub>O (250 mL) was cooled to 0 °C in an ice-bath, and hexafluorophosphoric acid (264 mL, 40% aqueous solution) was added slowly with rapid stirring. The resulting biphasic mixture was stirred for 2 hours., then allowed to come to room temperature, whence the upper, aqueous phase was decanted. The lower, ionic liquid phase was washed with water (5 × 500 mL), and saturated aqueous NaHCO<sub>3</sub> solution (2 × 500 mL) to ensure neutrality, and then extracted into dichloromethane (400 mL). The organic phase was dried over MgSO<sub>4</sub>, filtered, the solvent removed under reduced pressure and the ionic liquid dried for 6 hours at 70 °C *in vacuo*. Yield 400 g, (1.41 mol, 80%) as a colourless liquid (Calculated for C<sub>8</sub>H<sub>15</sub>N<sub>2</sub>PF<sub>6</sub>: C, 33.81; H, 5.32; N, 9.86. Found: C, 33.62; H, 5.37; N, 9.90%).

### 2.1.3 Organism source

The microorganism used, *Rhodococcus* R312, was a kind gift from Professor N. J. Turner (University of Edinburgh, UK) and was stored on nitrile-metabolising (Section 2.1.4) agar at 4°C (Kerridge, 1995).

### 2.1.4 Culture storage (short-term)

*Rhodococcus* R312 was maintained on ‘nitrile-metabolising’ agar plates, at room temperature (Kerridge, 1995). ‘Nitrile metabolising’ agar was composed of the following components (in 1 L deionised water): Bacteriological peptone – 5 g.L<sup>-1</sup>, Lablemco powder – 5 g.L<sup>-1</sup>, Yeast extract – 0.5 g.L<sup>-1</sup>, NaCl – 2 g.L<sup>-1</sup>, Oxoid agar No. 1 – 15 g.L<sup>-1</sup>. Subcultures were made at weekly intervals. Regular streaking for single colony formation was performed to assess culture purity.

### **2.1.5 Culture storage (long term)**

#### **2.1.5.1 Agar slopes**

Isolates were stored on 'nitrile-metabolising' agar slopes and were stored at 4 °C for up to 4 months. Subcultures were made at monthly intervals.

#### **2.1.5.2 Glycerol stocks**

A loopful of bacteria was transferred to growth media as described in either 2.2.1 or 2.2.2. This was mixed with sterile glycerol (final concentration 50% (v/v)) and stored at -20 °C for up to one year.

## **2.2 MEDIA COMPOSITION AND CONDITIONS FOR GROWTH**

### **2.2.1 Rich growth medium (RGM)**

Initially the microorganism was cultivated in a rich growth medium adapted from Nagasawa *et al.* (1986). The medium was made up in three separate solutions as described: Solution 1 (in 120 mL deionised water) was composed of Special peptone - 1 g.L<sup>-1</sup>, Malt extract - 0.6 g.L<sup>-1</sup>, Yeast extract - 0.6 g.L<sup>-1</sup>; Solution 2 (in 80 mL deionised water) Glucose - 20 g.L<sup>-1</sup>; Solution 3 (concentrated solution) FeSO<sub>4</sub>.7H<sub>2</sub>O - 0.002 g.L<sup>-1</sup> (final concentration). Solutions 1 and 2 were sterilised by autoclaving at 15 psi for 20 minutes. Solution 3 was made up as a concentrated stock solution. After cooling solution 2 was added to solution 1 under aseptic conditions and solution 3 was added by passage through a 0.22 µm sterilised millipore filter.

### 2.2.2 Tryptic soy broth (TSB) medium

To achieve greater biomass production the microorganism was also cultivated on a Tryptic Soy Broth (TSB) medium adapted from Chartrain *et al.* (1998) containing 30 g.L<sup>-1</sup> of TSB powder. This was dissolved into deionised water and autoclaved at 15 psi for 20 minutes.

## 2.3 FERMENTATION CONDITIONS AND BIOMASS HARVESTING

### 2.3.1 Shake flask fermentations

200 mL liquid volume fermentations were carried out in 2 litre baffled conical flasks in a orbital shaking incubator operated at 200 rpm and 30 °C. Cells were subsequently harvested by centrifugation at the end of the exponential growth phase. This was typically two days after inoculation at an OD<sub>600</sub> of 1.0 with rich growth media and at an OD<sub>600</sub> of 12.0 with tryptic soy broth media (Section 2.2.1 and 2.2.2). The cells were then resuspended in an appropriate biotransformation buffer before use (usually 0.1 M KH<sub>2</sub>PO<sub>4</sub>-K<sub>2</sub>HPO<sub>4</sub> phosphate buffer, pH 7) as described in Section 2.4.1. Shake flasks were regularly sampled using aseptic techniques to monitor optical density and biomass wet weight and cell dry weight (Section 2.7.1).

### 2.3.2 Stirred tank fermentations

All stirred tank fermentations were performed with a series 2000 TCS box controller produced by Turnbull Control Systems (Worthing, UK). Logging and set points were controlled using Bioview, a specialist fermenter control software package, produced by Adaptive Biosystems (Watford, UK). The oxygen uptake rate (OUR), carbon evolution rate (CER) and respiratory quotient (RQ) were measured online using a VG Prima mass spectrometer produced by VG Gas Analysis, Ltd. (Cheshire, UK). Dissolved oxygen tension (DOT) was measured

online with an Ingold DO probe produced by Ingold Messtechnik Ag (Urdorf, Switzerland).

### 2.3.2.1 7 L Fermentation

The 5 L fermentation was performed in an Inceltech (Pangbourne, UK) 7 L fermenter. The main tank was 40 cm high and 15 cm in diameter with an H:T ratio of 2.63. Agitation was provided by a two-stage 5 cm diameter Rushton turbine impeller. The reactor was filled with 4.5 L sterile 30 g.L<sup>-1</sup> TSB in deionised water and 1 mL PPG (surfactant) which was sterilized in place at 121 °C for one hour. The reactor was run at 30 °C, 700 rpm, at aeration rate of 0.5 VVM. The fermentation was initiated by inoculation with 500 mL of *Rhodococcus* R312 cell suspension which had also been grown in 30 g.L<sup>-1</sup> TSB (harvested at OD<sub>600</sub> = 12). pH was kept at 7 by the controlled addition of 4M NaOH and 4M phosphoric acid. Foaming was regulated by the controlled addition of PPG antifoam in response to the antifoam probe. The fermentation was stopped at approximately 25 hours when OD<sub>600</sub> = 16. Samples were collected from the sample port every hour and analysed for biomass wet weight, dry cell weight (Section 2.7.1) and activity (Section 2.5).

### 2.3.2.2 20 L Fermentation

The 15 L fermentation was performed in an Inceltech (Pangbourne, UK) 20 L fermenter. The main tank was 53 cm high and 22 cm in diameter with an H:T ratio of 2.4. Agitation was provided by a three-stage 7 cm diameter Rushton Turbine impeller. The reactor was filled with 14 L sterile 30 g.L<sup>-1</sup> TSB in deionised water and 4 mL PPG (surfactant) which was sterilized in place at 121 °C for one hour. The reactor was run at 30 °C, 500 rpm, at an aeration rate of 0.5 VVM. The fermentation was initiated by inoculation with 1 L of R312 in 30 g.L<sup>-1</sup> TSB (harvested at OD<sub>600</sub> = 12). pH was kept at 7 by the controlled addition of 4M NaOH and 4M phosphoric acid. Foaming was regulated by the controlled addition of PPG antifoam in response to the antifoam probe. The fermentation was stopped at approximately 31 hours when OD<sub>600</sub> = 16 and liquid volume used to aseptically

innoculate the 450L fermenter (Section 2.3.2.3). Samples were collected at the end of the fermentation and analysed for biomass wet weight, dry cell weight (Section 2.7.1) and activity (Section 2.5).

### 2.3.2.3 450 L Fermentation

Cells for large scale (75 L) biotransformation experiments were produced in a 300 L fermentation in a 450 L Chemap AG (Volketswil, Switzerland) fermenter. The main tank was 220 cm high and 59 cm in diameter with an H:T ratio of 3.7. Agitation was provided by a three-stage 20 cm diameter Rushton Turbine impeller. The reactor was filled with 285 L sterile 30 g.L<sup>-1</sup> TSB in deionised water and 60 mL PPG (surfactant) which was sterilized in place at 121 °C for one hour. The reactor was run at 30 °C, 180 rpm, at an aeration rate of 0.5 VVM. The fermentation was initiated by aseptically pumping the 15 L inoculum of biomass rich fermentation broth from the Inceltech 20 L (2.3.2.1). pH was kept at 7 by the controlled addition of 4M NaOH and 4M phosphoric acid. Foaming was regulated by the controlled addition of antifoam in response to the antifoam probe. The fermentation was stopped and harvested after 16 hours when OD<sub>600</sub>=16. Samples were collected at the end of the fermentation and analysed for biomass wet weight, dry cell weight (Section 2.7.1) and activity (Section 2.5). The 300 L of fermentation broth from the Chemap fermenter was then harvested and processed through a Carr Powerfuge (Franklin, MA, USA) to recover the biomass from the liquid fermentation medium (Section 2.4.2).

## 2.4 CELL PREPARATION

### 2.4.1 Small scale

Cells harvested from shake flask fermentation were centrifuged at 10,000 rpm, 4 °C for 20 minutes in a Sorvall Super T21 centrifuge (Stevenage, UK). The harvested cells were then washed twice with 0.1 M KH<sub>2</sub>PO<sub>4</sub>-K<sub>2</sub>HPO<sub>4</sub> phosphate buffer (pH 7) and were then resuspended at a typical concentration of 10-15 g<sub>ww</sub>.L<sup>-1</sup> for subsequent experiments.

### 2.4.2 Large scale

The 300 L of fermentation broth from the Chemap AG 450 L reactor (Section 2.3.2.3) was processed through a Carr Powerfuge (Franklin, MA, USA) separation system to separate the biomass from the supernatant. The powerfuge processed batches of up to 50 L at a time and was set to run at 15200 RPM at a flow rate of 1000 mL.min<sup>-1</sup>. 3.6 Kg biomass in dry solid form was recovered and stored in polythene bags at 4 °C. Harvested cells were resuspended and prepared for experiments at 75 L scale as required. Cells for biotransformation and mixing studies were resuspended in 0.1 M potassium phosphate buffer, pH 7 at a concentration of 15 g<sub>ww</sub>.L<sup>-1</sup> in a mixing vat.

### 2.5 NHase AND AMIDASE ACTIVITY ASSAYS

To determine the activity of the NHase and amidase enzymes 200 µL samples of aqueous cell suspension were added to 0.8 mL 0.1 M phosphate buffer, pH 7, and 1 mL of an identical buffer solution containing 0.2 g.L<sup>-1</sup> 1,3-DCB (final mixed concentration 0.1 g.L<sup>-1</sup>). 200 µL samples of this mixture were removed at 20 second time intervals for one minute and immediately added to 50 µL of 10 M HCl<sub>(aq)</sub> in a 2 mL Eppendorf tube to quench the transformation. The samples were then centrifuged at high speed for 10 minutes to pellet the biomass after which 100 µL of the clarified aqueous phase was removed, filtered through a Whatman 0.2 µm syringe filter (Maidstone, UK) and analysed for substrate and product concentrations by HPLC as described in Section 2.7.5. Plots of amide and acid concentration against time were then used to calculate the initial rates of formation. One unit of NHase (or amidase) activity was defined as the amount of enzyme catalysing the production of 1 µmol 3-cyanobenzamide or (3-cyanobenzoic acid) per minute. This was expressed as units per mg of wet weight of bacterial mass (U.mg<sup>-1</sup>).

## 2.6 BIOTRANSFORMATION OF 1,3-DCB BY *Rhodococcus* R312

### 2.6.1 Shake flask biotransformations

#### 2.6.1.1 Single-phase biotransformations

5 mL of buffered aqueous phase, pH 7, containing 50  $\text{g}_{\text{ww}}\cdot\text{L}^{-1}$  (wet weight) *Rhodococcus* R312 cells was initially incubated for 30 minutes at 30 °C in a shaking incubator at 200 rpm. The equivalent dry cell weight biomass concentration is 10  $\text{g}_{\text{dcw}}\cdot\text{L}^{-1}$  (1  $\text{g}_{\text{ww}}\cdot\text{L}^{-1}$  is equivalent to 0.2  $\text{g}_{\text{dcw}}\cdot\text{L}^{-1}$  in this case). To start the transformation 5 mL of an aqueous buffer solution, pH 7, containing 0.2  $\text{g}\cdot\text{L}^{-1}$  1,3-DCB (final concentration 0.1  $\text{g}\cdot\text{L}^{-1}$ ) was added to the agitated cell suspension. 200  $\mu\text{L}$  samples were taken at 1 minute intervals for a pre-defined period and immediately added to 50  $\mu\text{L}$  of 10 M  $\text{HCl}_{(\text{aq})}$  to quench the reaction (Kerridge, 1995). The samples were then further analysed as described in Section 2.7.5.

##### 2.6.1.1.1 Amidase inhibition study

5 mL of a buffered aqueous phase, pH 7, containing 25  $\text{g}_{\text{ww}}\cdot\text{L}^{-1}$  *Rhodococcus* R312 cells were incubated on a shaking incubator at 200 rpm and 30 °C for 30 minutes in the presence of 0.5, 5 and 50 mM urea. To start a transformation 5 mL of an aqueous phase, pH 7, containing 0.2  $\text{g}\cdot\text{L}^{-1}$  1,3-DCB was added to the cells. 200  $\mu\text{l}$  samples were taken at three minute intervals for fifteen minutes and immediately added to 50  $\mu\text{l}$  of 10 M  $\text{HCl}_{(\text{aq})}$  to quench the reaction (Kerridge, 1995). The samples were then further analysed as described in Section 2.7.5.

##### 2.6.1.1.2 Stability of *Rhodococcus* R312 NHase activity with variable pH and temperature

The influence of pH and temperature on the initial activity of the *Rhodococcus* R312 NHase enzyme has been previously investigated (Kerridge, 1995). In this work the pH and temperature stability (initial activity measured over time) of the

NHase in a single-phase aqueous reaction system was examined. Initially 50  $\text{g}_{\text{ww}}\cdot\text{L}^{-1}$  of biocatalyst in 5 mL of 0.1 M potassium phosphate buffer was placed in a 25 mL shake flask. To assess the effect of temperature, at pH 7, the shake flask was placed in a water bath at a specified temperature for 1 hour after which time the cells were assayed for NHase and amidase activity as described in Section 2.5. The effect of pH, at 30 °C, was similarly assessed by suspending the cells in an appropriate buffer at a specific pH (see table 2.1 for list of buffers) before again assaying for NHase and amidase activity. Experiments were performed in triplicate.

Buffer	PH Range
0.1 M Citric acid - $\text{Na}_2\text{HPO}_4$	4-5
0.1 M $\text{K}_2\text{HPO}_4$ - $\text{KH}_2\text{PO}_4$	6-9
0.1 M $\text{NaHCO}_3$ – NaOH	10-11

**Table 2.1** Buffer comparison and pH range used in biotransformation experiments

### 2.6.1.2 Two-phase biotransformations

#### 2.6.1.2.1 Solvent selection and partition coefficients

A suitable organic phase for the biotransformation of 1,3-DCB was selected on the basis of biocompatibility (retention of biocatalytic activity after exposure to solvent), substrate saturation concentration and partition coefficient together with background information available in the literature (Sangster, 1989). To determine saturation concentrations of 1,3-DCB in the various solvents (and ionic liquid [bmim][PF<sub>6</sub>]) excess quantities of 1,3-DCB were initially added and equilibrated at 30°C before filtering the suspension through a 0.2  $\mu\text{m}$  syringe filter (Maidstone, UK) and determining the dissolved concentration of substrate by HPLC as described in Section 2.7.5. Product saturation concentrations in phosphate buffer were determined in the same manner.

Equilibrium partition coefficients of the substrate and product were determined using an equal volumes of the extracting phase, 0.1 M phosphate buffer and substrate containing toluene phase or [bmim][PF<sub>6</sub>] in a tightly sealed vial. After vigorous mixing followed by phase separation under gravity for 24 hours, samples from each phase were removed and the 1,3-DCB concentration determined using HPLC analysis as described in Section 2.7.5.

#### **2.6.1.2.2 NHase and amidase activity of *Rhodococcus* R312 in aqueous-toluene systems**

The NHase and amidase activities of *Rhodococcus* R312 cells in an aqueous-toluene reaction system were examined under variable conditions of cell concentration, substrate concentration and phase volume ratio ( $V_r = V_{org}/V_{aq}$ ). Experiments were carried out in 25 mL shake flasks containing a final total liquid volume of 10 mL. Cells were initially suspended in 0.1 M potassium phosphate buffer, pH 7, the substrate-containing toluene phase added at the desired  $V_r$  and the two-phase mixture was then agitated in a shaking incubator at 200 rpm and 30 °C. To assess the enzyme activities 200 µL samples of the dispersion were taken at appropriate time intervals and rapidly added to 50 µL of 10 M HCl<sub>(aq)</sub> in a 2 mL Eppendorf tube to quench the transformation (Section 2.5). The samples were then further analysed as described in Section 2.7.5. All experiments were performed in triplicate.

#### **2.6.1.2.3 Biotransformation with variable biomass concentrations**

To assess the influence of variable cell concentrations experiments were carried out at a  $V_r$  of 0.1 with a toluene phase initially containing 20 g.L<sup>-1</sup> 1,3-DCB as described in Section 2.6.1.2.2. Cell concentration was investigated over a range of 1.25 to 200 g<sub>ww</sub>.L<sup>-1</sup>. All experiments were performed in triplicate.

#### 2.6.1.2.4 Biotransformation with variable phase volume ratios

To assess the activity of biocatalyst at various phase volume ratios defined as  $V_r = V_{org}/V_{aq}$ , the volumes of the aqueous and toluene phases were modified accordingly using an aqueous phase containing  $50 \text{ g}_{ww} \cdot \text{L}^{-1}$  of cells and a toluene phase initially containing  $20 \text{ g} \cdot \text{L}^{-1}$  1,3-DCB. Experiments were performed as described in Section 2.6.1.2.2 with the phase volume ratio varied over a range of 0.05 to 0.3. All experiments were performed in triplicate.

#### 2.6.1.2.5 Biotransformation activity with variable initial substrate concentration

To assess the activity of the biocatalyst over a range of initial 1,3-DCB concentrations experiments were performed at a  $V_r$  of 0.1 and a biomass concentration of  $50 \text{ g}_{ww} \cdot \text{L}^{-1}$  *Rhodococcus* R312 cells as described in Section 2.6.1.2.2. The initial substrate concentration was investigated over a range of 5 to  $25 \text{ g} \cdot \text{L}^{-1}$ . All experiments were performed in triplicate.

#### 2.6.1.2.6 25 mL shake flask two-phase biotransformation of 1,3-DCB by *Rhodococcus* R312

In a 25 mL shake flask, a volume of buffered aqueous phase (depending on phase ratio), pH 7, containing  $50 \text{ g}_{ww} \cdot \text{L}^{-1}$  *Rhodococcus* R312 cells was initially incubated for 30 minutes at  $30 \text{ }^\circ\text{C}$  in a shaking incubator at 200 rpm. To start the transformation a volume of toluene containing a given concentration of 1,3-DCB was added to the agitated cell suspension. 200  $\mu\text{L}$  samples were taken at time intervals for two hours and immediately added to 50  $\mu\text{L}$  of 10 M  $\text{HCL}_{(aq)}$  to quench the reaction (Kerridge, 1995). The samples were then further analysed as described in Section 2.7.5.

#### 2.6.1.2.7 Comparative two-phase biotransformations of 1,3-DCB using aqueous-toluene and aqueous-[bmim][PF<sub>6</sub>] systems

The substrate-containing phase, either toluene or [bmim][PF<sub>6</sub>] (2 mL) (Section 2.1.2), containing 1 g.L<sup>-1</sup> 1,3-DCB was added to 8 mL of 0.1 M potassium phosphate buffer, pH 7, containing 100 g<sub>ww</sub>.L<sup>-1</sup> of the biocatalyst, *Rhodococcus* R312, in a 25 mL shake flask. The flask was then placed in a shaking incubator operated at 200 rpm and 30 °C. Samples of the mixture (200 µL) were subsequently removed at designated time intervals and immediately added to 50 µL of 10 M HCl<sub>(aq)</sub> in a 2 mL Eppendorf tube to quench the transformation. The samples were then centrifuged at high speed for 10 minutes to separate the two liquid phases after which 100 µL of the aqueous phase was removed, filtered through a 0.2 µm syringe filter (Whatman, UK) and analysed for substrate and product concentrations by HPLC (Section 2.7.5). All experiments were performed in triplicate.

#### 2.6.1.2.8 Activity of *Rhodococcus* R312 cells after exposure to a second phase

The activity of the *Rhodococcus* R312 cells was also determined during prolonged agitation in either water-toluene or water-[bmim][PF<sub>6</sub>] two-phase systems. Experiments were performed described in Section 2.6.1.2.2 except that the concentration of *Rhodococcus* R312 in the aqueous phase was 50 g<sub>ww</sub>.L<sup>-1</sup> and no substrate was present. The residual specific activity of the cells was then determined by diluting 200 µL of an aqueous phase sample to 5 g<sub>ww</sub>.L<sup>-1</sup> with 800 µL 0.1 M potassium phosphate buffer, pH 7, and 1 mL of the same buffer containing 0.2 g.L<sup>-1</sup> 1,3-DCB (final concentration 0.1 g.L<sup>-1</sup>). Samples of this reaction mixture were then removed at 20 second intervals and the specific activity of the cells was determined by monitoring the initial rate of amide formation by HPLC as described in Section 2.7.5. All experiments were performed in triplicate.

## 2.6.2 Stirred tank biotransformations

### 2.6.2.1 Stirred tank geometry and operation

Droplet size analysis and biotransformation experiments were carried out in two stirred vessels of similar geometry each fitted with a three-stage Rushton turbine impeller. The Inceltech (Wokingham, UK) LH SGI 75 L stainless steel solvent reactor was operated in a dedicated pilot plant facility designed according to both solvent and biological containment regulations. The 3 L glass vessel was located in a fume hood. The dimensions of both vessels and impellers used are given in Figure 2.1. To minimise the risk of explosion, the impeller in the 3 L vessel was stirred by an air-driven motor. In the 75 L reactor a constant positive pressure of nitrogen was maintained in the headspace to exclude any oxygen and a spark proof motor was used. Both vessels were thoroughly cleaned and rinsed with deionised water between runs.

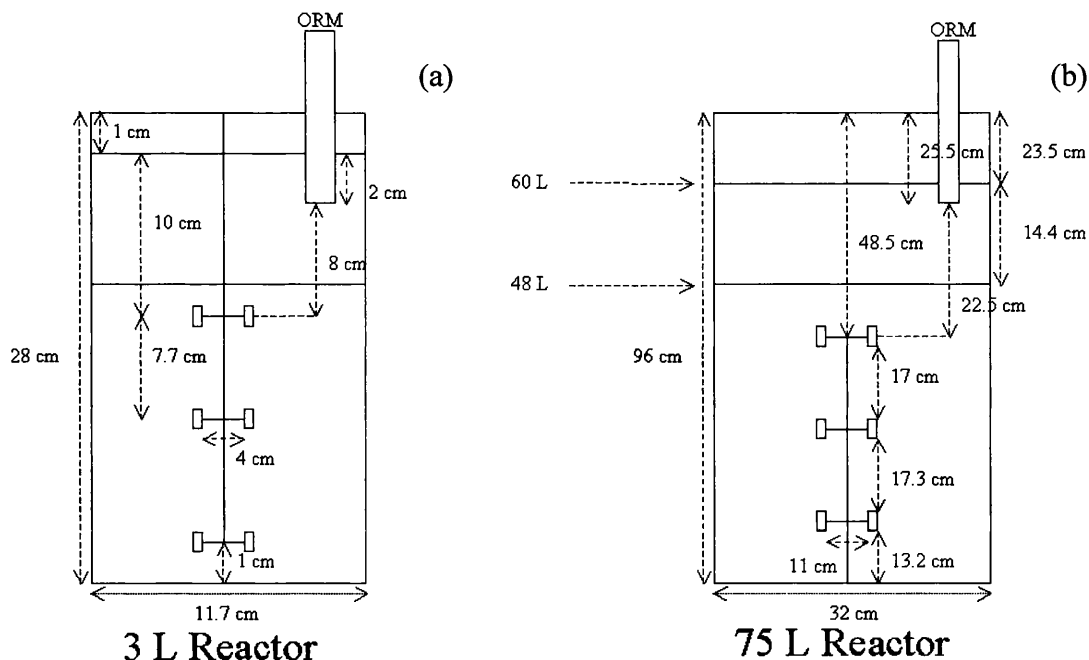


**Figure 2.1** Scale diagrams of the 3 L and 75 L vessels

### 2.6.2.2 Two-phase biotransformations of 1,3-DCB (3 L scale)

Biotransformation experiments in the 3 L reactor were conducted in a fume hood which was switched on for the duration for the experiment due to the flammable nature of toluene. Initially the 3 L reactor (Figure 2.1 (a)) was filled with 2.4 L pH 7 0.1 M phosphate buffer containing  $15 \text{ g}_{\text{ww}}\cdot\text{L}^{-1}$  of the biocatalyst, *Rhodococcus* R312. The ORM probe (Section 2.6.2.4) and the impeller were then placed in the vessel. Finally 600 mL of the toluene phase containing  $25 \text{ g}\cdot\text{L}^{-1}$  1,3-DCB was carefully poured on top of the aqueous phase (to prevent mixing) and the impeller switched on at the required speed. Samples of the mixture (1 mL) were subsequently removed at designated time intervals and immediately added to 250  $\mu\text{L}$  of 10 M  $\text{HCl}_{(\text{aq})}$  in a 2 mL Eppendorf tube to quench the transformation. The samples were then centrifuged at high speed for 10 minutes to separate the two liquid phases after which 100  $\mu\text{L}$  of the aqueous phase was removed, filtered through a 0.2  $\mu\text{m}$  syringe filter (Whatman, UK) and analysed for substrate and product concentrations by HPLC (Section 2.7.5). The vessel was cleaned and rinsed with deionised water between use.

### 2.6.2.3 Two-phase biotransformations of 1,3-DCB using an aqueous-toluene system (75 L scale)

The Inceltech (Wokingham, UK) LH SGI 75 L stainless steel solvent reactor was operated in a dedicated pilot plant facility designed according to both solvent and biological containment regulations. Initially the 75 L reactor (Figure 2.1 (b)) was filled with 48 L pH 7 0.1 M phosphate buffer containing  $15 \text{ g}_{\text{ww}}\cdot\text{L}^{-1}$  of the biocatalyst, *Rhodococcus* R312. Then 12 L of toluene phase containing  $25 \text{ g}\cdot\text{L}^{-1}$  1,3-DCB was carefully pumped into the top of the reactor from a connected side tank. The impeller was then switched on and set to the required speed. Samples of the mixture (5 mL) were subsequently removed at designated time intervals, immediately added to 1.25 mL of 10 M  $\text{HCl}_{(\text{aq})}$  in a 25 mL glass tube to quench the transformation and analysed by HPLC (Section 2.7.5). A positive pressure of nitrogen was maintained in the head space of the 75 L reactor during all biotransformation experiments to exclude oxygen that could combust on mixing

with toluene vapour. The 75 L reactor was maintained and cleaned as described in Appendix A1.

#### 2.6.2.4 On-line measurement of droplet size distributions

Drop size distributions were recorded using an Optical Reflectance Measurement (ORM) particle size analyser (MTS, Dusseldorf, Germany), which can provide *in-situ* and on-line measurements. The technique uses a laser beam which, through a lens, is focused a short distance in front of the probe tip, to a high intensity focal point and is rotated at a known velocity within the sample. When the rotating beam intercepts a drop, light is scattered back, through the optical system of the instrument, to a detector and the chord length of the drop is determined. Measurements over a period of time will produce a distribution of drop chord lengths. This is then transformed to a drop diameter distribution assuming that the drops have a particular shape. Since the laser beam is focused only at a short distance away from the instrument and does not pass through the dispersion, the measurements are not limited by the dispersed phase concentration (Hobbel *et al.*, 1991), a common problem with other light-based drop size analysers. As it can also be used *in-situ* it does not require any manipulation of the dispersion before the measurement. The technique has previously been used in various aqueous-organic systems, where it has been found to respond swiftly to any changes in process conditions which affect drop size (El-Hamouz and Stewart, 1996; Rimpler and Daniels, 1996; Simmons *et al.*, 2000).

The calibration of the ORM instrument was set using a drop size distribution calibration curve obtained with a Malvern Mastersizer 3600 (E-Type, Malvern Instruments Ltd., Worcester, UK). A series of standard size microspheres (Polymer Laboratories, UK) was then used to check the satisfactory calibration of the ORM instrument before use.

The probe tip was mounted vertically in approximately the same position in the 3 L and 75 L reactors (as shown in Figure 2.1). Droplet measurements were recorded from the start of agitation and subsequently every 60 seconds.

### 2.6.2.5 Droplet size measurement

Droplet size was analysed in the 3 L reactor shown in Figure 2.1 for an 80 % aqueous 20 % toluene two-phase system agitated between 600 and 900 rpm. In addition the affect of the addition of  $20 \text{ g.L}^{-1}$  1,3-dicyanobenzene with and without  $15 \text{ g.L}^{-1}$  *Rhodococcus* R312 was examined.

The vessel was initially filled with 2.4 L of either aqueous buffer or aqueous buffer containing biocatalyst. The impeller and probe were then secured in the vessel and the second phase, toluene was carefully poured onto the aqueous phase. The impeller was set to the required agitation rate and the timer was started.

In both reactors the two phases were mixed at the designated speeds for fifteen minutes then measurements were recorded. All 3 L non-biomass experiments were performed in triplicate with the maximum coefficient of variance for the measured steady-state mean drop size being 3%.

Droplet size was also analysed in the scaled-up 75 L reactor shown in Figure 2.1 over a range of speeds (see chapter 6).

### 2.6.2.6 Power consumption and phase continuity

Power consumption and phase continuity during agitation of single phase and two-phase liquid-liquid systems were measured in the 3 L vessel (Figure 2.1). For the two-phase experiments the phase continuity was also monitored using a micro-conductivity probe, made in-house, connected to an Alpha 800 conductivity meter (Courtcloud Ltd, UK). This minimised the disturbance of the flow field during measurements. For power consumption measurements the entire vessel was placed on a turntable supported on an air layer (air bearing technique). All experiments were performed in triplicate with the maximum coefficient of variance for the calculated power input being 2.7 %. During agitation the force,  $F$  (N), required to stop the rotation of the vessel on the air-bearing, was recorded with a load cell and the power input into the vessel was calculated according to Equation 2.1:

$$P=2\pi NRF \quad (2.1)$$

Where, P is the power consumption (W), N is the impeller rotational speed ( $s^{-1}$ ) and R is the distance (m) between the load cell and the centre of the tank.

For power measurements with the two-phase mixture the vessel was first filled with the aqueous phase followed by the organic phase at appropriate volume fractions and agitation was then started. Initial experiments had showed that 600 rpm was the minimum rotational speed necessary to ensure complete mixing of both phases at all the volume fractions tested. Power measurements were recorded for stirring speeds varying from 650 to 1100 rpm after 30 min to ensure that the system had reached steady state. Drop size measurements were recorded on-line from the commencement of agitation as described in Section 2.6.2.4. These confirmed that a steady-state droplet size had been reached.

## 2.7 ANALYTICAL TECHNIQUES AND PHYSICAL MEASUREMENTS

### 2.7.1 Off-line fermentation growth measurements: Optical density, Wet weight and Dry Cell weight determination

Optical density (OD) measurements were used to monitor cell growth during fermentation. Samples in a 1 mL disposable cuvette were measured at an absorbance of 600 nm in a Beckman DU640 spectrophotometer (Fullerton, CA, USA). Sterile fermentation medium was used as a blank. Accurate results were in the range 0-0.5, more concentrated samples were diluted with sterile fermentation medium. All measurements were performed in triplicate with the maximum coefficient of variance for the OD being 1 %. Biomass dry cell weights (dcw) was determined using pre-dried pre-weighed 1.5 mL eppendorf tubes. 1 mL samples were placed in the tube and spun in a Centaur Centrifuge for 20 minutes. The supernatant was discarded and the tube and pellet were dried in a high temperature oven for 24 hours and then weighed. The tube and pellet were then dried out for a further 24 hours to ensure that all water had evaporated. All

measurements were performed in triplicate with the maximum coefficient of variance for the dry cell weight being 8.5 %. Biomass wet weight (ww) was determined using a pre-dried pre-weighed 1.5 mL eppendorf tubes. 1 mL samples were placed in the tube and spun in a Centaur Centrifuge for 20 minutes. The supernatant was discarded and the tube and pellet inverted on blotting tissue. When no more water could be observed the tube and pellet were weighed. All measurements were performed in triplicate with the maximum coefficient of variance for the biomass wet weight being 7 %.

### 2.7.2 Density

Liquid density was determined by gravimetric analysis using 1 mL liquids volumes and a Mettler-Toledo AB54 mass balance (Leicester, UK) and the average of three measurements. All measurements were performed in triplicate with the maximum coefficient of variance for the density being 9 %.

### 2.7.3 Viscosity

Liquid viscosity was measured using a ‘cup and bob’ type Contraves Rheomat 115 (Contraves AG, Zurich, Switzerland) rheometer. The liquid was measured by pipetting the liquid into the ‘cup and bob’. The outer cylinder (cup) is stationary whilst the inner cylinder (bob) is rotated. The rheometer gives the braking torque exerted on the inner cylinder rotated in the dispersion. Which is a function of the shear stress and the shear rate exerted on the inner cylinder. These are related to the apparent fluid viscosity by Equation 2.2:

$$\mu = \frac{\tau I}{\gamma} \quad (2.2)$$

Where  $\mu$  is the apparent viscosity (Pa.s),  $\tau$  is the shear stress (Nm<sup>-2</sup>) per unit torque,  $I$  is the torque read out obtained from the rheometer control panel and  $\gamma$  is the shear rate (s<sup>-1</sup>). To simplify calculations the manufacturers of the rheometer have put together a series of values,  $\eta$  (Equation 2.3) where:

$$\eta = \frac{\tau}{\dot{\gamma}} \quad (2.3)$$

So the calculations reduce to Equation 2.4:

$$\mu = \eta l \quad (2.4)$$

The actual shear stress at each rheometer setting is determined by multiplying the manufacturers value of shear stress per unit torque by the torque reading at each setting. Liquid viscosity was investigated over a shear rate range from 24 to 3680 s<sup>-1</sup>. The final values recorded were the average of three measurements. The bob and cup were cleaned, rinsed and dried with deionised water between use. All measurements were performed in triplicate with the maximum coefficient of variance for the viscosity being 7.1 %.

#### 2.7.4 Surface tension and interfacial tension

Liquid surface tension and interfacial tension were measured using a Kruss K12 Processor Tensiometer (Palaiseau, France). Surface tension was determined using the Wilhelmy plate method. Liquid sample of ~40 mL were placed in wide glass vessel beneath a vertical Plate that was attached to the tensiometer balance and lowered onto the liquid surface. The force due to wetting was then measured by the instrument. Interfacial tension was determined by the dynamic Wilhelmy method. The plate was initially lowered onto a liquid of known surface then ~20 mL of the liquid was carefully poured over the first liquid without breaking the surface tension. The balance then raised the plate out of the interface between the two liquids and measured the wetting force. The final values recorded were the average of three measurements. All measurements were performed in triplicate with the maximum coefficient of variance for the surface and interfacial tension being 2.6 % and 2.5 % respectively.

### 2.7.5 Quantitative HPLC assay

Quantitative data on reaction samples were determined using HPLC. The substrate, 1,3-DCB, and products of the biotransformation, 3-cyanobenzamide and 3-cyanobenzoic acid, were separated and quantified using a Dionex HPLC system fitted with a 4.6 mm x 25 cm (5  $\mu$ m) Zorbax Rx-C8 reverse phase column. The mobile phase was a 1:1 v/v acetonitrile:phosphorylated water mixture pumped isocratically at a flow rate of 1 mL.min<sup>-1</sup>. Compound peaks were detected by UV absorbance at 230 nm, the retention times of the nitrile, amide and acid being 6.0, 3.3 and 4.2 minutes respectively. Control experiments showed that toluene was retained in the column and had to be washed out of the system. However [bmim][PF<sub>6</sub>] the ionic liquid did not interfere with the HPLC. All measurements were performed in triplicate with the maximum coefficient of variance for the density being 2.3 %.

Calibration of the system was performed before each use, using 1,3-DCB and 3-cyanobenzoic acid. Figure 2.2 shows typical calibration curves for the substrate and one of the products. The calibration curves of 1,3-DCB and 3-cyanobenzoic acid HPLC peak area were used to calculate substrate/product concentration as determined by Equations 2.5 and 2.6. As the amide product was not commercially available and due to the high level of similarity in molecular structure and calibration gradients, as well agreement with mass balance calculations the average of the two gradients was used to calculate the 3-cyanobenzamide concentration shown in Equation 2.7.

$$1,3\text{-DCB (g.L}^{-1}\text{)} = \text{Peak area}/10948800 \quad (2.5)$$

$$3\text{-cyanobenzoic acid (g.L}^{-1}\text{)} = \text{Peak area}/11637300 \quad (2.6)$$

$$3\text{-cyanobenzamide (g.L}^{-1}\text{)} = \text{Peak area}/11293050 \quad (2.7)$$

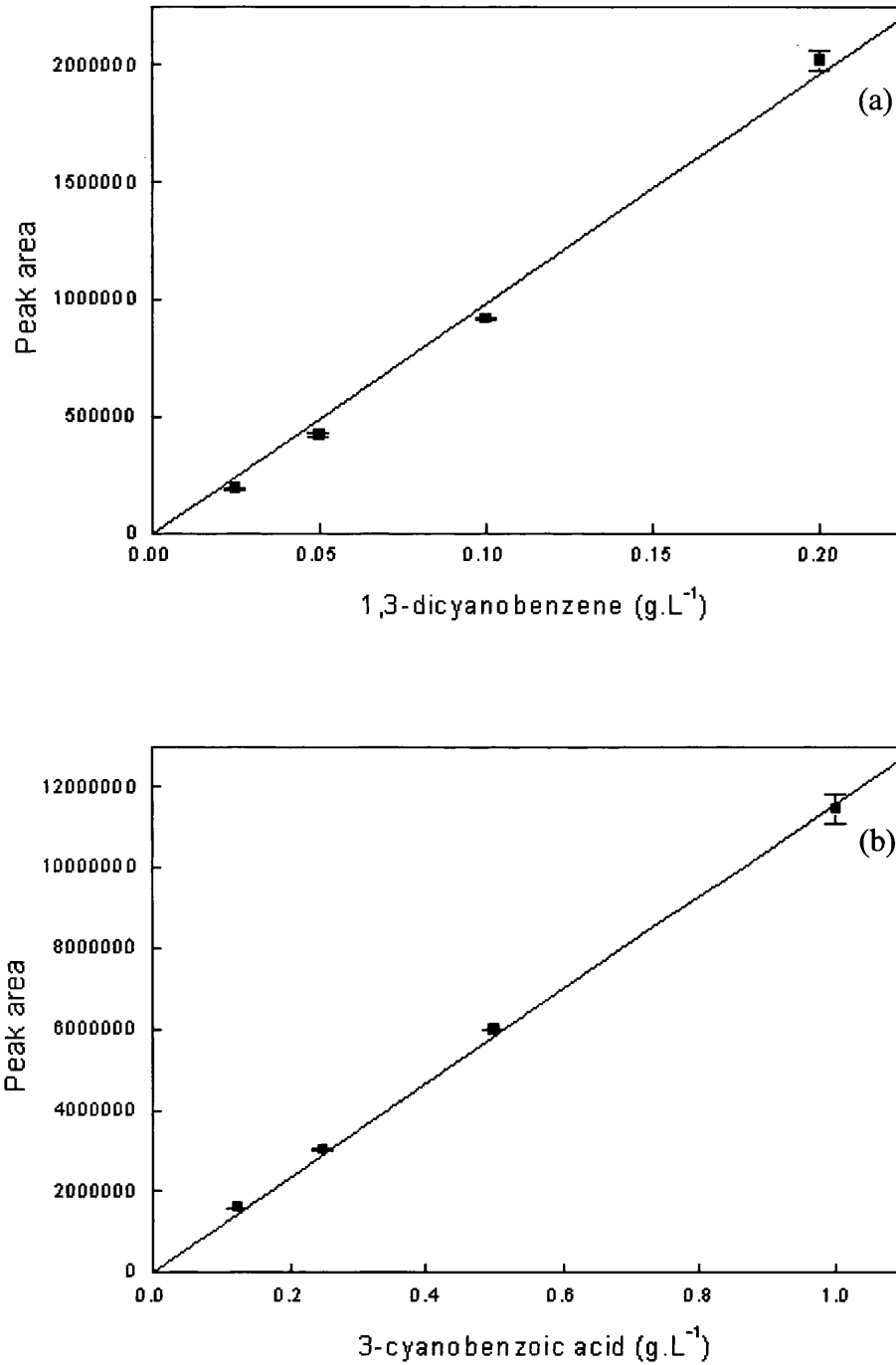


**Figure 2.2** (a) 1,3-DCB and (b) 3-cyanobenzoic acid calibration curves as measured by HPLC (Section 2.7.5).

# 3. BIOCATALYST SELECTION AND PRODUCTION

## 3.1 INTRODUCTION

In this chapter the selection and production of the chosen biocatalyst, *Rhodococcus* R312, are investigated. A number of fermentation processes for the production of *Rhodococci* with NHase activity are already described in the literature (Osprian *et al.*, 1999; Chartrain *et al.*, 1998; Nagaswa *et al.*, 1986) therefore the design and implementation of a new fermentation process was not necessary for this project. However, the large scale hydrodynamics and biotransformation studies described in Chapters 6 and 7 required significant quantities of biomass and so a fermentation process suitable for scale-up to 450 L scale had to be investigated.

Initially a defined media from earlier work was selected (Kerridge, 1995) but this proved to be difficult to use especially at large scale because some of the components were insoluble and fermentations were slow typically taking five days, and only achieved low cell concentrations ( $OD_{600}=1$ ). After further investigation a medium from other studies into the production of *Rhodococcus* R312 (Nagasawa *et al.*, 1986) was selected due to improved fermentation kinetics. This medium is referred to throughout this work as the Rich Growth Medium (RGM) and its components were described in detail in 2.2.1. However, this medium only achieved modest biomass production and hence a third medium was used to produce the biocatalyst in sufficient quantity. This medium is referred to as Tryptic Soy Broth (TSB) and is described in Section 2.2.2.

### 3.1.1 Objectives

This Chapter covers the selection of a suitable NHase biocatalyst for the biotransformation of 1,3-DCB. The Chapter will examine and utilise existing

fermentation process in the literature for the production of the chosen biocatalyst *Rhodococcus* R312. It will seek to establish a reproduceable and scaleable fermentation process with a sufficient biocatalyst yield and NHase activity. As mentioned in Section 1.3 the NHase enzyme of *Rhodococcus* R312 is known to be constitutively expressed and the activity is not influenced by the carbon and nitrogen source used in the growth medium (Tourneix *et al.*, 1986). This chapter therefore focuses on increasing the yield of biomass from the fermentation rather than increasing the enzyme activity through media selection

## 3.2 MATERIALS AND METHODS

### 3.2.1 Chemicals and microorganism

The microorganism storage and cultivation media used in this chapter are as described in Sections 2.1 and 2.2.

### 3.2.2 Experimental methods

*Rhodococcus* R312 was cultivated on a Rich Growth Medium (RGM) (2.2.1) and Tryptic Soy Broth (TSB) medium (Section 2.2.2) in the fermentations described in this Chapter. NHase and amidase activity assays were performed as described in Section 2.5. Biomass weight and optical density was determined as described in 2.7.1. The whole cell *Rhodococcus* biocatalyst was produced by shake flask (SF) fermentation and 7, 20 and 450 L stirred tank reactor (STR) fermentation as described in Section 2.3.1, 2.3.2.1, 2.3.3.2 and 2.3.2.3 respectively. The fermentation reactors were operated as described in section 2.3.2 with a series 2000 controller. The logging and set points were controlled using Bioview, a specialist fermenter control software package, produced by Adaptive Biosystems, Watford, UK. The oxygen uptake rate (OUR), carbon evolution rate (CER) and respiratory quotient (RQ) were measured online.

### 3.3 RESULTS AND DISCUSSION

#### 3.3.1 Biocatalyst selection and form

The first step in the development of a process for the biocatalytic production of 3-cyanobenzamide is necessarily the selection of an appropriate biocatalyst. Based on information in the literature (Cohen *et al.*, 1990) the regio-selective hydration of 1,3-dicyanobenzene catalysed by nitrile hydratase was chosen as the most direct route. Furthermore, the NHase from *Rhodococcus* R312 was selected since the enzyme is known to be regioselective, to act on aromatic substrates such as 1,3-DCB (Crosby *et al.*, 1994; Martínková *et al.*, 1995) and to be expressed constitutively (Bui *et al.*, 1984a). It is also known that the organism does not contain a nitrilase activity which might convert the starting substrate directly into the acid product in a single step (Kerridge, 1995).

Initially *Rhodococcus* R312 was cultivated on a rich growth medium in shake flasks as described in Section 2.2.1. This achieved satisfactory levels of biomass production of around 2.5-3.0 g<sub>ww</sub> l<sup>-1</sup> as shown in Figure 3.1. NHase activity was confirmed to be expressed constitutively with a maximum activity observed after 30 hours when the cells were in the deceleration phase. Use of a rich medium was preferable to a defined growth medium (Kerridge, 1995) which required over twice as long to achieve a similar biomass concentration.

Although the R312 strain does not possess a nitrilase activity it does, however, express an amidase activity that is the second enzyme in the two-step nitrile degradation pathway. This will further hydrate the desired 3-cyanobenzamide product to the corresponding acid. Figure 3.1 shows the activity of the amidase during the cultivation of the R312 cells. The enzyme is also expressed constitutively but at levels some 15 times less than the NHase (assuming a harvest time of 30 hours).

Since the aim of this process is the production of the amide product, the option of using an isolated form of the NHase was explored. This is the most direct process option available to overcome problems with further metabolism of the amide

which would occur in a whole cell biocatalyst. Bearing in mind the final application of the biocatalyst preparation, the direct immobilisation of NHase on

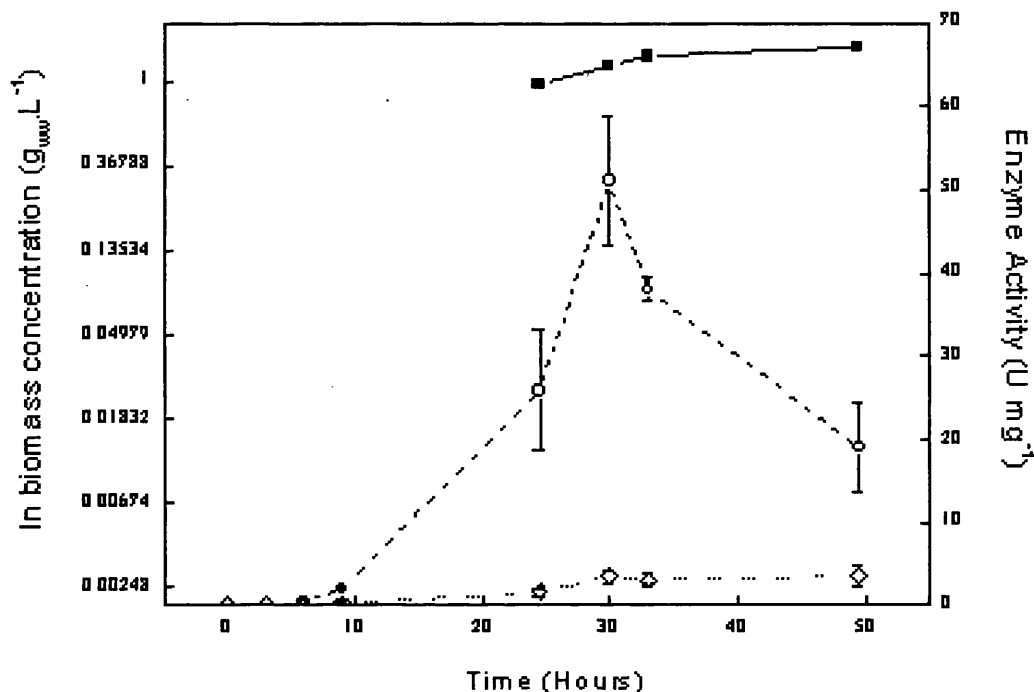


**Figure 3.1** Shake flask fermentation profile for growth of *Rhodococcus* R312 on RGM; (■) ln of biomass concentration, (○) NHase activity, (◇) amidase activity. Fermentation conditions as described in Section 2.3.1. NHase and amidase activity determined as described in Section 2.5.

Eupergit C was initially attempted. However, levels of enzyme release were low ( $<0.028$  U mg<sup>-1</sup> in terms of total cell protein) due to the thick, and mechanically robust, cell walls of the *Rhodococci* and no selective purification of the NHase activity over that of the amidase was found during fractional precipitation (data not shown). Literature data obtained during the purification of NHase for structural studies also suggested that the enzyme is rather unstable (Huang *et al.*, 1997). For these reasons the development of an immobilised NHase preparation was not pursued further.

The advantages of finally opting for the whole cell biocatalyst are that it can be produced more rapidly and cheaply than any immobilised enzyme preparation. In this case, however, it will be necessary to try to maximise the activity of the NHase while simultaneously minimising the activity of the amidase in order to prevent overmetabolism of the desired product. A further option would be to clone

just the NHase gene and to overexpress it in an alternative host but this is beyond the scope of the current investigation.

### 3.3.2 Shake flask fermentations

#### 3.3.2.1 Growth of *Rhodococcus* R312 on RGM

Initially *Rhodococcus* R312 was grown on the RGM (Section 2.2.1) in shake flasks as described in detail in Section 2.3.1. The RGMs primary carbon source was glucose, the secondary carbon sources and a nitrogen source was provided by the more complex ingredients special peptone, malt extract and yeast extract. The medium produced relatively low concentrations of biomass  $\sim 1.0 \text{ g}_{\text{dcw}} \cdot \text{L}^{-1}$  over 48 hours of growth with an optimum activity of  $\sim 50 \text{ U} \cdot \text{mg}^{-1}$  achieved at 30 hours (see Figure 3.1). Although this medium provided sufficient biomass for lab scale biotransformation experiments the process considerations for larger experiments required a medium that promoted greater growth.

#### 3.3.2.2 Growth of *Rhodococcus* R312 on TSB

The TSB medium (Section 2.2.2) was also investigated initially as a growth medium for the production of the biocatalyst due to its previous application in the production of other *Rhodococci* species (Chartrain *et al.*, 1998). In shake flask experiments, *Rhodococcus* R312 grew more rapidly on TSB compared to RGM, achieving a dry cell weight after 48 hours of  $\sim 5 \text{ g} \cdot \text{L}^{-1}$  compared to  $\sim 1 \text{ g} \cdot \text{L}^{-1}$  for RGM (data not shown). Due to the rapid growth of the organism on TSB and the high production of biomass ( $18 \text{ g}_{\text{ww}} \cdot \text{L}^{-1}$ ) the medium was selected for use in reactor fermentations. Although it is proprietary information the TSB medium is known to contain two main carbon sources: glucose ( $2.5 \text{ g} \cdot \text{L}^{-1}$ ) and Casein peptone ( $17 \text{ g} \cdot \text{L}^{-1}$ ) and a nitrogen source soy peptone ( $3 \text{ g} \cdot \text{L}^{-1}$ ) (containing amino nitrogen, total nitrogen, water with a typical carbon content of 41.8%) (Smith and Dell, 1990).

### 3.3.3 Scale-up of stirred tank reactor (STR) fermentations

TSB medium 7, 20 and 450 L STR fermentations were subsequently used to produce sufficient quantities of biomass for the large-scale biotransformations and reactor hydrodynamics described in Chapter 6 and Chapter 7. The reactors were scaled-up on the basis of constant tip speed (ND) rather than power per unit volume to reduce the impact of shear forces on the biocatalyst as a consequence of scale-up. However, it would be of interest in further investigations to compare the two fermentation scale-up criteria. Table 3.1 shows the reactor impeller diameter (D) and corresponding impeller speeds (N) used calculated on the basis of constant tip speed.

Reactor scale (L)	D <sub>i</sub> , impeller diameter (M)	Agitation rate (rpm)	N, impeller speed (s <sup>-1</sup> )
7	0.05	700	11.7
20	0.07	500	8.3
450	0.2	180	3

**Table 3.1** STR fermentation tip speed scale-up data.

#### 3.3.3.1 7 L Stirred tank reactor fermentation

The 7 L reactor was operated and inoculated as described in Section 2.3.2.1. Figure 3.2 (a) and (b) shows the change in biomass and activity for a typical 7 L fermentation. The biomass increased steadily during the fermentation and dry cell weight reached a maximum around  $\sim 7 \text{ g.L}^{-1}$  at 15 hours ( $\text{OD}_{600}=13.5$ ,  $28 \text{ g}_{\text{ww}}.\text{L}^{-1}$ ). Figure 3.3 (a) and (b) shows the corresponding online change in DOT, CER, OUR and RQ over the course of the fermentation. The OUR and CER values peaked at 8 hours ( $18$  and  $14 \text{ mmol.L}^{-1}.\text{h}^{-1}$ ) and the respiratory quotient remained at around 1 throughout the duration of the fermentation indicating that the organism had a steady supply of carbon source. The OUR/CER peak corresponded to the lowest DOT value of 45% at 8 hours indicating that this is the most rapid period of growth of the organism.

As can be seen from figure 3.2 (b) the rapid increase in growth corresponds strongly with an increase in NHase enzyme activity. Enzyme activity increases rapidly up to 8 hours, and it then remains approximately constant at  $\sim 90 \text{ U.mg}^{-1}$  until 19 hours when the stationary phase is reached at which point the activity starts to decrease. This is similar to a published 10 L *Rhodococcus* R312 fermentation that used a specific medium (Osprian *et al.*, 1999). Combining the information in graphs 3.2 and 3.3 indicated that the best time to harvest the fermentation to obtain the largest concentration of active cells is between 15 and 20 hours at this reactor scale. After this period the fermentation enters a stationary phase and appears to be entering the death phase at the end of the monitoring period at 25 hours.

### 3.3.3.2 20 L and 450 L stirred tank reactor fermentations

The 20 L and 450 L reactor was operated and inoculated as described in 2.3.2.2 and 2.3.2.3 respectively. Both STR reactors demonstrated a similar profile therefore only the profile for the final fermentation in the 450 L reactor is shown here. Figure 3.4 (a) and (b) shows the online change in DOT, CER, OUR and RQ over the course of the 450 L fermentation. Unlike the 7 L reactor the biomass growth and activity was not monitored continuously for the duration of the fermentation. The OUR and CER peaked at 8 hours ( $16$  and  $11 \text{ mmol.L}^{-1}.\text{h}^{-1}$ ) and the respiratory quotient remained at around 1 throughout the duration of the fermentation. The OUR/CER peak value corresponded to the lowest DOT value of 18% at 10 hours indicating that this is the most rapid period of growth of the organism. The divergence in OUR/CER in Figure 3.4 (b) was due a temporary technical problem with the monitoring equipment during the fermentation.

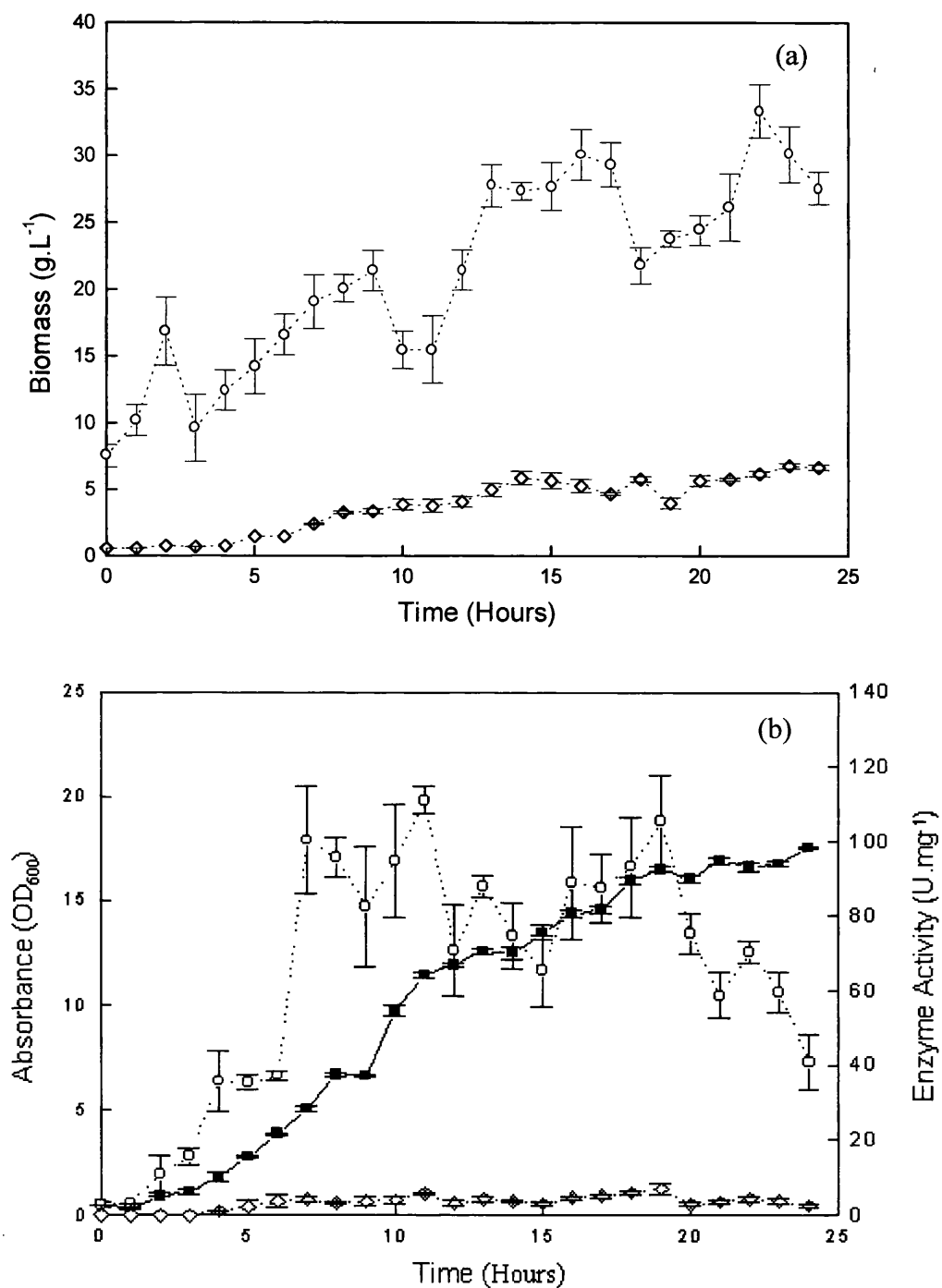


**Figure 3.2** Off-line measurements for 7 L fermentation profile for growth of *Rhodococcus* R312 on TSB. **(a)** (○) Biomass – wet weight (g.L<sup>-1</sup>), (◇) Biomass – dry cell weight (g.L<sup>-1</sup>); **(b)** (■) Optical density (OD<sub>600</sub>), (○) NHase activity, (◇) amidase activity. Fermentation conditions as described in Section 2.3.2.1. NHase and Amidase activity determined as described in Section 2.5. Error bars show the standard deviation over three replicate measurements.

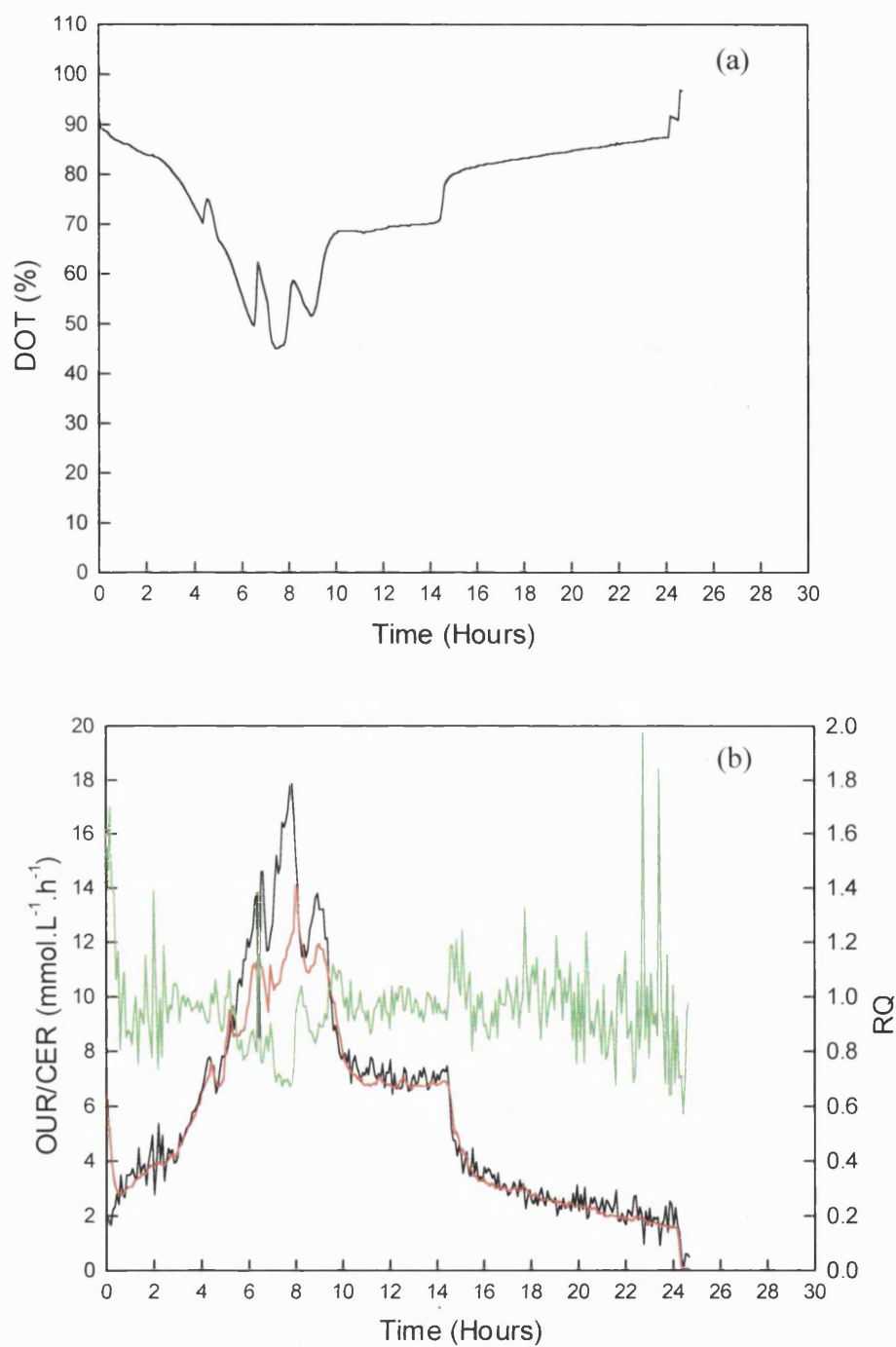


**Figure 3.3** On-line fermentation data for a 7 L TSB fermentation. **(a)** DOT (%) (-); **(b)** OUR (-), CER (-), RQ (-). Fermentation carried out as described in Section 2.3.2.1.

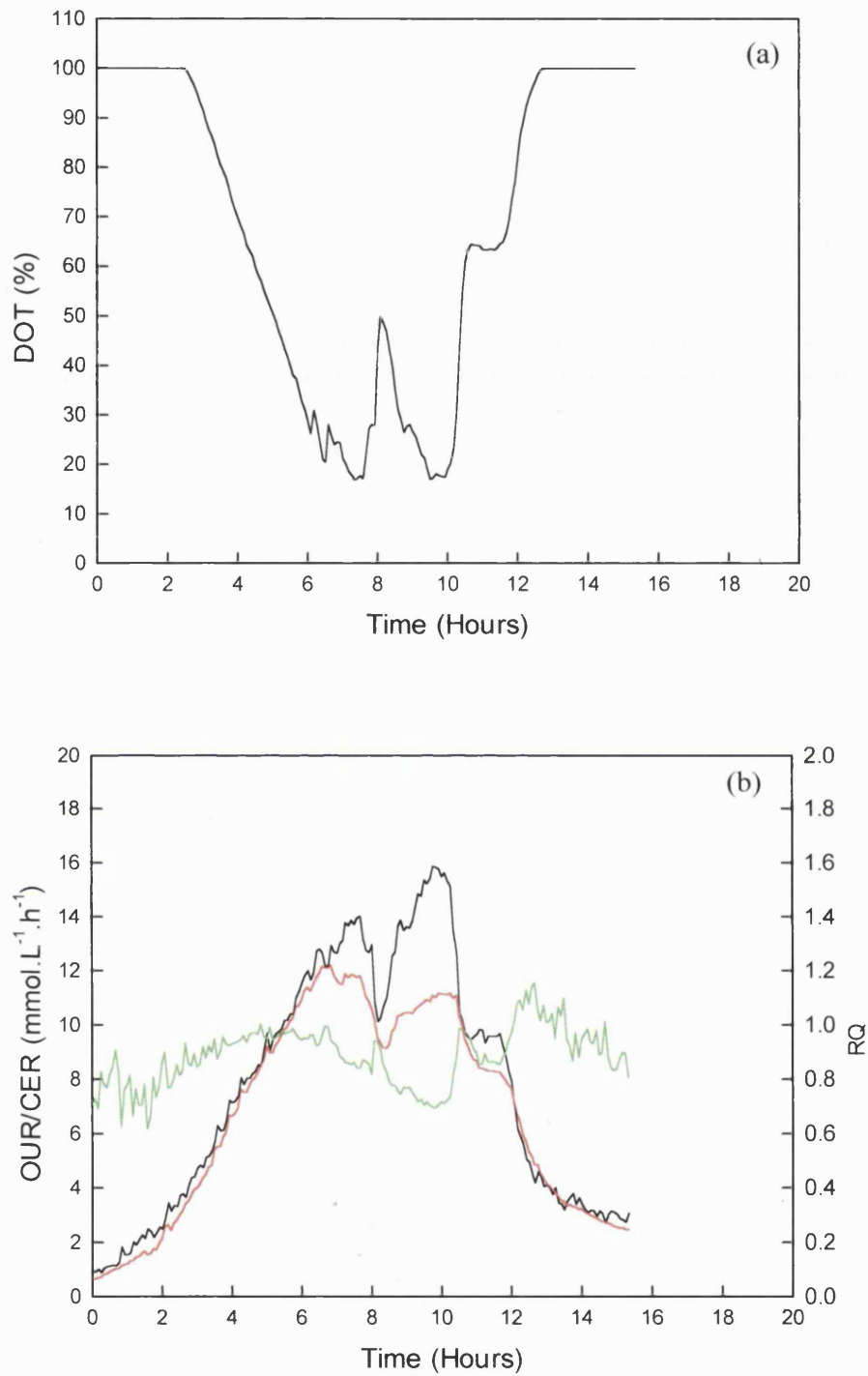


**Figure 3.4** On-line fermentation data for a 450 L TSB fermentation. **(a)** DOT (%) (-). **(b)** OUR (-), CER (-), RQ (-). Fermentation carried out as described in Section 2.3.2.3.

### 3.3.4 Biocatalyst recovery and suspension

After the biocatalyst was harvested from shake flask fermentations it was prepared for biotransformation by resuspension in buffer, pH 7 as described in 2.4.1. The biocatalyst was recovered from reactor fermentations and stored for experiments as described in 2.4.2. A total of 3.6 kg of solid biomass was recovered from the 450 L fermentation for use in drop size and biotransformation experiments in the 75 L reactor.

## 3.4 CONCLUSIONS

During the course of the project two different types of medium were used to produce the biocatalyst *Rhodococcus* R312. The first medium, rich growth medium (RGM) was based on an early rich medium (Nagasawa *et al.*, 1986) used in the production of the *Rhodococcus* R312. The second medium described, TSB was adapted from (Chartrain *et al.*, 1998) and was used to increase the production of biomass to  $\sim 7 \text{ g}_{\text{dcw}} \cdot \text{L}^{-1}$  with a view to producing as much biomass as possible for biotransformation and drop size experiments in the large scale 75 L reactor. The TSB fermentation was successfully scaled-up to 450 L on the basis of constant tip speed and the resulting biomass was recovered and processed for use (see Chapters 6 and 7).

One of the most important objectives of this chapter was to produce the maximum concentration of active cells for biocatalysis. Table 3.2 compares the biomass yields and enzyme activities of *Rhodococcus* R312 biomass produced by the different fermentations and media covered in this chapter. As mentioned in the introduction a number of fermentation processes for *Rhodococcus* R312 have already been described in the literature and it was beyond the scope of this thesis to fine tune or investigate a new process. Therefore existing methods were used and the key criteria of biomass dry cell weight and enzyme activity are described for each process in Table 3.2. As the data clearly shows TSB is the better medium for *Rhodococcus* R312 production compared to the RGM. Although cells produced by TSB media appear to have a more active NHase the trends and constraints of the two-phase process investigated in Chapters 4 and 5 will still

hold. Changing the medium from RGM to TSB resulted in a seven fold increase in biomass which made the production of biomass for the 75 L biotransformation experiments discussed in Chapter 7 practical. Scale-up on the basis of tip speed seemed to produce similar fermentation conditions at the 7 and 450 L scale. Both the OUR and CER values peaked at similar times and values. In the 7 L reactor OUR/CER peaked at 8 hours at 18 and 14 mmol.L<sup>-1</sup>.h<sup>-1</sup>, and in the 450 L reactor at 16 and 11 mmol.L<sup>-1</sup>.h<sup>-1</sup>. Biocatalyst recovered from the fermentations also had similar levels of activity as shown in Table 3.2. NHase is constitutively expressed in the biocatalyst so this is to be expected but the similarity of fermentation profiles and activities indicate that constant tip speed is a good ‘rule of thumb’ for scale-up of this particular fermentation.

Fermentation Process	Config.	Max. Biomass Conc. (g <sub>dcw</sub> .L <sup>-1</sup> )	Max. NHase activity (U.mg <sup>-1</sup> )	Max. amidase activity (U.mg <sup>-1</sup> )
2L, RGM	SF	~ 1	~ 50 (at 30 h)	~ 5 (at 48 h)
2L, TSB	SF	~ 7	~ 85 (at 13 h)	~ 5 (at 30 h)
7 L TSB	STR	~ 7	~ 115 (at 11 h)	~ 7 (at 19 h)
20 L TSB	STR	~ 5	~ 90 (at 14 h)	~ 5 (at 16 h)
450 L TSB	STR	~ 5	~ 100 (at 16 h)	~ 6 (at 16 h)

**Table 3.2** Fermentation process comparison data. SF: Shake flask; STR: Stirred tank reactor.

In the following chapter the kinetics and optimisation of the biotransformation, for the hydration of poorly water soluble aromatic dinitrile using biomass produced by fermentation will be examined.

## 4. PROCESS SELECTION AND OPTIMISATION FOR AROMATIC NITRILE HYDRATION

### 4.1 INTRODUCTION

#### 4.1.1 The importance of nitrile hydration

The biotransformation of nitriles is of interest because a number of industrially important organic compounds are currently produced from the amide or acid derivatives of nitrile starting materials (Jallageas *et al.*, 1980). Nitrile hydratase (NHase), as described in Section 1.2.3, is the most widely studied enzyme for the hydrolysis of nitriles to amides and has been shown to have applications in the industrial production of acrylamide and nicotinamide (Yamada and Kobayashi, 1996) as well as in waste water treatment (Kobayashi and Shimizu, 1998). In whole-cell biocatalysts, however, this enzyme is part of the two-step nitrile metabolism pathway (see lower half of Figure 4.1), the second enzyme being an amidase which hydrolyses the amide derivative of the nitrile substrate to the corresponding acid. Many species of micro-organism have been discovered that possess this two-step NHase-amidase pathway and/or a nitrilase enzyme that will hydrolyse a nitrile to the corresponding acid in a single step. Nitrile hydratase enzymes generally operate under mild conditions (20-30°C, pH 7-8) and can accept a broad range of aliphatic, aromatic and hetero-cyclic substrates which is important with regard to synthetic applications. They also exhibit regio- and stereo-selectivity (Cohen *et al.*, 1992; Beard *et al.*, 1993; Crosby *et al.*, 1994; Meth-Cohn and Wang, 1997b).

To date there has been little investigation into the design of large scale biotransformation processes for the hydration of poorly water soluble nitrile compounds. The biotransformation of such molecules using two-liquid phase systems was first conceived in the 1930's (Halling and Kvittingen, 1999). However, it was not until the 1970's that applications of this form of biotransformation were again investigated. Initial research focused on the biotransformation of steroids (Cremonesi *et al.*, 1975; Buckland *et al.*, 1975) but the technology was rapidly adapted for use with other poorly water soluble substrates (Klibanov *et al.*, 1975). With details of several industrial two-phase conversions published (Heath *et al.*, 1997; Chartrain *et al.*, 1998) and

complete process descriptions available for the production of diltiazem (Lopez and Matson, 1997) and 1-alkanols (Mathys *et al.*, 1999) two-phase biotransformations, after 30 years of research, represent a maturing process technology. New developments in the design and operation of such processes have recently been reviewed (Lye and Woodley, 2001).

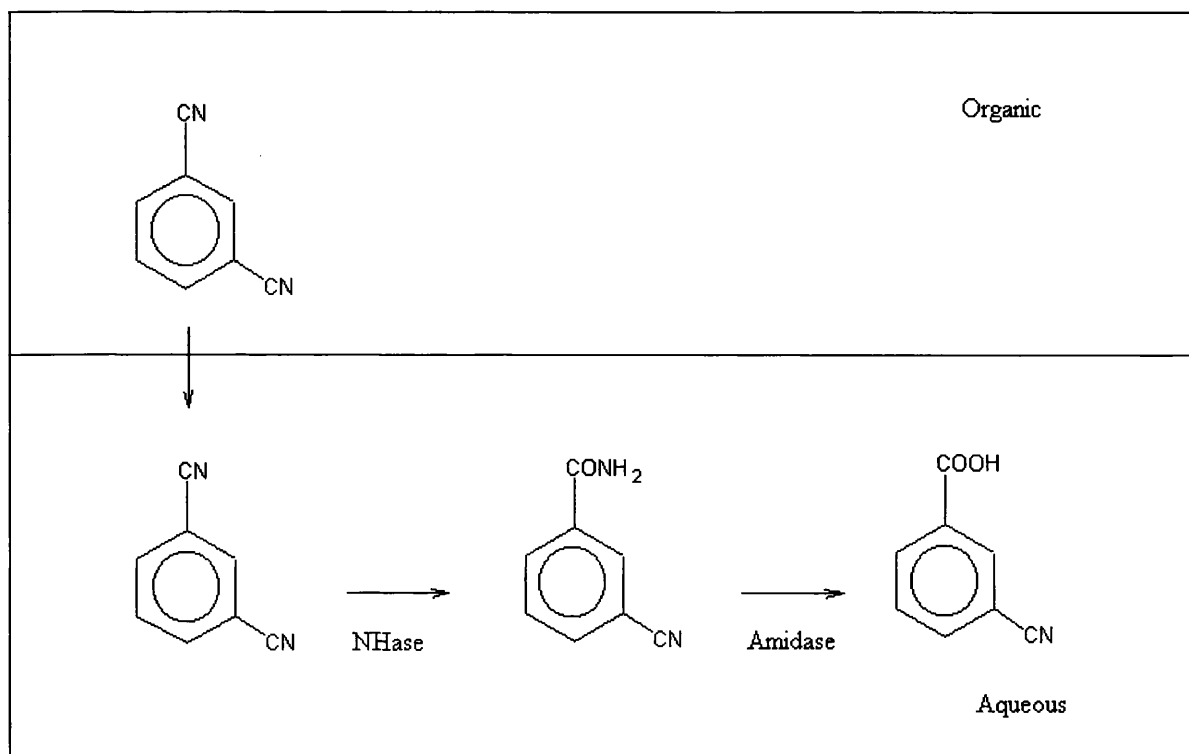


**Figure 4.1** Mass transfer and reaction steps in the two-phase biotransformation of 1,3-DCB using the two-step nitrile degradation pathway of *Rhodococcus* R312.

The use of two liquid-phase systems solves several process issues as described in section 1.2. Water immiscible organic solvents can act as a reservoir for poorly water soluble compounds and can be used to control substrate delivery to the aqueous phase in the case of inhibitory or toxic substrates. When favourable partition coefficients exist, products can also be extracted back into the solvent phase to overcome issues of product inhibition and aid product recovery. In these ways the productivity, or space-time yield, of the biotransformation can be greatly increased (León *et al.*, 1998). However, new problems arise such as solvent toxicity to the biocatalyst (Osborne *et al.*, 1990) and interfacial effects including stable emulsion formation as a result of biosurfactant production by the micro-organism (Schmid *et al.*, 1998). Experimental characterisation of a two-phase system however can provide an understanding of the interaction between its components: biocatalyst, organic solvent, substrate and products and environmental factors that have a direct affect on enzyme activity i.e. temperature and pH. By manipulating the

relative concentrations of these key system components a process can be optimised to maximise production of a given molecule and reduce the effects of solvent toxicity.

### 4.1.2 Objectives

This chapter follows on from the selection and production of the biocatalyst *Rhodococcus* R312 in Chapter. It covers the selection, characterisation and design of a two-phase process for the production of 3-cyanobenzamide (3-CB) from 1,3-dicyanobenzene (1,3-DCB). The aim is to establish a viable, well understood biotransformation for use as a model system to investigate the scale-up of a two-phase process in subsequent chapters. The production of the amide rather than the usual acid product has been deliberately chosen to aim for, as this would enable alternative chemistries to be used for the subsequent modification of the molecule. It also provides an interesting case study on the process engineering options available to overcome problems associated with competing enzyme activities (conversion of the 3-cyanobenzamide product into 3-cyanobenzoic acid (3-CA) by the amidase in this case). While molecular genetic techniques, such as cloning and overexpression of the NHase in an alternative host, will ultimately be more powerful they will be considerably slower to implement than any engineering solution. This initial selection and optimisation of the bioconversion was conducted following a systematic procedure for the design of biocatalytic processes (Woodley and Lilly, 1992). This is based upon analysis of the properties of the substrate and product molecules, the properties of the biocatalyst, the reaction conditions and the interactions between these factors. The properties and conditions of the reaction were combined in a process table (Table 4.2).

The work presented in this chapter has been published as: Cull, S.G., Woodley, J.M. and Lye, G.J. (2001) Process selection and characterisation for the biocatalytic hydration of poorly water soluble aromatic dinitriles. *Biocatalysis and Biotransformation*, **19**, 131-154.

## 4.2 MATERIALS AND METHODS

### 4.2.1 Chemicals and microorganism

The organic solvents and biological agents used in this chapter are as described in Section 2.1.

### 4.2.2 Experimental methods

Production of the whole cell *Rhodococcus* biocatalyst is as described in Section 2.3.1 using rich growth media (Section 2.2.1). Cells were processed for single and two-phase biotransformations as described in section 2.4.1. NHase and amidase activity assays were performed as described in Section 2.5. Single-phase biotransformations, amidase inhibition experiments and pH and temperature stability studies were performed as described in Section 2.6.1, 2.6.1.1, and 2.6.1.1.1 respectively. Solvent selection studies, two-phase activity studies with variable: biomass, phase volume ratio, initial substrate concentration and shake flask two-phase biotransformations were performed as described in Section 2.6.1.2.1, 2.6.1.2.3, 2.6.1.2.4, 2.6.1.2.5 and 2.6.1.2.6 respectively.

## 4.3 RESULTS AND DISCUSSION

### 4.3.1 Single-phase biotransformation of 1,3-DCB

Initially the single-phase transformation of 1,3-DCB by *Rhodococcus* R312 was conducted to examine the reaction kinetics. Figure 4.2 shows a kinetic profile for a single-phase biotransformation of 1,3-DCB as described in Section 2.6.1. The starting concentration of 1,3-DCB (~ 0.8 mM) is close to the aqueous saturation limit of the substrate. The profile shows that the substrate is rapidly taken up by the cells while the relative levels of NHase and amidase activity present in the cells (*c.f.* data in Figure 3.1) result in a peak of 3-cyanobenzamide production (within 30 seconds or less) followed by its gradual conversion into the acid by-product. The mass balance on substrate and product molecules at the end of the conversion process closed to within 2%. The low starting concentrations suggest that the space-time yield of such a process would be extremely low. Therefore a second phase in which higher starting concentrations of substrate could be dissolved would be of great benefit in making this biotransformation a more viable process.

Previous aqueous phase biotransformations of nitriles using a range of NHase-containing microorganisms and substrates have operated at mild conditions around pH 7-8 and 25-35 °C (Beard *et al.*, 1993; Cohen *et al.*, 1990; Cohen *et al.*, 1992; Crosby *et al.*, 1992; Crosby *et al.*,

1994; Kerridge, 1995; Martínková *et al.*, 1995; Blakey *et al.*, 1995; Meth-Cohn and Wang, 1997a; Meth-Cohn and Wang, 1997b; Eyal and Charles, 1990a; Eyal and Charles, 1990b). Similar experiments were conducted here but with the aim of finding conditions which optimised the activity of the NHase while minimising that of the amidase. Experiments to find the optimum pH and temperature for the production of 3-cyanobenzamide were conducted as described in Section 2.6.1.1.1. The results shown in Figure 4.3 confirm the optimum NHase activity for 1,3-DCB hydration is in the range 20-30 °C but also show that the amidase enzyme has an optimum activity at a higher temperature of around 40 °C. Further experiments investigating the effect of pH exposure on the activity of each of the enzymes (Figure 4.4) indicate that the optimum pH for NHase activity is in the range 7-8 while there is no distinct optimum for the amidase. Clearly a biotransformation operated in the pH range 7-8 and at a temperature of 20-30 °C would appear to favour the NHase activity and hence production of the amide product.

A further solution to overcome the activity of the amidase and result in an increased final concentration of 3-cyanobenzamide would be to specifically inhibit the activity of the amidase enzyme. Literature data suggested urea as a potential inhibitor (Jakoby and Fredericks, 1964). However, in the case of single-phase transformations of 1,3-DCB (Section 2.6.1.1) with the whole cell *Rhodococcus* R312 biocatalyst used here, urea appeared to have no effect on the amidase activity over the concentration range of 0.5-50 mM.

### 4.3.2 Two-phase biotransformation of 1,3-DCB

Because of the low aqueous solubility of the starting substrate the option of using a two-phase biotransformation process was explored (Faber, 1997; Van Sonsbeek *et al.*, 1993; Lye and Woodley, 2001). The addition of a second organic phase to the system would facilitate the dissolution of much higher concentrations of substrate and hence improve the space-time yield of the process. The use of a two-phase biotransformation process initially requires the selection of an appropriate solvent and necessitates investigation of substrate mass transfer rates and interfacial effects.

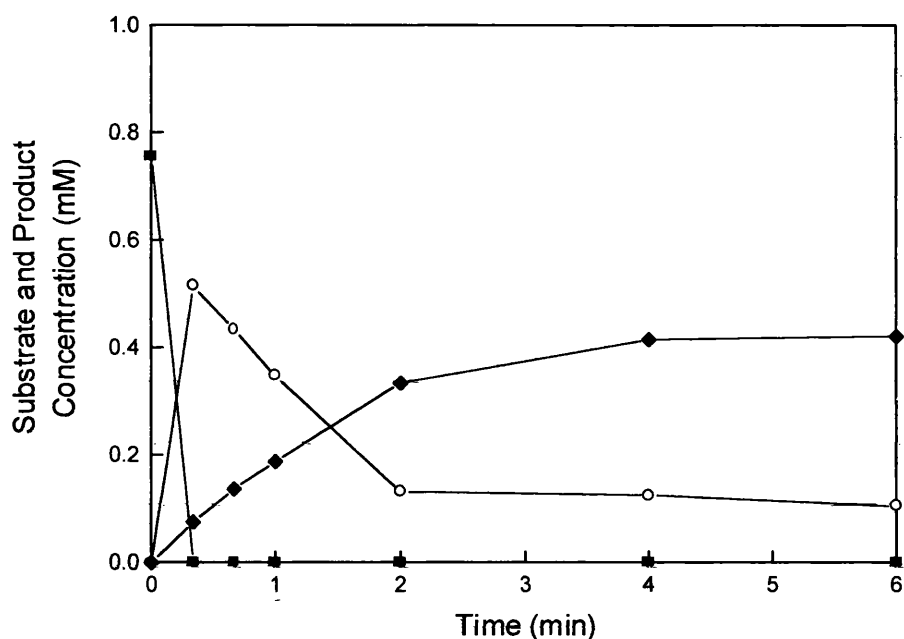


**Figure 4.2** Single-phase *Rhodococcus* R312 biotransformation kinetics; (■) 1,3-DCB, (○) 3-CB and (◆) 3-CA concentration. Cells produced as described in Section 2.3.1 and harvested at 30 hours. The reaction was initiated by the addition of 1,3-DCB (final concentration  $0.1 \text{ g}\cdot\text{L}^{-1}$ ) to  $50 \text{ g}_{\text{ww}}\cdot\text{L}^{-1}$  cells. Biotransformation conditions are as described in Section 2.6.1.

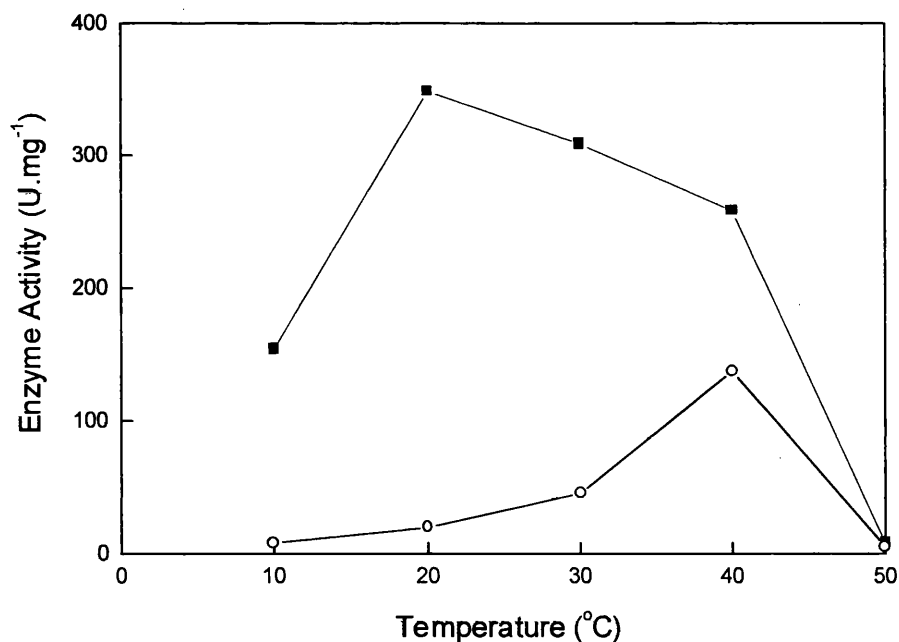


**Figure 4.3** Single-phase NHase and amidase activities as a function of temperature; (■) NHase activity, (○) amidase activity. Cells produced as described in Section 2.3.1 and harvested at 30 hours. Activity measurements performed at pH 7 as described in Section 2.6.1.1.1.

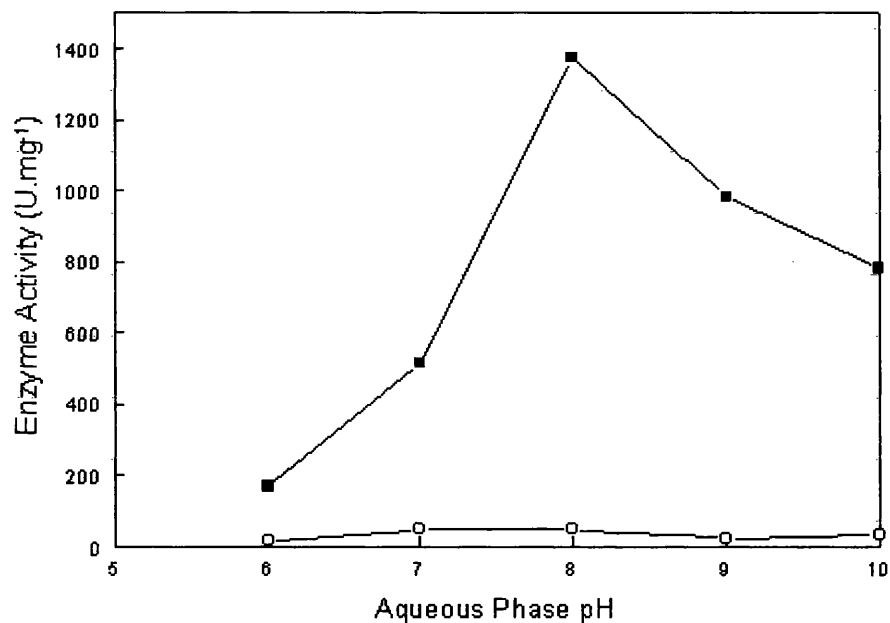


**Figure 4.4** Single-phase NHase and amidase activities as a function of pH; (■) NHase activity, (○) amidase activity. Cells produced as described in Section 2.3.1 and harvested at 30 hours. Activity measurements performed at 30 °C as described in Section 2.6.1.1.1.

#### 4.3.2.1 Solvent selection

Previous work on solvent selection strategies indicate that the ideal solvent for biphasic biotransformations is biocompatible, non-hazardous, non-biodegradable and has a high capacity for both substrate and product molecules (Bruce and Daugulis, 1991). In this case, however, the products of the conversion (3-CB and 3-CA) are more water soluble than the substrate hence the main criteria for solvent selection are biocompatibility, safety and high substrate saturation concentrations. Biocompatibility is related to the critical concentration of a particular solvent in the cellular membrane (León *et al.*, 1998; Osborne *et al.*, 1990). A concentration below this point will have relatively little effect on activity while a concentration above it is toxic and will result in damage to the biocatalyst and an eventual loss of activity. Biocompatibility is most commonly described by the Log P parameter (Laane *et al.*, 1987). This is the partition coefficient of the solvent in an octanol-water two-phase system and has an empirical correlation with the retention of cellular activity (Osborne *et al.*, 1990). Generally solvents with Log P values below 2 are hydrophilic, partition strongly into the cell walls of bacteria and rapidly deactivate the catalyst. Solvents with Log P values above 4 are hydrophobic and are unlikely to cause deactivation (Vermuë *et al.* 1993). Solvents with intermediate Log P values may be used,

but the degree of biocompatibility depends on the concentration and characteristics of the particular biocatalyst/solvent combination.

In order to select a suitable solvent for the biotransformation of 1,3-DCB a number of commonly used organic solvents were chosen from the literature and the saturation concentrations of the substrate in these determined. The results are shown in Table 4.1. Toluene was eventually selected for further use because it has a relatively high Log P value of 2.9 and a reasonable 1,3-DCB saturation concentration of  $\sim 30 \text{ g l}^{-1}$ . This is nearly 90 times higher than that which could be achieved in a single aqueous phase system. Other solvents such as 1,2-dichloroethane and dichloromethane clearly dissolve even higher concentrations of 1,3-DCB but are either chlorinated, thus presenting serious safety and environmental issues, or have low Log P values and could severely damage the biocatalyst.

Solvent	Saturation concentration of 1,3-DCB ( $\text{g.L}^{-1}$ )	Log P value
Chloroform	68	2
Dichloromethane	100	1.3
Ethyl acetate	40	0.7
Hexane	Negligible	3.8
Hexadecane	Negligible	8.8
Octanol	Negligible	3.1
1,2-Dichloroethane	60	3.6
Pristane	Negligible	Unknown
Silicone oil	Negligible	Unknown
Toluene	30	2.9

**Table 4.1** Log P values and 1,3-DCB saturation concentrations of the solvents screened for use in a two-phase biotransformation process. Solvent saturation concentrations were determined as described in Section 2.6.1.2.1 and Log P values were derived from the literature (Vermue *et al.*, 1993 and Laane *et al.*, 1987) where possible.

#### 4.3.3.2 Operating parameters for the two-phase process

The mass transfer and reaction steps involved in the two-phase biotransformation of 1,3-DCB were previously indicated in Figure 4.1. To aid in the design of the process all characteristics of the biotransformation were recorded in a process constraints table (Table 4.2). This table

BIOTRANSFORMATION DESIGN DATA AND PROCESS CONSTRAINTS			
(1) SUBSTRATE (S) AND PRODUCT (P <sub>1</sub> AND P <sub>2</sub> ) PROPERTIES	1,3-dicyanobenzene (S)	3-cyanobenzamide (P <sub>1</sub> )	3-cyanobenzoic acid (P <sub>2</sub> )
Molecular formula	C <sub>8</sub> H <sub>4</sub> N <sub>2</sub>	C <sub>8</sub> H <sub>6</sub> N <sub>2</sub> O	C <sub>8</sub> H <sub>5</sub> NO <sub>2</sub>
Molecular weight (g)	128	146.15	147.13
Boiling/melting point (°C)	ND/161	ND/230	ND/217
Solubility in water (g.L <sup>-1</sup> )	0.341	15.4	2.31
Solubility in toluene (g.L <sup>-1</sup> )	~30	~0	~0
Partition coefficient (K <sub>1,3-DCB</sub> (= C <sub>aq</sub> /C <sub>tol</sub> ))	0.025	~ND	~0
(2) ENZYME AND REACTION PROPERTIES	Nitrile Hydratase		Amidase
<b>(2.1) Reaction characteristics:</b>			
Equilibrium position (effect of T°C, pH, etc.)	ND		ND
Acid/base production	None		Produces acid product and NH <sub>3</sub>
Water consumption/production	Consumption		Consumption
Gas consumption/production	None		NH <sub>3</sub> production
Heat evolution	Negligible		Negligible
<b>(2.2) Biocatalyst (B) characteristics:</b>			
Single/multiple enzyme transformation	Single		Single
Cofactor requirements	None		None
Enzyme location (e.g. membrane-associated)	Cytosol		Cytosol
Biocatalyst requirements for water	Stoichiometric		Stoichiometric
<b>(2.3) Interaction between B, S and P:</b>			
Substrate/Product inhibition	Amidase competitively inhibited by 3-CB (Fournaud <i>et al.</i> , 1998)		
Activity (dependence on pH, T°C etc.)	Optimal activity achieved at 12-50 g.L <sup>-1</sup> substrate, pH 7-8, 20-30°C		
Substrate/product toxicity	None observed		
Stability (dependence on pH, T°C etc.)	Substrate and product are most stable at pH 7-8 and 20-30°C		

ND: Not determined/unknown.

**Table 4.2.** Process constraints table for the hydration of 1,3-DCB by the whole cell NHase of *Rhodococcus* R312. Substrate partition coefficient was determined as described in Section 2.6.1.2.1. Values for interaction between B, S and P taken from activity and optimisation data shown in Figures 4.3-4.9.

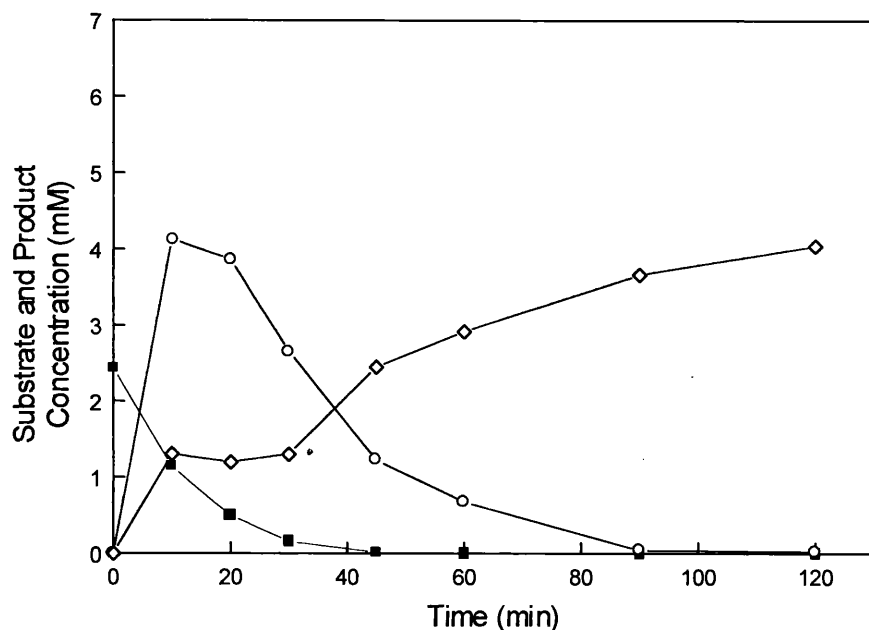


**Figure 4.5** Two-phase *Rhodococcus* R312 biotransformation kinetics for a mass transfer limited system; (■) 1,3-DCB, (○) 3-CB, (◇) 3-CA. Cells produced as described in Section 2.3.1 and harvested at 30 hours. The biotransformation was performed as described in Section 2.6.1.2.6 with a phase volume ratio of 0.1 and initial [1,3-DCB] concentration in the toluene phase of  $20 \text{ g.L}^{-1}$ . The biocatalyst concentration was  $50 \text{ g}_{\text{ww}}\text{.L}^{-1}$ .

contains all the known information on the process including the substrate and product properties and biocatalyst properties.

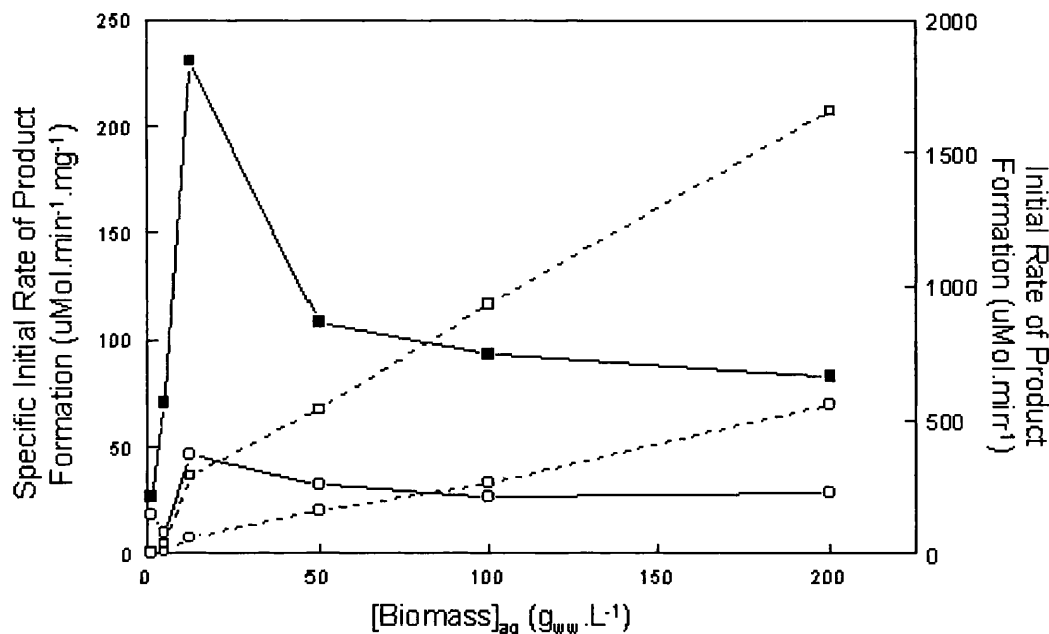
The most important parameters to investigate regarding the operation and performance of such a process include the biocatalyst concentration present in the aqueous phase, the phase volume ratio used ( $V_r = V_{\text{org}}/V_{\text{aq}}$ ) and the initial concentration of substrate in the toluene phase. These three parameters have a direct effect on 3-cyanobenzamide production and must be optimised in the process. A typical, though non-optimised, kinetic profile for the two-phase bioconversion of 1,3-DCB is shown in Figure 4.5. The 1,3-DCB initially partitions into the aqueous phase to a level close to the saturation concentration. This is then taken up by the cells and the profiles of amide and acid production are seen to be similar to those observed in the single-phase transformation (Figure 4.2).

In the two-phase process 1,3-DCB will continuously partition into the aqueous phase to replace that which is hydrolysed. For the transformation shown in Figure 4.5, however, the rapid decline in the aqueous phase concentration of the substrate suggests that the rate of 1,3-DCB mass

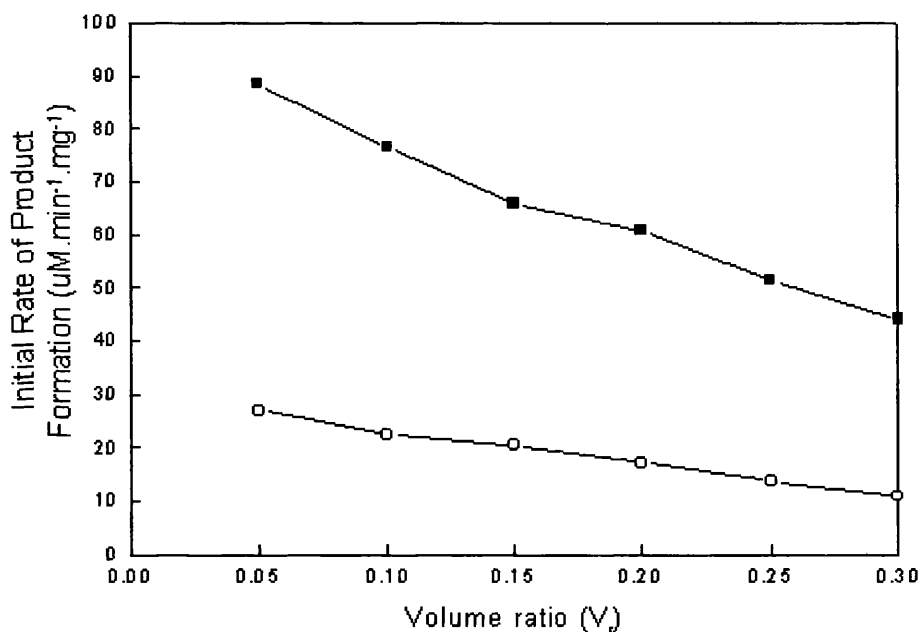
transfer is significantly less than the rate of its conversion by the NHase *i.e.* under these conditions the biotransformation is mass transfer limited.

Figure 4.6 shows the overall initial rates of amide and acid production (dashed lines) in the two-phase process as a function of the biocatalyst concentration. This rate data was derived from the aqueous phase concentration-time profiles of amide and acid production which, in each case, were similar to those observed in Figure 4.5. It is clear that the initial rate of production of both molecules increases in proportion to the amount of biocatalyst present. The solid lines in Figure 4.6, however, show the same data plotted on a specific basis per unit mass of biocatalyst. In this way it becomes clear that the most efficient use of the biocatalyst activity is made at concentrations around  $12 \text{ g}_{\text{ww}}\cdot\text{L}^{-1}$  (equivalent to  $2.4 \text{ g}_{\text{dcw}}\cdot\text{L}^{-1}$ ), an important issue when considering that a scaled-up process will require significant production of biocatalyst. At higher biocatalyst concentrations the concentration of substrate measured in the aqueous phase rapidly fell to levels well below those expected based on the substrate partition coefficient ( $K = C_{\text{aq}}/C_{\text{org}} = 0.025$  at  $20 \text{ g}\cdot\text{L}^{-1}$  1,3-DCB). This indicates that at all biocatalyst concentrations greater than  $12 \text{ g}_{\text{ww}}\cdot\text{L}^{-1}$  the system will be mass transfer limited. Conversely, at biocatalyst concentrations below  $12 \text{ g}_{\text{ww}}\cdot\text{L}^{-1}$  the system was found to be kinetically controlled.

The effect of the phase volume ratio on the initial rate of product formation per unit mass of biocatalyst is shown in Figure 4.7. The volume ratio was varied over a relatively narrow range in which it could be ensured that the solvent droplets would remain as the dispersed phase (Lilly and Woodley, 1985). The graph clearly shows that both amide and acid production is reduced at high values of  $V_r$ . This is probably due to either a general solvent toxicity effect, which increases in proportion to the amount of toluene present, or damage resulting from the interaction of the *Rhodococcus* R312 cells with the aqueous-toluene interface, the area of which will also increase with the phase volume ratio. At low volume ratios (0.05-0.15) measurement of the aqueous phase 1,3-DCB concentration over time again showed that the systems were mass transfer limited. This could be due to either the decreased interfacial area available for mass transfer at low  $V_r$  values or the 'dilution effect' on the substrate as it passes into the aqueous phase (Chae and Yoo, 1997). Based on these considerations it would appear that the most suitable  $V_r$  at which to operate the process would be in the range 0.15-0.2.



**Figure 4.6** Initial rates of amide and acid production as a function of biocatalyst concentration in a aqueous-toluene two-phase system. Rate values expressed on both an overall basis [(- □ -) amide, (- o -) acid] and a specific basis per gram wet weight of biomass [(■) amide, (○) acid]. Cells produced as described in Section 2.3.1 and harvested at 30 hours. The experiments were performed as described in Section 2.6.1.2.3.



**Figure 4.7** Initial specific rates of amide and acid production as a function of phase volume ratio ( $V_r = V_{org}/V_{aq}$ ); (■) amide, (○) acid. Cells produced as described in Section 2.3.1 and harvested at 30 hours. The experiments were performed as described in Section 2.6.1.2.4 with an initial [1,3-DCB] concentration in the toluene phase of 20 g.L<sup>-1</sup>. The biocatalyst concentration was 50 g<sub>ww</sub>.L<sup>-1</sup>.

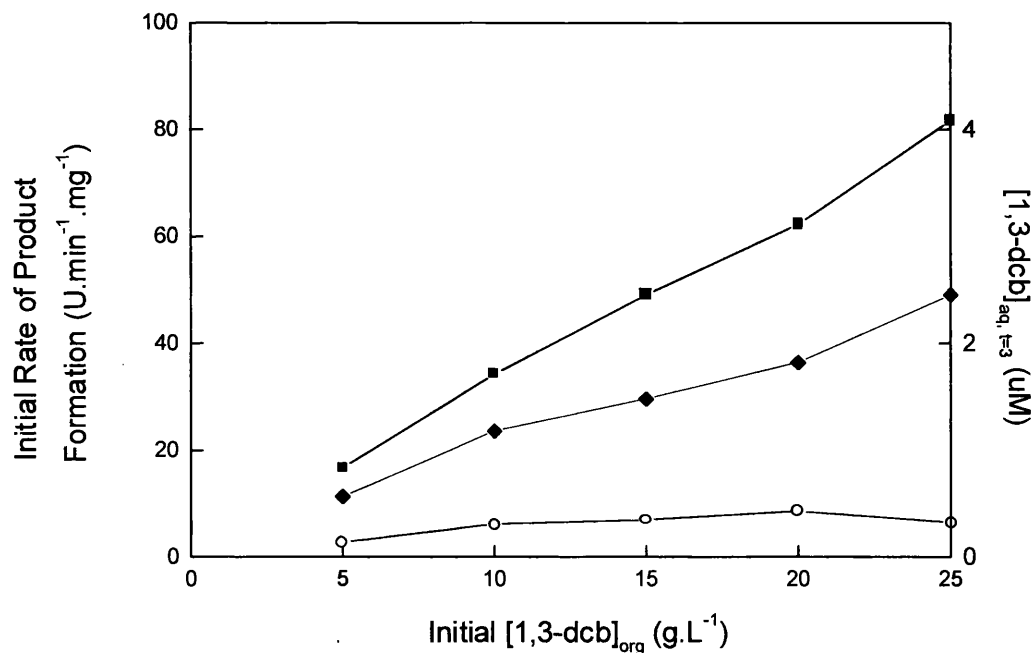


**Figure 4.8** Initial specific rates of amide and acid production as a function of initial substrate concentration in the toluene phase; (■) amide, (○) acid. The corresponding equilibrium concentrations of substrate, 1,3-DCB, in the aqueous phase (◆) are also shown. Cells produced as described in Section 2.3.1 and harvested at 30 hours. The experiments were performed as described in Section 2.6.1.2.5. The initial biocatalyst concentration was 50 g<sub>ww</sub>.L<sup>-1</sup>.

Figure 4.8 shows the effect of the initial substrate concentration in the organic phase on the initial rates of product formation. The maximum organic phase concentration of substrate investigated, 25 g.L<sup>-1</sup>, is already close to the solubility limit of the molecule in toluene (Table 4.2). Also plotted is the corresponding aqueous phase concentration of 1,3-DCB measured at equilibrium in a cell-free system; this represents the maximum substrate concentration to which the cells in the aqueous phase would be exposed during the course of a two-phase transformation. As can be seen from Figure 4.8 the rate of amide formation increases in direct proportion to the substrate concentration present in the aqueous phase (linear regression on a plot of the initial rate of amide formation against [1,3-DCB]<sub>aq</sub> gave a correlation coefficient of 0.997). This would suggest that the substrate is not toxic or inhibitory to the NHase enzyme over the concentration range investigated. It also confirms that the decrease in activity with  $V_r$  seen in Figure 4.7 is most probably due to the toxicity of the toluene. Interestingly, however, the initial rate of acid production is seen to be largely independent of the substrate concentration present in either the aqueous or organic phases. This is probably due to inhibition of the amidase by the increasing concentrations of 3-cyanobenzamide formed in the cells during the transformation (Fournaud *et al*, 1998; Maestracci *et al*, 1988). In this case operation at high initial 1,3-DCB

concentrations will kinetically favour amide production. Finally, at initial substrate concentrations of less than 10 g.L<sup>-1</sup> mass transfer limitations were observed due to the low driving force available for mass transfer (data not shown). Based on these considerations it would appear that an initial substrate concentration in the range 10-25 g.L<sup>-1</sup> would provide suitable operating conditions.

### 4.3.3 Biotransformation process design and operating conditions

Previous work on a wide range of transformations led to the identification of a systematic design procedure for biocatalytic processes (Woodley and Lilly, 1992). This was based upon analysing the properties of each component in the system and their interactions in a series of defined experiments. Table 4.2 indicates the key features of the design procedure and summarises the results obtained with the current biotransformation. Clearly the major process constraints are the low aqueous solubility of the substrate molecule, which led to the selection of a two-phase process, and the need to minimise the activity of the amidase in order to maximise production of the desired 3-cyanobenzamide product.

Once the process has been defined, in this case a whole-cell catalysed conversion in a two-liquid-phase reactor, it is necessary to rapidly establish suitable operating conditions or a 'window of operation' (Woodley and Titchener-Hooker, 1996). A window is an area of operational space determined by the constraints of the bioprocess whether they are biological, physical, chemical, engineering or economic. Although the window does not define the optimum conditions for a process they place the process in an area that is close to this without the need for extensive factorial experiments which can be expensive and time consuming. Given the data presented in Figures 4.6-4.8 it is logical to define the operating window for the current process based on substrate concentration, catalyst concentration and phase volume ratio as all these parameters have a significant effect on the productivity of the transformation. These parameters were also the important variables in an operating window developed for the production of *cis*-glycols in a similar two-liquid phase process (Collins *et al.*, 1995).

Figure 4.9 shows a three-dimensional operating window for the two-phase hydration of 1,3-DCB by the whole cell NHase biocatalyst. The scales on the axes represent the ranges over which each variable was investigated. The area within the rectangular window defines operating

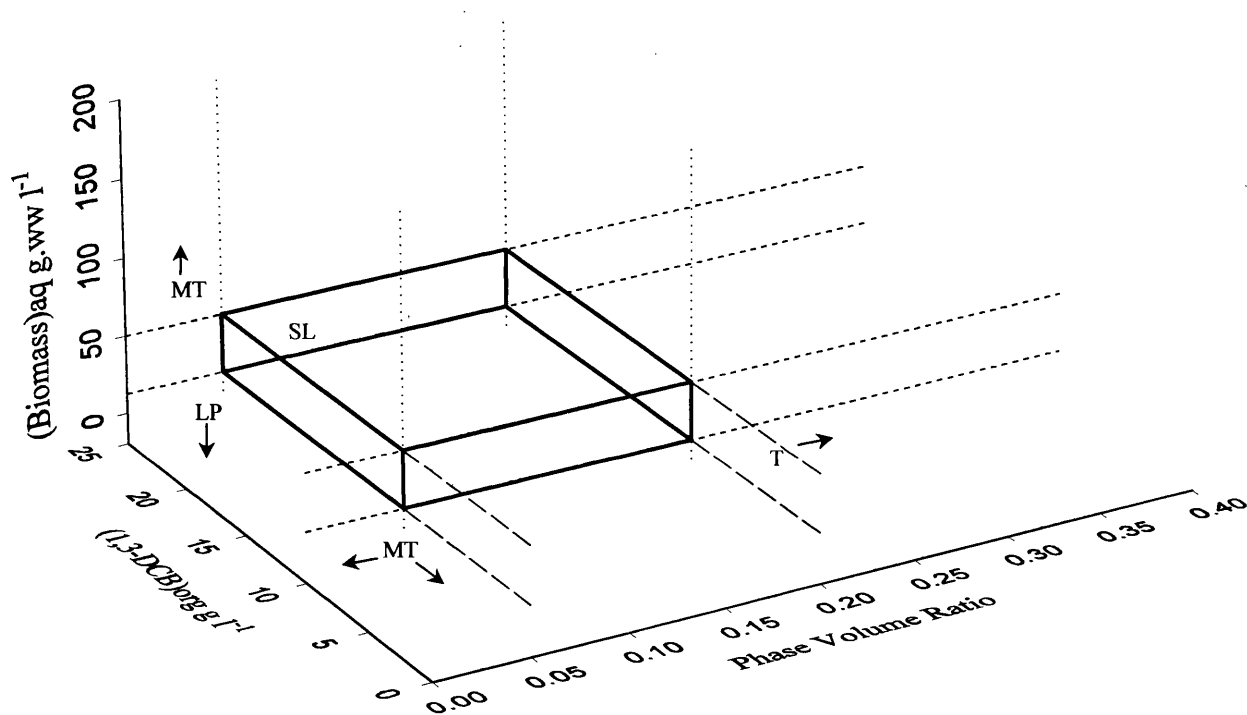


**Figure 4.9** Operating window for the *Rhodococcus* R312 catalysed transformation of 1,3-DCB in an aqueous-toluene two-phase system at pH 7 and 30°C. Axes indicate range over which variables were investigated: (MT) substrate mass transfer limitation; (LP) low amide productivity ( $< 30 \mu\text{mol min}^{-1} \text{mg}^{-1}$ ); (T) toluene toxicity limitation; (SL) substrate solubility limit. The window was compiled from data shown in Figures 4.6-4.8.

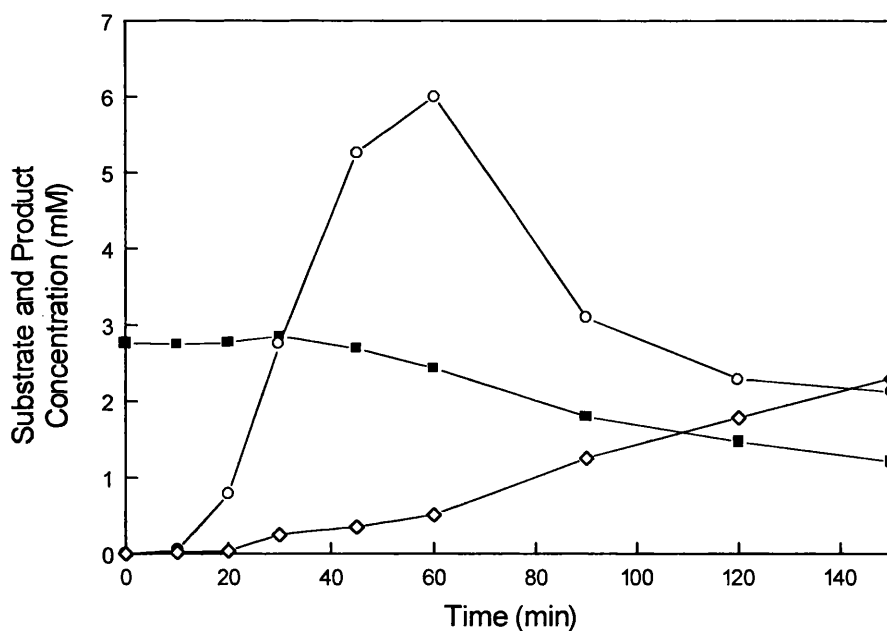


**Figure 4.10** Two-phase *Rhodococcus* R312 biotransformation kinetics for final optimised conditions; (■) 1,3-DCB, (○) 3-CB, (◇) 3-CA. Cells produced as described in Section 2.3.1 and harvested at 30 hours. The biotransformation was as described in Section 2.6.1.2.6 with a phase volume ratio of 0.2 and the initial [1,3-DCB] concentration in the toluene phases of 25 g.L<sup>-1</sup>. The biocatalyst concentration was 12.5 g<sub>ww</sub>.L<sup>-1</sup>.

conditions under which; (1) the system is not substrate mass transfer limited during amide synthesis, (2) amide synthesis is kinetically favoured over its further conversion to the corresponding acid and (3) the minimum specific initial rate of amide synthesis is 30 μmol min<sup>-1</sup> mg<sup>-1</sup>. Substrate mass transfer limitations are avoided by operation at relatively low biocatalyst concentrations (Figure 4.6) and high concentrations of substrate in the organic phase (Figure 4.8). Damage to the catalyst due to phase toxicity effects is avoided by not operating at large values of  $V_r$  (Figure 4.7). Currently the boundaries of the window are defined by straight lines which assumes the three parameters can be considered independently. Clearly this is an initial approximation but the operating window allows us to rapidly define the region of experimental space in which the process can be most feasibly operated.

To confirm the utility of the operating window approach, Figure 4.10 shows the time course of a biotransformation carried out at a position within the defined window of operation for this process. The particular conditions chosen were those where the rate of amide production was expected to be highest *i.e.* a biocatalyst concentration of 12.5 g<sub>ww</sub>.L<sup>-1</sup>,  $V_r = 0.2$ , and an initial organic phase substrate concentration of 25 g<sub>ww</sub>.L<sup>-1</sup>. After 60 minutes of operation a maximum

concentration of 6 mM 3- cyanobenzamide was obtained. This represents a 12 fold improvement in what was achieved in the single-phase biotransformation process (*c.f.* data in Figure 4.2). The low rate of acid by-product formation during this time, due to inhibition of the amidase activity by the amide product (Fournaud *et al.*, 1998), meant that less than 8 % w/w of the amide produced was lost due to further metabolism by the amidase.

#### 4.4 CONCLUSIONS

This chapter covered the application of a structured approach (Woodley and Lilly, 1992) to the design of a biotransformation process for the specific case of aromatic nitrile hydration. It has shown that the use of a two-phase process leads to a considerable enhancement in both the rate of product synthesis and the final product yield compared to what could be achieved in a single-phase process.

Isolation of the NHase at process scale however was not feasible due to the rigid cell wall of the bacteria and the poor stability of the isolated enzyme. The whole cell form of the biocatalyst was thus used even though the activity of the associated amidase could overmetabolise the amide product into the corresponding acid. To overcome productivity limitations imposed by the characteristically low aqueous solubility of this class of substrate ( $\sim 0.34 \text{ g l}^{-1}$  in the case of 1,3-DCB) the use of an aqueous-organic two-phase bioreactor was investigated. After screening a wide range of solvents to act as a substrate reservoir toluene was selected as the organic phase due to the most favourable combination of Log P value (2.9) and 1,3-DCB saturation concentration ( $\sim 30 \text{ g l}^{-1}$ ). The effects of phase volume ratio (0.05-0.3), wet weight biomass concentration ( $1.25\text{-}200 \text{ g}_{\text{ww}} \text{ l}^{-1}$ ) and substrate concentration in the organic phase ( $5\text{-}25 \text{ g l}^{-1}$ ) were then combined to define a suitable operating window where the maximum space-time yield of amide formation could be obtained. Compared to a single-phase transformation, the two-phase process yielded 12 times as much of the amide product of which less than 8% w/w was lost due to overmetabolism.

Having established and optimised the two-phase biotransformation of 1,3-DCB the hydrodynamics of the system can now be investigated as a basis for the successful scale-up of the process. This will be discussed in Chapter 6. Before that, however, the issue of replacing

toluene (relatively low Log P value) as the substrate reservoir will be addressed in Chapter 5 where room temperature ionic liquids will be examined as possible solvent replacements.

# 5. USE OF ROOM TEMPERATURE IONIC LIQUIDS AS ORGANIC SOLVENT REPLACEMENTS

## 5.1 INTRODUCTION

### 5.1.1 Can ionic liquids replace organic solvents in two-phase bioprocesses?

Organic solvents are widely used in a range of multiphase bioprocess operations including two-phase biotransformation reactions and the liquid-liquid extraction of antibiotics. There are, however, considerable problems associated with the safe handling of these solvents which relate to their toxic and flammable nature. There are also issues of biocompatibility associated with organic solvents. They are frequently toxic and this can reduce activity of an enzyme or biocatalyst and hence the space-time production of a biotransformation. Recently, room-temperature ionic liquids have emerged as a potential replacement for organic solvents in catalytic processes on both a laboratory and industrial scale (Holbrey and Seddon, 1999b). This chapter will examine the possible application of an ionic liquid [bmim][PF<sub>6</sub>] in the two-phase biotransformation of 1,3-DCB.

A wide range of reactions have been reported, including advances in alkylation reactions (Earle *et al.*, 1998), Diels-Alder cyclisations (Earle *et al.*, 1999; Jaeger and Tucker, 1989), hydrogenation of aromatics (Adams *et al.*, 1999), transition metal catalysed hydrogenation (Chauvin *et al.*, 1995), Heck coupling chemistry (Carmichael *et al.*, 1999; Herrmann and Bohm, 1999), and the development of commercially competitive processes for dimerisation, oligomerisation and polymerisation of olefins (Ambler *et al.*, 1996; Abdul-Sada *et al.*, 1995a and 1995b; Chauvin *et al.*, 1988 and 1989). Since the work in this chapter was published (Cull *et al.*, 2000) others have shown that enzymes can be used in single phase ionic liquid biotransformations in near anhydrous (Erbeldinger *et al.*, 2000) and anhydrous conditions (Lau *et al.*, 2000) for synthetically useful reactions. The 'designer solvent' potential has also been shown by Kragl (Kaftzik *et al.*, 2001) who demonstrated that the enantiomeric excess of a lipase could be enhanced by selecting certain ionic liquids. Also microscopy studies on *Rhodococcus* R312 cells used in the

single phase biotransformation of 1,3-DCB using [bmim][PF<sub>6</sub>] have shown that the cells show no evidence of lysis. That cells also remain viable and can be plated on agar media (Roberts and Lye, 2001) emphasises the non-toxicity of the ionic liquid.

Ionic liquids, also known as molten salts, are solutions composed entirely of ions. They have, among a unique set of chemical and physical properties (Seddon, 1997; Chauvin, 1996; Chauvin and Olivier-Bourbigou, 1995), effectively no measurable vapour pressure, which lends them ideally as replacements for volatile, conventional organic solvents. The wide and readily accessible range of room-temperature ionic liquids with corresponding variation in physical properties, prepared by simple structural modifications to the cations (Gordon *et al.*, 1998; Holbrey and Seddon, 1999a) or changes in anion (Wilkes and Zaworotko, 1992; Bonhôte *et al.*, 1996), offers the opportunity to design an ionic liquid solvent system optimised for a particular process; in other words, these can be considered as “designer solvents” (Freemantle, 1998). Table 5.1 shows the properties of room temperature ionic liquids, all of which are potentially of use in process design. The structure of the ionic liquid used in this chapter [bmim][PF<sub>6</sub>] is illustrated in Figure 5.1 as well as examples of cations and anions typically combined to form ionic liquids.

<b>Properties of room temperature ionic liquids</b>
Non-Volatile, non-flammable, low toxicity
Liquid and stable over a wide temperature range (typically -80 °C to 200 °C)
Relatively low viscosity with Newtonian rheology
Non-corrosive and compatible with common materials of construction
Good solvents for many organic, inorganic and polymeric materials
Immiscible with a wide range of organic solvents
Immiscible (or miscible) with water
Able to suppress solvation and solvolysis phenomena
Tuneable physicochemical properties (‘designer solvents’)

**Table 5.1** Physicochemical properties of ionic liquids (from Roberts and Lye, 2001).

### 5.1.2 Objectives

This chapter investigates the application of a room temperature ionic liquid, 1-butyl-3-methylimidazolium hexafluorophosphate (Figure 5.1), as a potential replacement for toluene in the *Rhodococcus* R312 catalysed biotransformation of 1,3-dicyanobenzene (1,3-DCB) previously studied in Chapter 4. Having selected and optimised the aqueous-toluene biotransformation system in Chapter 4, [bmim][PF<sub>6</sub>] was considered as a potential alternative to toluene due its reduced toxicity and flammability. Specifically this Chapter investigates the physical properties of the ionic liquid and its suitability as a solvent phase for the biotransformation of 1,3-DCB with regard to solute mass transfer between the phases and compatibility with the whole cell biocatalyst used.

The work in this chapter has also been published as: S.G. Cull, J.D. Holbrey, V. Vargas-Moore, K.R. Seddon and G.J. Lye (2000) *Room temperature ionic liquids as replacements for organic solvents in multiphase bioprocess operations*, *Biotechnology and Bioengineering* **69**, 227-233.

## 5.2 MATERIALS AND METHODS

### 5.2.1 Chemicals and microorganism

The organic solvents, inorganic and biological agents are as described in Section 2.1.

### 5.2.2 Experimental methods

Production of the whole cell *Rhodococcus* biocatalyst using RGM in shake flask fermentations is as described in Sections 2.2.1 and 2.3.1 respectively. Cells were prepared for two-phase hydrodynamics experiments as described in Section 2.4.1. Phase physical properties of density, viscosity and substrate partition coefficients were determined as described in Sections 2.7.2, 2.7.3 and 2.6.1.2.1 respectively. The saturation concentration of substrate was determined as described in Section 2.6.1.2.1. Comparative two-phase biotransformations and activity assays were performed as described in Sections 2.6.1.2.7 and 2.6.1.2.8.

The ionic liquid [bmim][PF<sub>6</sub>] was a kind gift from Dr J.D. Holbrey and was synthesised in the QUESTOR centre of the Queens University Belfast as described in Section 2.1.2.

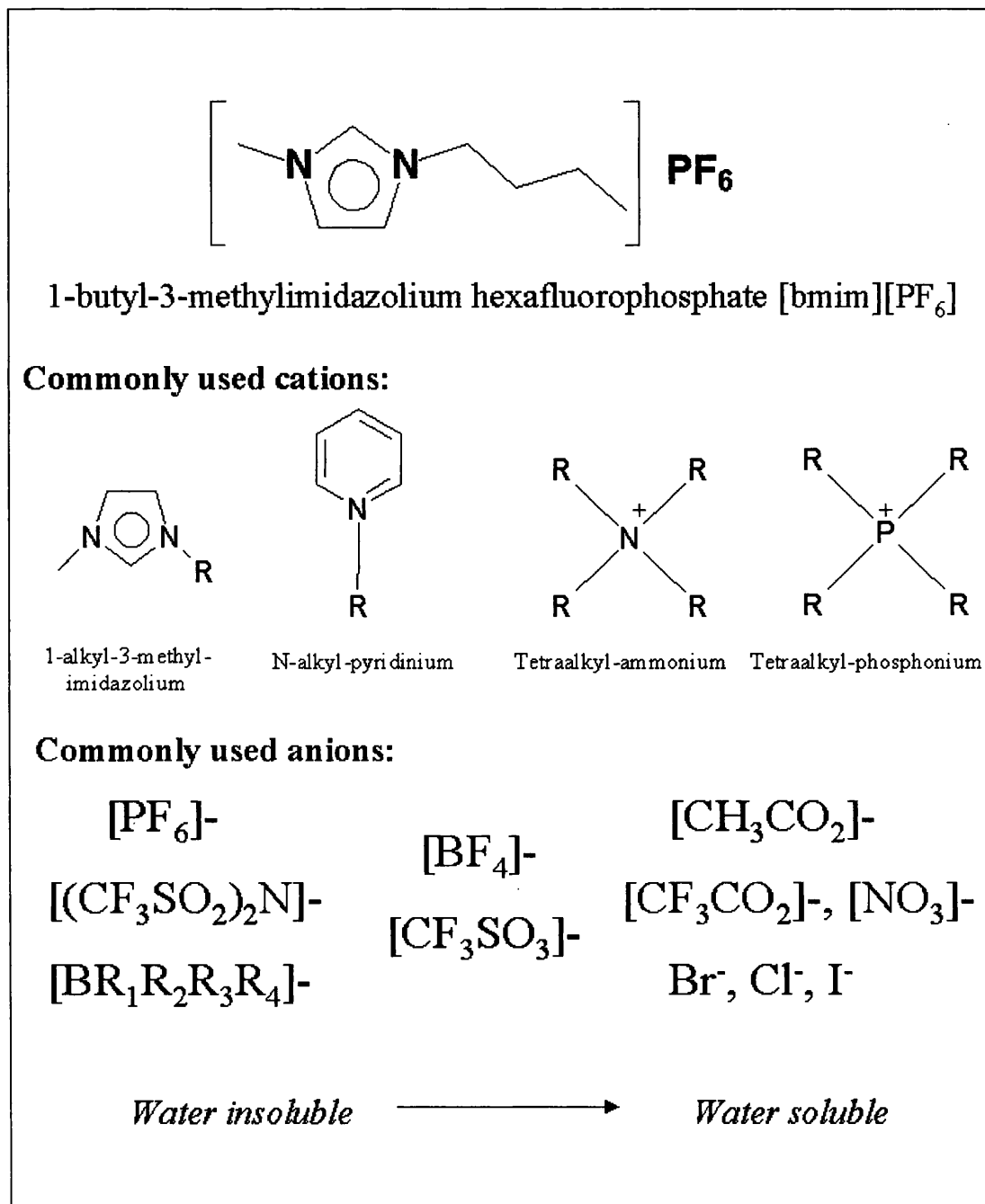


**Figure 5.1** Chemical structure of [bmim][PF<sub>6</sub>] and examples of cations and anions commonly used in the creation of ionic liquids (from Roberts and Lye, 2001).

## 5.3 RESULTS AND DISCUSSION

### 5.3.1 Ionic liquid selection and physical properties

The ionic liquid [bmim][PF<sub>6</sub>] was initially selected for use in the biotransformation because it was one of the most widely used ionic liquids in chemical catalysis, it has a low toxicity and flammability and is also water immiscible. It also has a high solubility for organic molecules used in catalysis. It possesses a large cation, [bmim] and a small inorganic anion, which accounts for the low melting point and relatively low viscosity at room temperature.

Before performing biotransformation experiments it was necessary to first determine the relative solubility of the substrate in each of the two-phase systems. Table 5.2 shows the experimentally determined saturation concentrations of 1,3-DCB in toluene and [bmim][PF<sub>6</sub>] phases (Section 2.6.1.2.1), together with equilibrium distribution coefficients of the substrate (2.7.5) and the physical properties of the liquids. The saturation concentration of 1,3-DCB in toluene is seen to be considerably higher than that for the ionic liquid though both are still greater than the saturation concentration of 1,3-DCB in the aqueous biotransformation buffer which is only 0.34 g.L<sup>-1</sup>. The equilibrium partition coefficients are similar in the two systems and of an order of magnitude which will facilitate the continuous delivery of low levels of the substrate, from either the toluene or [bmim][PF<sub>6</sub>] phase, into the conjugate aqueous phase during the biotransformation. One of the future advantages of using ionic liquids, however, is the potential to be able to rationally control both the solubility and partitioning of substrate molecules. This can be achieved by variation of the cations (Gordon *et al.*, 1998) and anions (Wilkes and Zaworotko, 1992) for example.

Table 5.2 also shows that the ionic liquid is more dense ( $\rho = 1190 \text{ kg.m}^{-3}$ ) than both the toluene and the aqueous phases ( $\rho \sim 1000 \text{ kg.m}^{-3}$ ) and will therefore be present as the lower phase in most two-phase systems. The viscosity of the ionic liquid over a range of shear rates from 24 to 877 s<sup>-1</sup> was found to be 0.29278 kg.m<sup>-1</sup>.s<sup>-1</sup> which is approximately 300 times that of water ( $\mu \sim 0.001 \text{ kg.m}^{-1}.\text{s}^{-1}$ ) and approximately 600 times greater than that of toluene. Both the ionic liquid and toluene displayed a Newtonian behaviour. Simple

mixing trials, in which equal volumes of the two phase were mixed on an orbital shaker at 200 rpm in the absence of cells, showed that the majority of phase separation occurred in the water-[bmim][PF<sub>6</sub>] system after approximately 10 minutes. This was somewhat slower than in the water-toluene system where the majority of phase separation occurred in approximately half this time.

Property	Toluene	[bmim][PF <sub>6</sub> ]
[1,3-DCB] <sub>sat</sub> (g l <sup>-1</sup> )	~30	~1.0
$K_{1,3\text{-DCB}}$ (= $C_{\text{aq}}/C_{\text{tol}}$ or $C_{\text{aq}}/C_{\text{il}}$ )	0.025	0.013
Density (kg m <sup>-3</sup> )	867	1190
Rheological behaviour	Newtonian	Newtonian
Viscosity (kg m <sup>-1</sup> s <sup>-1</sup> )	$5.1 \times 10^{-4}$	$2.9 \times 10^{-1}$

**Table 5.2.** Physical and equilibrium properties of toluene and [bmim][PF<sub>6</sub>] systems (aqueous phase consisted of 0.1 M phosphate buffer, pH 7). Density, viscosity and substrate partition coefficients were performed as described in Sections 2.7.2, 2.7.3 and 2.7.1.2.1 respectively. The saturation concentration of 1,3-DCB in the two phases was performed as described in Section 2.6.3.1.

### 5.3.2 Two-phase biotransformation of 1,3-DCB

The hydration of 1,3-DCB by the nitrile hydratase of *Rhodococcus* R312 is a reaction of scientific and industrial interest of which a number of illustrations already exist in the literature (e.g. Martinkova *et al.*, 1995; Crosby *et al.*, 1994; Maddrell *et al.*, 1996). However, as discussed in Chapter 4 the substrate is very poorly water soluble and the organic solvent toluene has been used to increase the space-time yield of the product 3-cyanobenzamide in a two-phase biotransformation. For the process discussed in the majority of this thesis toluene was selected as the organic phase, after initially screening a wide range of solvents, because it has a high saturation concentration of 1,3-DCB, a desirable substrate partition coefficient ( $C_{\text{aq}}/C_{\text{org}}$ ), is unchlorinated and has an acceptable Log P of 2.9 (Laane *et al.*, 1987). Like most organic solvents, however, toluene has a damaging effect on the cell wall of the biological catalyst and is hazardous to work with, particularly at large scale, because of its toxicity and flammability. The potential replacement of toluene with a room-temperature ionic liquid such as [bmim][PF<sub>6</sub>] would be both scientifically interesting in relation to cell wall-ionic liquid interactions, and highly

desirable from an industrial perspective. As previously stated the ionic liquid [bmim][PF<sub>6</sub>] was selected due to its low flammability, low toxicity, water immiscibility and previous use with small molecule substrates that are also used in biocatalysis.

Aqueous phase reaction profiles for the *Rhodococcus* R312 catalysed transformation of 1,3-DCB in water-toluene and aqueous-[bmim][PF<sub>6</sub>] two-phase systems are shown in Figures 5.2 and 5.3 respectively. Note that the initial concentration of substrate present in the non-aqueous phase was the same in each case. Both figures show the expected conversion of 1,3-DCB first to 3-cyanobenzamide and then 3-cyanobenzoic acid. The slower initial rates of both amide and acid production in the aqueous-[bmim][PF<sub>6</sub>] system could be due either to the slower rate of 1,3-DCB mass transfer from the more viscous [bmim][PF<sub>6</sub>] phase (see also respective  $K_{1,3\text{-DCB}}$  values in Table 5.2) or inhibitory/toxic effects of the ionic liquid towards the *Rhodococcus* R312 cells. The rapid initial decline in the aqueous phase concentration of 1,3-DCB also suggests that the rate of amide production is limited by substrate mass transfer rather than cellular activity (c.f. Figure 5.2 where there is an approximately constant level of 1,3-DCB maintained in the aqueous phase due to its continuous supply from the conjugate toluene phase). Even though the initial rate of 3-cyanobenzamide production was lower in the water-[bmim][PF<sub>6</sub>] system, the yield of product in the aqueous phase was slightly higher.

To investigate the toxic/inhibitory effects of toluene and [bmim][PF<sub>6</sub>] the residual activity of the cells was measured as a function of time during an extended period of mixing in each of the two-phase systems. Figure 5.4 shows the retention of nitrile hydratase activity in aqueous-toluene and aqueous-[bmim][PF<sub>6</sub>] systems relative to a single aqueous phase control sample (the large error bars are associated with the difficulty of removing a representative sample of cells during mixing of the two-phase systems). It is apparent from Figure 5.4 that toluene has a more detrimental effect on the activity of the cells compared to [bmim][PF<sub>6</sub>] where, during the early period of mixing, the specific activity of the biocatalyst is an order of magnitude larger. Although the activity of the biocatalyst in the aqueous-toluene rises this is due to toluene damaging the cell wall and membrane and therefore allowing for the better transfer of substrate and product out of the cell. However, over longer time periods the aqueous-toluene drops to zero (data not shown). The higher aqueous-[bmim][PF<sub>6</sub>] activity would suggest, then, that the slower initial rate of amide production observed in Figure 5.3, for the [bmim][PF<sub>6</sub>] system, is due to the reduced rate

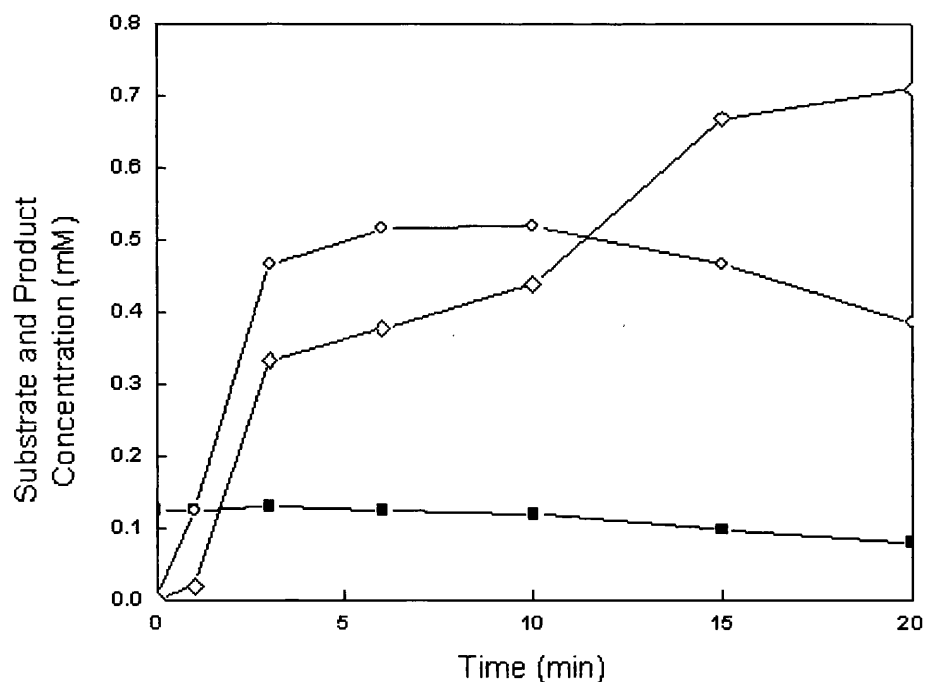


**Figure 5.2** *Rhodococcus* R312 catalysed transformation of 1,3-DCB in an aqueous-toluene two-phase system; (■) 1,3-DCB, (O) 3-CB, (◇) 3-CA. Cells produced as described in Section 2.3.1 and harvested at 30 hours. The biotransformation was as described in Section 2.6.1.2.7 with a phase volume ratio of 0.2 and the initial [1,3-DCB] concentration in the toluene phase of  $1 \text{ g.L}^{-1}$ . The biocatalyst concentration was  $100 \text{ g}_{\text{ww}}.\text{L}^{-1}$ .

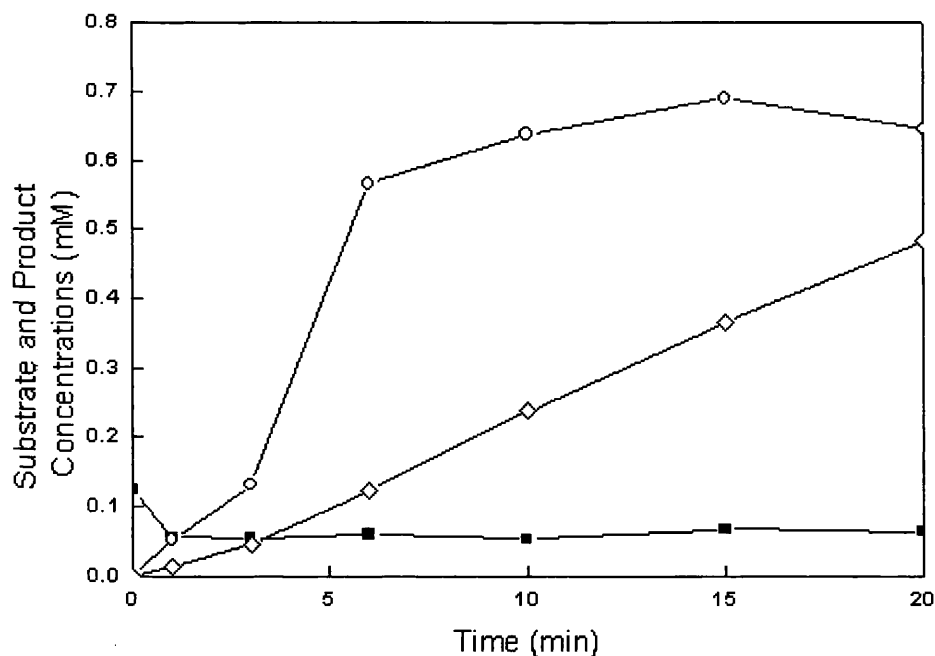


**Figure 5.3** *Rhodococcus* R312 catalysed transformation of 1,3-DCB in an aqueous-[bmim][PF<sub>6</sub>] two-phase system; (■) 1,3-DCB, (O) 3-CB, (◇) 3-CA. Cells produced as described in Section 2.3.1 and harvested at 30 hours. The biotransformation was as described in Section 2.6.1.2.7 with a phase volume ratio of 0.2 and the initial [1,3-DCB] concentration in the [bmim][PF<sub>6</sub>] phase of  $1 \text{ g.L}^{-1}$ . The biocatalyst concentration was  $100 \text{ g}_{\text{ww}}.\text{L}^{-1}$ .

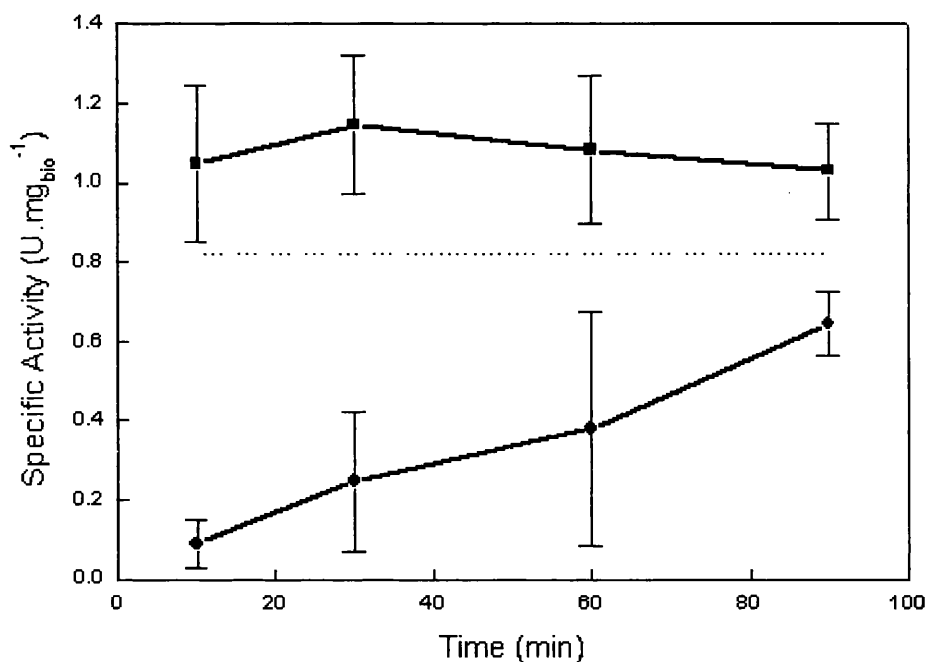


**Figure 5.4** Retention of *Rhodococcus* R312 nitrile hydratase activity in (●) aqueous-toluene and (■) aqueous-[bmim][PF<sub>6</sub>] two-phase systems; (···) activity of single aqueous phase control. Cells produced as described in Section 2.3.1 and harvested at 30 hours. The activity assay was as described in Section 2.6.1.2.8 with a phase volume ratio of 0.2. The biocatalyst concentration was 50 g<sub>ww</sub>.L<sup>-1</sup>.

Visual observations, after settling of the two phase-systems under gravity, showed that in the water-toluene system the cells were aggregated together and that the majority were closely associated with the liquid-liquid interface. This had the effect of stabilising the oil-in-water emulsion formed during the course of the biotransformation which resulted in the formation of a stable 'interphase' in which the majority of toluene was located. In the water-[bmim][PF<sub>6</sub>] system, however, the cells showed little aggregation and were more evenly dispersed throughout the bulk of the aqueous phase. This has obvious benefits for the subsequent downstream processing of the reactor phases, where product recovery and breakage of the emulsion can be difficult (Schroën and Woodley, 1997), and for the recycling and reuse of the [bmim][PF<sub>6</sub>] phase. Recent experiments by others (Roberts and Lye, 2001) have also shown that the *Rhodococcus* R312 cells remain viable after suspension in both single phase ionic liquids and aqueous-ionic liquid biphasic systems suggesting that the biocatalyst might also be able to be recycled. This would certainly not be 'possible' in the aqueous-toluene system.

## 5.4 CONCLUSIONS

The work in this chapter demonstrates for the first time that room temperature ionic liquids, such as [bmim][PF<sub>6</sub>], can be considered as direct replacements for conventional organic solvents in two-phase biocatalytic processes. The replacement of organic solvents with these ionic liquids would enable major process design and economic constraints associated with the toxicity and flammability of organic solvents to be overcome. Further research is clearly required in order to show the generic nature of the results, to explore the process implications of using ionic liquids and the rational selection or design of ionic liquids for particular applications.

Biotransformation of 1,3-DCB in both aqueous-toluene and aqueous-[bmim][PF<sub>6</sub>] systems showed similar profiles for the conversion of 1,3-DCB initially to 3-cyanobenzamide and then 3-cyanobenzoic acid. The initial rate of 3-cyanobenzamide production in the aqueous-[bmim][PF<sub>6</sub>] system was somewhat lower, however, due to the reduced rate of 1,3-DCB mass transfer from the more viscous [bmim][PF<sub>6</sub>] phase. It was also shown that the specific activity of the biocatalyst in the aqueous-[bmim][PF<sub>6</sub>] system was almost an order of magnitude greater than in the aqueous-toluene system which suggests that the rate of 3-cyanobenzamide production was limited by substrate mass transfer rather than the activity of the biocatalyst.

Although the results are very promising the focus of the remaining chapters in this thesis will be on the scale-up of two-phase biocatalytic processes. The current difficulty and expense of obtaining large quantities of ionic liquids requires that the scale-up studies be performed with the aqueous-toluene system, the conditions for which were previously optimised in Chapter 4.

## 6. TWO-PHASE REACTOR HYDRODYNAMICS AND SCALE-UP

### 6.1 INTRODUCTION

Having defined the optimal conditions for the lab-scale two liquid phase bioconversion in Chapter 4 this chapter focuses on scale-up of the process. Measurement of interfacial area and definition of basis for scale-up for the successful scale-up of the process in both 'clean' systems and systems containing biomass are investigated. As outlined in Chapter 1, the maintenance of a constant interfacial area is a key parameter for the successful scale-up of a bioreactor as this strongly influences the rate of substrate mass transfer between the phases and consequently the rate of reaction.

#### 6.1.1 The hydrodynamics of two-phase bioreactors

Currently there is little information available on the hydrodynamics and phase behaviour of two-phase bioconversion processes carried out in stirred-tank reactors. Knowledge of the droplet size distribution, in particular, is critical for estimation of the interfacial area and hence the rate of solute transfer between the phases. To date, however, little is known on how the droplet size distribution varies as a function of reactor design and operation, while none of the suggested scale-up criteria are generally accepted (Zhou and Kresta, 1998). From a hydrodynamic standpoint, two-phase bioconversion processes can be classified according to the metabolic state of the biocatalyst:

**(a) Processes employing growing cells.** Bioconversions requiring actively growing cells necessitate the use of complex growth media and frequently result in the production of extracellular, surface-active, metabolites as a consequence of solvent exposure throughout the fermentation (Schmid *et al.*, 1998). Recent results have shown that droplet coalescence is hindered in such systems and that the equilibrium drop size distribution is primarily determined by the surface activity of the broth components rather than the agitation

conditions (Kollmer *et al.*, 1999). These processes are also likely to require the supply of a gaseous substrate such as oxygen.

**(b) Processes employing resting cells.** Bioconversions using resting cells (or immobilised enzymes) are generally carried out in simpler systems in which the cells are first recovered from the fermentation broth and then resuspended in a simple aqueous buffer. The substrate-containing solvent phase is then added to begin the bioconversion. In these processes, unless the substrate or product molecules are surface active, the equilibrium drop size distribution should be primarily determined by the agitation conditions. Unless a redox enzyme is involved, the supply of gaseous oxygen is not necessarily required.

In bioconversions employing resting cells the drop size distribution will thus be primarily determined by the competing phenomena of drop break-up and coalescence. From the different suggested mechanisms, break-up in the inertial subrange of turbulence will be the prevailing one in dilute dispersions (Kumar *et al.*, 1998). The maximum drop size that can resist break-up,  $d_{max}$ , will depend on the balance between external turbulent fluctuations, which tend to break the drops, and surface tension, which tends to stabilise them (Hinze, 1955). In a stirred vessel  $d_{max}$  will be given by:

$$d_{max} \propto We_T^{-0.6} \quad (6.1)$$

where  $We_T$  is the stirred tank Weber number (Zhou and Kresta, 1998). The maximum droplet size is thus determined by the continuous phase density,  $\rho_c$ , the impeller rotational speed,  $N$ , the impeller diameter,  $D_i$ , and the interfacial tension,  $\sigma$ . The dispersed phase viscosity can help stabilise the drops and its effect is often accounted for by introducing a viscosity number. This can, however, be ignored for systems with small viscosity differences between the phases.

Coalescence of drops will occur at high dispersed phase volume fractions and will result in increased drop sizes. The mechanisms relevant to drop-drop coalescence have been detailed by Chesters (Chesters, 1991). However, even when coalescence is prevented, increasing the volume fraction of the dispersed phase will decrease the turbulence intensity and, therefore, increase the dispersed phase droplet size. To account for the effect

of volume fraction on  $d_{max}$ , investigators have used a linear concentration correction function with the general form:

$$d_{max} / D_i = c_1 (1 + c_2 \phi) We_T^{-0.6} \quad (6.2)$$

where  $D_i$  is the impeller diameter,  $c_1$  and  $c_2$  are constants and  $\phi$  is the volume fraction of the dispersed phase. Instead of  $d_{max}$ , a more useful parameter, particularly for mass transfer operations, is the Sauter mean diameter,  $d_{32}$ , which is often assumed to be proportional to  $d_{max}$ . A number of correlations taking the form of Equation 6.2 have been proposed in the literature and some of those most relevant to this work are given in Table 6.1. The constant  $c_2$  is considered equal to 3 when it accounts for turbulence damping at low dispersed phase concentrations (Doulah, 1975), or higher than 3 for coalescing systems (Pacek *et al.*, 1998). Equation 6.2 predicts an increase in the drop size with increasing dispersed phase volume fraction. At high dispersed phase volume fractions (usually above 40%), however, a further increase in the dispersed concentration results in decreasing drop size (Kumar *et al.*, 1998; Boye *et al.*, 1996). This behaviour has been attributed to alternative mechanisms of drop break-up for Reynolds numbers below 1000 (Kumar *et al.*, 1998) but is not relevant to the work performed here.

Author	Correlation equation	$D_i$ (cm)	$T$ (cm)	$\phi$	Impeller characteristics
Chen and Middleman (1967)	$d_{32}/D_i = 0.053(We, T)^{-0.6}$	5.1-15.2	10-45.7	0.001-0.005	Single 6-bladed RT
Brown and Pitt (1970)	$d_{32}/D_i = 0.051(1+3.14\phi) \times (We, T)^{-0.6}$	10	30	0.05-0.3	Single 6-bladed RT
Van Heuven and Beek (1971)	$d_{32}/D_i = 0.047(1+2.5\phi) \times (We, T)^{-0.6}$	3.75-40	12.5-120	0.04-0.35	Single 6-bladed RT
Calabrese <i>et al.</i> (1986)	$d_{32}/D_i = 0.053(We, T)^{-0.6} \times (1+0.91Vi^{0.84})^{3/5}$	7.1-19.6	14.2-39.1	<0.005	Mainly single 6-bladed RT
Godfrey and Grilc (1977)	$d_{32}/D_i = 0.058(1+3.6\phi) \times (We, T)^{-0.6}$	5.1	15.2	0.05-0.5	Single 6-bladed RT

**Table 6.1** Literature correlations for the prediction of Sauter mean drop diameter in agitated liquid-liquid systems (compiled from Zhou and Kresta (1998)). RT = Rushton turbine.

### 6.1.2 Current scale-up methodologies

The existing scale-up literature for two-liquid phase reactors mainly relates to simple chemical systems. Scale-up has tended to focus on the maintenance of consistent characteristics such as interfacial area. The two most popular criteria for scale-up in geometrically similar liquid-liquid agitated systems are constant power input per unit volume ( $P/V$ ) and constant impeller tip speed respectively (Okufi *et al.*, 1990). Podgorska and Baldyga (Podgorska *et al.*, 2001) recently proposed that the fluid circulation time in the vessel is also relevant and suggested instead the following four criteria for scale-up: (i) equal power input per unit mass and geometric similarity, (ii) equal average circulation time and geometric similarity, (iii) equal power input per unit mass, equal average circulation time and no geometric similarity, (iv) equal impeller tip speed and geometric similarity. The study demonstrated that in fast coalescing systems both criteria (i) and (iii) resulted in small changes in the drop size distribution during scale-up, while in slow coalescing systems none of the criteria seemed to perform satisfactorily.

Literature on the scale-up of complex two-liquid phase bioconversion processes is extremely limited. Previous investigators have simply indicated that during scale-up consistency should be maintained in all reactor conditions and have postulated that scale-up on the basis of constant  $P/V$  was appropriate (Woodley, 1990) but this has not been experimentally verified to date.

### 6.1.3 Objectives

The overall goal in this chapter is to carry out an investigation into the hydrodynamics and scale-up of the two-phase system previously defined in Chapter 4. The hydrodynamics will be investigated in a clean system (without biomass or substrate) and with the addition of biomass to examine the affect of biomass on drop size and drop size distribution. Correlation equations from the literature will also be used to try to predict the affect of biomass and change in drop size upon reactor scale. The results of the investigation will be used to define scale-up criteria and test the suitability of current correlation equations.

Experiments were performed in the two geometrically similar 3 L and 75 L reactors, while the dynamic variation of droplet size distribution, as a function of power input and reactor size, was measured on-line using a light back-scattering technique. For scale-up, the two commonly used criteria of constant P/V and constant impeller tip speed were investigated.

The work presented in this chapter has been submitted for publication as: Cull, S.G., Lovick, J.W. Lye, G.J. and Angeli, P. (2001) Scale-down studies on the hydrodynamics of two-liquid phase biocatalytic reactors. In: *Bioprocess and Biosystems Engineering*.

## 6.2 MATERIALS AND METHODS

### 6.2.1 Chemicals and microorganism

The organic solvents and biological agents used in this chapter are as described in Chapter 2.1.

### 6.2.2 Experimental methods

Production of the whole cell *Rhodococcus* biocatalyst using 7, 20 and 450 L fermenters is as described in Sections 2.3.2.1, 2.3.2.2 and 2.3.2.3 respectively. Biomass was processed for 3 L and 75 L two-phase hydrodynamics experiments as described in Section 2.4.2 and 2.4.3. Phase physical properties such as density, viscosity and surface and interfacial tension were determined as described in Sections 2.7.2, 2.7.3 and 2.7.4 respectively.

The vessels used for the 3 L and 75 L hydrodynamic studies are as described in Section 2.6.2.1. On-line measurement of droplet size and distribution are as described in Section 2.6.2.4 and 2.6.2.5. Power consumption and phase continuity experiments were performed as described in Section 2.6.2.6

## 6.3 RESULTS AND DISCUSSION

### 6.3.1 Phase physical properties

As described in Chapter 4 toluene was selected as the organic solvent for the bioprocess due to its relatively low toxicity level (Log P = 2.9) and its ability to solubilise high concentrations of the 1,3-DCB substrate ( $\sim 25 \text{ g.L}^{-1}$ ). The aqueous phase used, consisted of 0.1 M potassium phosphate buffer which, at pH 7, provided the optimal conditions for nitrile hydratase activity. Table 6.2 summarises the measured physical properties of the individual phases used in the current work. For a ‘clean’ biphasic system (*i.e.* in the absence of substrate or biomass) of toluene-aqueous buffer, an interfacial tension of  $0.035 \text{ kg.s}^{-2}$  was determined. This is similar to values reported by previous investigators for a variety of model systems that had interfacial tension values between  $0.002 - 0.050 \text{ kg.s}^{-2}$  (Zhou and Kresta, 1998). The addition of substrate, 1,3-DCB, to the toluene phase had no apparent effect on the physical properties of the solvent or the measured interfacial tension at concentrations up to  $20 \text{ g.L}^{-1}$ . In contrast, the addition of  $15 \text{ g}_{\text{ww}}.\text{L}^{-1}$  of biomass to the aqueous phase was found to significantly reduce the interfacial tension to a value of around  $0.0013 \text{ kg.s}^{-2}$ . This low value is most likely due to the adsorption of biomass at the interface but may also be the result of small amounts of media components, especially antifoam, still present in the system after harvesting and resuspension of the biomass as described in Section 2.4.1.

Physical property	Phase composition		
	Aqueous phosphate buffer	Aqueous phosphate buffer plus $15 \text{ g}_{\text{ww}}.\text{L}^{-1}$ biocatalyst	Toluene
Formula	$\text{KH}_2\text{PO}_4 / \text{K}_2\text{HPO}_4$	$\text{KH}_2\text{PO}_4 / \text{K}_2\text{HPO}_4$	$\text{C}_6\text{H}_5\text{CH}_3$
Molecular weight	328	328	92
Density ( $\text{kg.m}^{-3}$ )	$1011 \pm 5$	$1034 \pm 6$	$857 \pm 3$
Dynamic viscosity (mPa.s)	$1.274 \pm 0.03$	$1.321 \pm 0.006$	$0.51 \pm 0.02$
Surface tension ( $\text{kg.s}^{-2}$ )	$71.9 \pm 0.05$	$34.9 \pm 0.5$	$28.1 \pm 0.3$

**Table 6.2** Experimentally determined phase physical properties. Density, dynamic viscosity and surface tension measurements performed as described in Section 2.7.2, 2.7.3 and 2.7.4 respectively.

It should be noted that adsorption of the biomass at the interface made accurate measurements of the interfacial tension difficult. The implications of the reduced interfacial tension on drop size distributions will be illustrated later.

### 6.3.2 Power curves for agitated liquid-liquid systems (3 L scale)

The power input for a homogenous liquid agitated in a tank fitted with a single Rushton turbine impeller can easily be found in the literature. For the particular tank and turbine geometry used in this work, however, it was necessary to determine the Power number,  $Po$ , experimentally. In general, when more than one impeller is used,  $Po$  will depend on the number of impellers, the spacing between them and the clearance of the lower impeller from the bottom of the vessel (Armenante *et al.*, 1998). For agitation of each of the ‘clean’ homogeneous phases used here, it was found that the Power number acquired a constant value of 11 for Reynolds numbers above 10,000 (data not shown). The measured power inputs for agitation rates of 400-1200 rpm were between 0.5 - 3.25 kW.m<sup>-3</sup>.

The power consumption was also measured during two-phase mixing using both toluene and pristane as the solvent phase as described in Section 2.6.2.6. Pristane ( $\rho = 790$  kg.m<sup>-3</sup>,  $\mu = 5$  mPa.s) is a solvent with a high Log P value, widely used in two-phase biotransformation processes, and was initially investigated as an alternative to toluene as described in Table 4.1. The power consumption results are shown in Figure 6.1 as  $Po$  against  $Re$  for both systems over a range of solvent volume fractions. For the determination of  $Re$  in the biphasic systems volume-averaged density values were used while viscosity values were calculated using:

$$\mu_m = \frac{\mu_c}{1-\phi} \left( 1 + \frac{1.5\phi\mu_d}{\mu_c + \mu_d} \right) \quad (6.3)$$

where,  $\phi$  is the volume fraction of the dispersed phase and  $\mu_c$  and  $\mu_d$  are the viscosity of the continuous and the dispersed phase respectively (Guilinger *et al.*, 1988). In this case the measured power inputs were slightly lower than for the single phase systems being in the range 0.15 - 2.31 kW.m<sup>-3</sup> for agitation rates of 600 - 1100 rpm.

$Po$  is again seen to be constant and equal to 11 for agitation at Reynolds numbers above 10000, similar to the case of single-phase systems. Reynolds numbers larger than 10,000 were achieved for water-continuous mixtures with dispersed phase volume fractions up to 30%. For the more concentrated water-continuous dispersions, and for oil-continuous dispersions,  $Re$  values fell below 10,000 and  $Po$  was less than 11. Chapter 4 previously investigated conditions to optimise the biocatalytic hydration of 1,3- DCB using toluene as the solvent phase at volume fractions between 5-30% (Cull *et al.*, 2001). The two-phase system comprising 20% v/v toluene and 80% v/v aqueous buffer containing  $15 \text{ g}_{\text{ww}}\cdot\text{L}^{-1}$  of biocatalyst was found to be most suitable as this maximised the synthesis of the 3-cyanobenzamide product and minimised the damaging effect of the toluene on the biocatalyst. Subsequent scale-up and droplet size distribution studies were thus performed solely with this system.

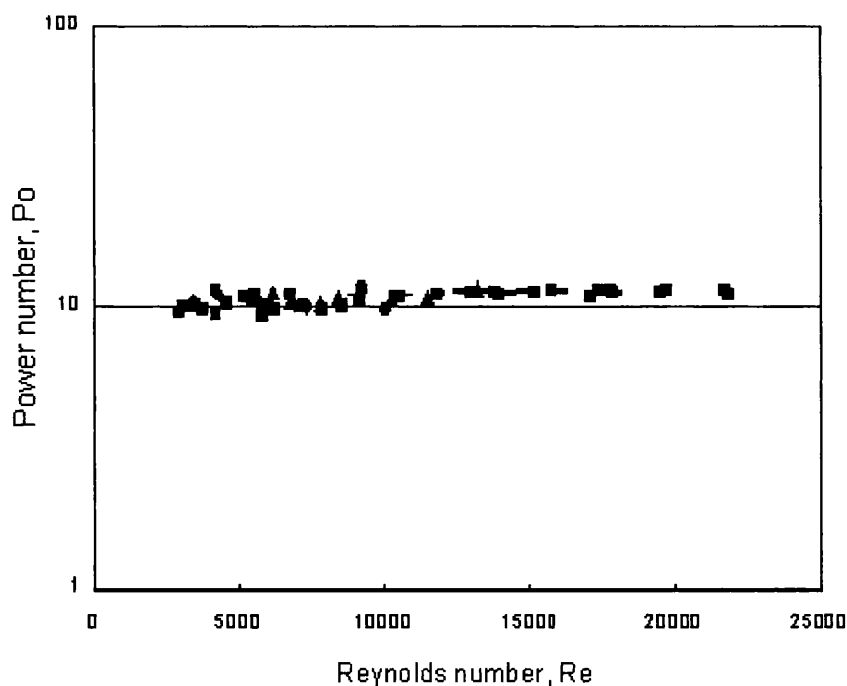


**Figure 6.1** Power curves for a variety of agitated two-liquid phase systems. Power measurements were made in the 3 L scale-down reactor for 10-30% v/v toluene-aqueous and 10-90% v/v pristane-aqueous systems mixed at agitation rates of 650-1100 rpm as described in Section 2.6.2.6.

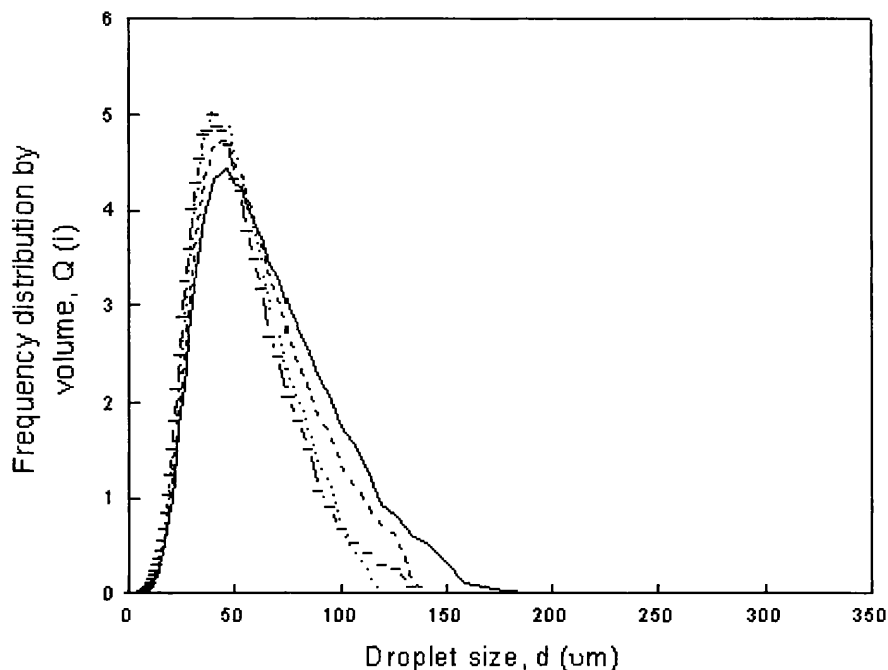


**Figure 6.2** Droplet size frequency distribution by volume as a function of agitation rate for a 20 % v/v aqueous-toluene system in the 3 L reactor in the absence of substrate and biomass: (—) 600 rpm; (---) 700 rpm; (....) 800 rpm; (-.-) 900 rpm. Droplet size measured as described in Section 2.6.2.5.

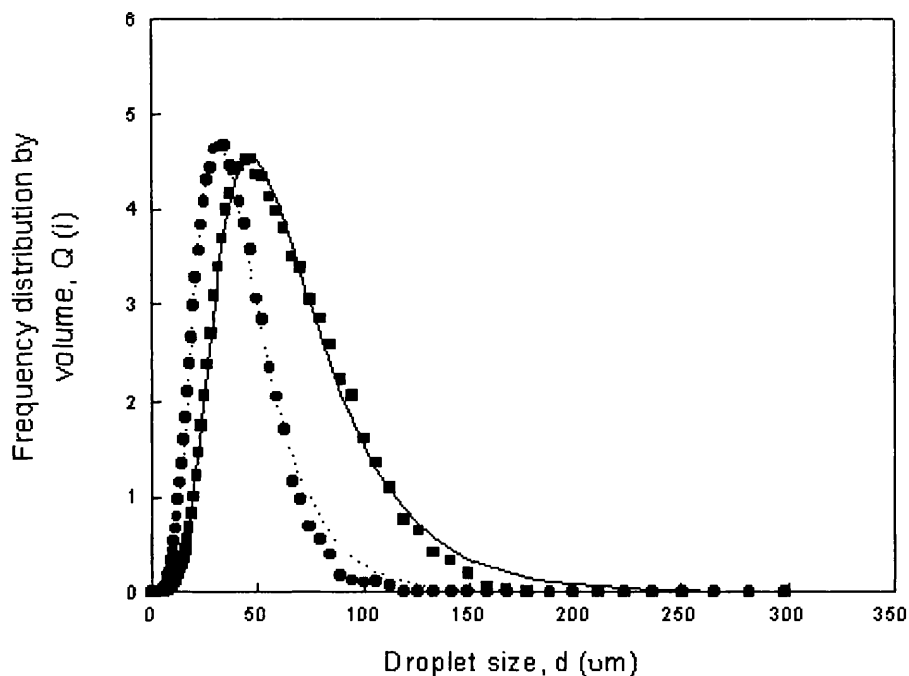


**Figure 6.3** Droplet size frequency distribution by volume for a 20 % v/v aqueous-toluene system agitated at 600 rpm in the 3 L reactor: (■) no substrate or biomass present; (●) 15  $g_{ww} \cdot L^{-1}$  biomass present. Lines show fitted Log-normal distributions as per Equation 6.4. Droplet size measured as described in Section 2.6.2.5.

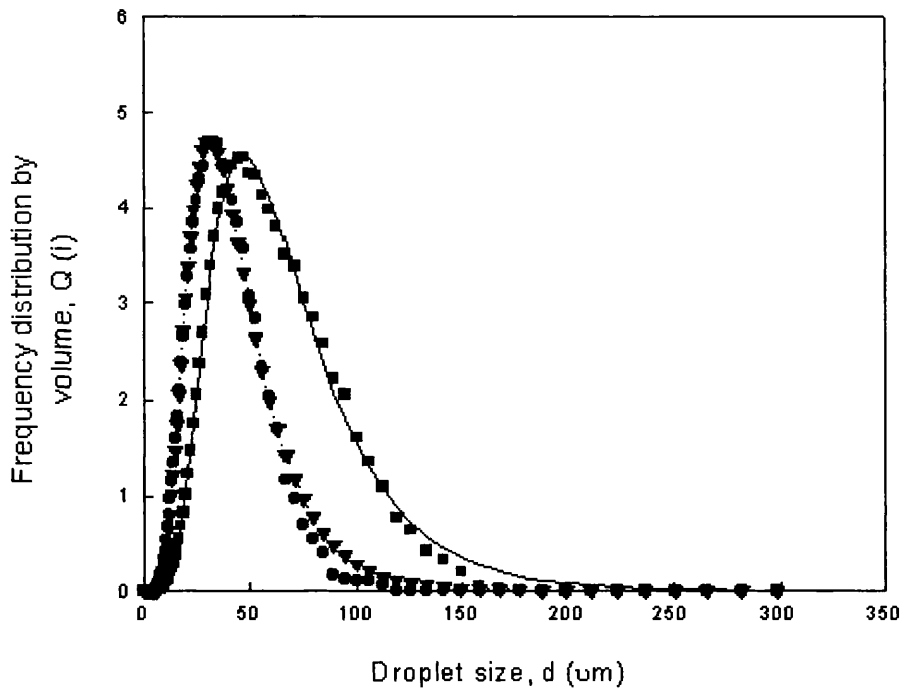


**Figure 6.4** Droplet size frequency distribution by volume for a 20 % v/v aqueous-toluene system agitated at 700 rpm in the 3 L reactor: (■) no substrate or biomass present; (●)  $15 \text{ g}_{\text{ww}}\cdot\text{L}^{-1}$  biomass present. Lines show fitted Log-normal distributions as per Equation 6.4. Droplet size measured as described in Section 2.6.2.5.

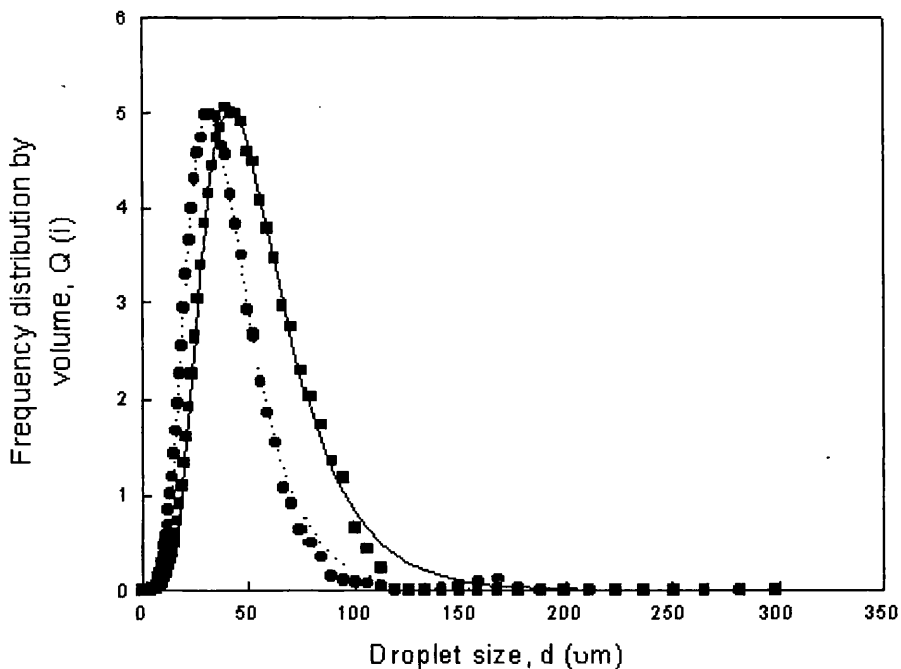


**Figure 6.5** Droplet size frequency distribution by volume for a 20 % v/v aqueous-toluene system agitated at 800 rpm in the 3 L reactor: (■) no substrate or biomass present; (●)  $15 \text{ g}_{\text{ww}}\cdot\text{L}^{-1}$  biomass present. Lines show fitted Log-normal distributions as per Equation 6.4. Droplet size measured as described in Section 2.6.2.5.

### 6.3.3 Effect of agitation rate and phase composition on drop size distributions (3 L scale)

Drop size distributions were initially measured in the 3 L scale-down reactor as described in Section 2.6.2.5 to examine the influence of agitation rate and phase composition on drop size distribution and Sauter mean drop diameter. Figure 6.2 shows that increasing the agitation rate in a ‘clean’ 20% v/v toluene-aqueous system resulted in narrower drop size distributions, shifted to smaller droplet sizes. The distributions shown were recorded 15 minutes after mixing began although the distributions did not change significantly from 10 minutes onwards. The addition of 20 g.L<sup>-1</sup> 1,3-DCB to the toluene phase produced no significant change in the measured size distributions or the Sauter mean diameters (data not shown). As stated previously in Section 6.3.1 addition of the substrate did not alter the physical properties of the toluene phase or the interfacial tension of the biphasic system.

Figures 6.2-6.5 however, shows that the addition of 15 g<sub>ww</sub>.L<sup>-1</sup> of biocatalyst to the aqueous phase shifted the measured distribution to smaller drop sizes for all agitation rates between 600-800 rpm. The individual *Rhodococcus* R312 cells are ~ 1 μm in diameter; this is below the detection limit of the ORM instrument and hence they are not registered in the size distribution. The reduction in droplet size with biomass present is attributed to the significantly reduced interfacial tension as described in Section 6.3.1. As Figure 6.2-6.5 show the difference between the droplet size distributions in the presence and absence of biomass decreased with increasing agitation rate. In all cases the measured drop sizes could be adequately described by a Log-normal distribution as indicated in Figure 6.3-6.5 for an agitation rate of 600-800 rpm. The Log-normal distribution is determined by equation 6.4 where A, B, C are system Log-normal coefficients and *d* is the drop diameter:

$$\frac{A}{(2\pi B)^{0.5} \times e^{((-1/2B) \times (\ln(d)-C)^2)}} \quad (6.4)$$

These distributions show a “tail” at the large end of the drop size spectrum. Mixing of the two-phases with biomass present also led to the formation of a stable inter-phase after phase separation. Visually the system comprised of clear upper (toluene) and lower (aqueous buffer) phases with an inter-phase of cells present between them.

Figure 6.6 shows the Sauter mean drop diameters, determined from the drop size distribution data, at agitation rates between 600 - 900 rpm for both 'clean' and biomass-containing phase systems. As expected from the distribution data, the Sauter mean drop size is seen to decrease slightly with increasing agitation rate from 42 to 36  $\mu\text{m}$  in the 'clean' system and from 31 to 27  $\mu\text{m}$  in the system with biomass. It is difficult to compare the magnitude of the drop sizes recorded, however, due to the limited amount of data available in the literature and the extremely different phase compositions and reactor geometries studied. Galindo *et al.* (2000) investigated droplet sizes in systems with up to four phases present for a highly viscous castor oil ( $\mu = 560 \text{ mPa s}$ ) dispersed in an aqueous salt solution. Experiments were performed at an agitation rate of 250 rpm in a tank fitted with a single Rushton turbine impeller. The drop sizes recorded using an *in-situ* video technique were between 750 – 1250  $\mu\text{m}$  for oil volume fractions between 2-16%. These very large drop sizes are in contrast to those reported by Schmid *et al.* (1998) who measured drop sizes of 10 - 13  $\mu\text{m}$  using an off-line laser refraction spectrometer in a 1.4 L 20% v/v decane-water system containing 1  $\text{g.L}^{-1}$  biosurfactant. These experiments were performed in a 3 L reactor fitted with two Rushton turbine impellers operated at agitation rates of 1500 - 2500 rpm. Clearly the Sauter mean drop sizes reported here lie somewhere between these two extremes and can be explained by the different agitation conditions, fluid properties and methods of drop size analysis used.

### 6.3.3.1 Prediction of Sauter mean drop diameter (3 L scale)

For process design purposes it is useful to be able to predict Sauter mean drop sizes and how these vary with reactor operation. Figure 6.6 also shows the comparison between experimental  $d_{32}$  values and the best predictions for drop size with and without biomass present using the literature correlations detailed in Table 6.1. These particular correlations were chosen from the many available as they were derived in systems with phase physical properties most similar to the ones used in this work. The majority of correlation equations take the general form previously shown in Equation 6.2 however virtually all were developed in vessels fitted with a single Rushton turbine impeller ( $Po = 6$ ). In the current work a three stage Rushton turbine impeller was used which results in a higher power input for the same agitation rate or higher  $Po$  values (see Figure 6.1). In order to account for this difference in power input the  $(We_T)^{-0.6}$  term in the equations in Table 6.1 was substituted by Equation 6.5:

$$We_T^{-0.6} \left( \frac{Po_{lit}}{Po_{ex}} \right)^{0.4} \quad (6.5)$$

where  $Po_{lit}$  is equal to 6 for a single Rushton turbine and  $Po_{ex}$  is equal to 11, as described in Section 6.3.2. The derivation of the power correction term is given in Appendix 2.

The predicted  $d_{32}$  values shown in Figure 6.6 are for the correlations with the closest predictions to the experimental values. For the ‘clean’ system the Chen and Middleman (1967) correlation was found to be the most appropriate. This over predicted the experimental values by 25 – 78%. This is probably due to the number of impellers used in this work. Generally, in stirred tanks drops break-up in the impeller region and coalesce in regions further away. In the correlations for  $d_{32}$  or  $d_{max}$ , the average energy dissipation rate is used which includes both these regions. In the reactor here, however, the use of three impellers decreases significantly the size of the coalescence region, which would be expected to lead to smaller drop sizes than those predicted. Further work on the variation of drop size at different locations in the reactor would provide useful insight. For the system with biomass present the Godfrey and Grilc correlation (1977) was most appropriate though this under predicted the experimental values by 39 – 59%. This under prediction could be a consequence of the very low interfacial tension measured (Section 6.3.1) or the stabilisation of the drops by surface active agents which could be present. It is also possible that the actual interfacial tension in the reactor is somewhat larger than measured at equilibrium in the static system due to the kinetics of biomass adsorption on the droplets during the course of the experiment. These results indicate that although reasonable drop size predictions can be made, further work is required to develop more accurate correlations for this typical bioreactor geometry widely used with biological two-phase systems.

Interestingly, it was also found that when  $d_{32}$  was plotted against  $We$  the exponent on  $We$  was larger than the commonly used value of (-0.6). Similar findings, reported by other investigators recently (Baldyga *et al.*, (2001), Pacek *et al.*, 1998), could imply that the mechanism of break-up in a turbulent dispersion is different than that originally suggested by Hinze (1955). Drop break-up mainly occurs in the impeller region where the isotropic

turbulence assumption of the Hinze theory least applies. The limited range of impeller speeds and dispersed phase volume fractions used in this work, however, does not allow any conclusions to be drawn in this respect.

### 6.3.4 Criteria for reactor scale-up to 75 L scale

As mentioned earlier the maintenance of constant power input per unit volume (or  $N^3 D_i^2 = \text{constant}$ ) and constant tip speed (or  $ND_i = \text{constant}$ ) were the two criteria used here for scale-up from the 3 L to the 75 L reactor. The respective agitation rates for scale-up using these two criteria are given in Table 6.3. Although the inclusion of the circulation time (as suggested by Podgorska and Baldyga (2001)) is an interesting concept when considering scale-up, its application is limited due to the difficulty in defining this parameter (Zhou and Kresta (1998)). Droplet size distributions were again measured in the 75 L reactor for

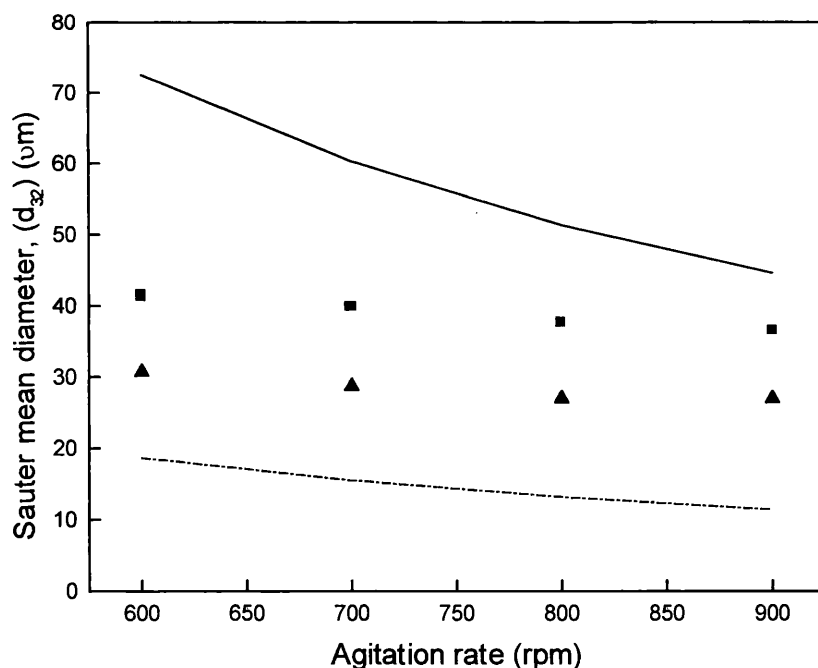


**Figure 6.6** Sauter mean diameter ( $d_{32}$ ) against agitation rate in 20 % v/v toluene-aqueous systems in the 3 L reactor: (■) without biomass present and (▲) with 15  $\text{g}_{\text{ww}}\cdot\text{L}^{-1}$  biomass present. Lines show predicted  $d_{32}$  values using correlations from Table 6.1 corrected for increased power input: (solid line) Chen and Middleman predictions for the biomass-free system; (dashed line) Godfrey and Grilc predictions for the biomass-containing system. Droplet size measurements were performed as described in 2.6.2.5

both a 'clean' 20% v/v toluene-aqueous buffer system and one in which 15 g<sub>ww</sub>.L<sup>-1</sup> of biomass was present.

Agitation rate at 3 L scale (rpm)	Agitation rate at 75 L scale (rpm)	
	P/V constant ( $N^3 D_i^2 = \text{constant}$ )	Tip speed constant ( $ND_i = \text{constant}$ )
600	305	218
700	357	255
800	408	291
900	459	328

**Table 6.3** Reactor agitation rates at 3 L and 75 L scales for scale-up using constant power input per unit volume and constant tip speed criteria.

Figure 6.7 compares the Sauter mean drop diameters measured in the small and large reactors using both scale-up criteria with the 'clean' system. Note that on the horizontal axis the agitation rates in the 3 L reactor are shown. It is apparent that scale-up on the basis of constant power input per unit volume is the best criterion for maintenance of interfacial area at the 75 L scale when considering mean drop size. In this case  $d_{32}$  values are found to be almost identical to those determined in the 3 L scale-down reactor for power inputs between 0.38 - 1.28 kW.m<sup>-3</sup>. This finding is in agreement with a recent investigation in a simple 'clean' phase system that showed that the mean drop size can either stay constant, or even decrease, during scale-up at constant power input per unit volume (Baldyga *et al.*, 2001). Scale-up on the basis of constant tip speed produced larger mean drop sizes than in the 3 L reactor in all cases (the corresponding power input values were between 0.14 - 0.45 kW.m<sup>-3</sup>). This could be due to an increase in circulation time and/or the decrease in average energy dissipation rate in the larger reactor (Podgorska and Baldyga, 2001).

Figures 6.8-6.11 show how the drop size distribution measured in the 3 L reactor, at an agitation rate of 600-900 rpm, compares to the equivalent distributions in the 75 L reactor for each of the scale-up criteria investigated. The distributions obtained in the larger reactor for scale-up on the basis of constant P/V are virtually identical to that found in the 3 L vessel in most cases. In contrast, the constant tip speed results show a distribution that is much wider and has a tail of larger drop sizes compared to that in the smaller reactor or for scale-up on the basis of constant P/V. The distributions here show that at the higher

agitation rates investigated the differences observed with the tip speed results were found to be less with increasing impeller speeds. When biomass was present in the system scale-up based on constant  $P/V$  again gave average drop sizes and size distributions closer to the 3 L reactor that when constant tip speed was used. All of the drop size distributions obtained in the 75 L reactor were again adequately described by a Log-normal distribution.

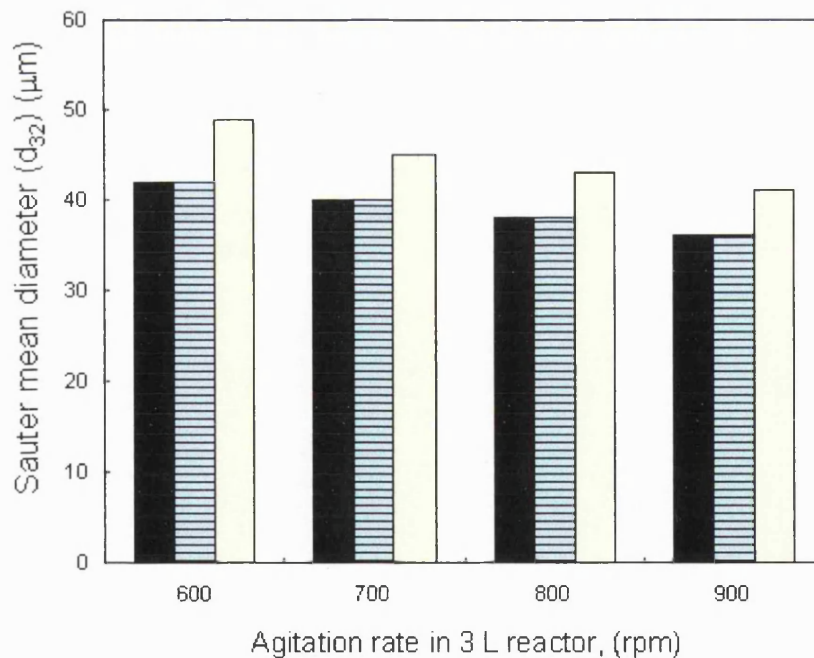


**Figure 6.7** Sauter mean diameter ( $d_{32}$ ) for a 20 % v/v toluene-aqueous system in the 3 L scale-down reactor (black bars) and the 75 L pilot scale reactor for scale-up under constant  $P/V$  (blue bars) and constant tip speed (yellow bars) criteria. Droplet size measured as described in Section 2.6.2.5.

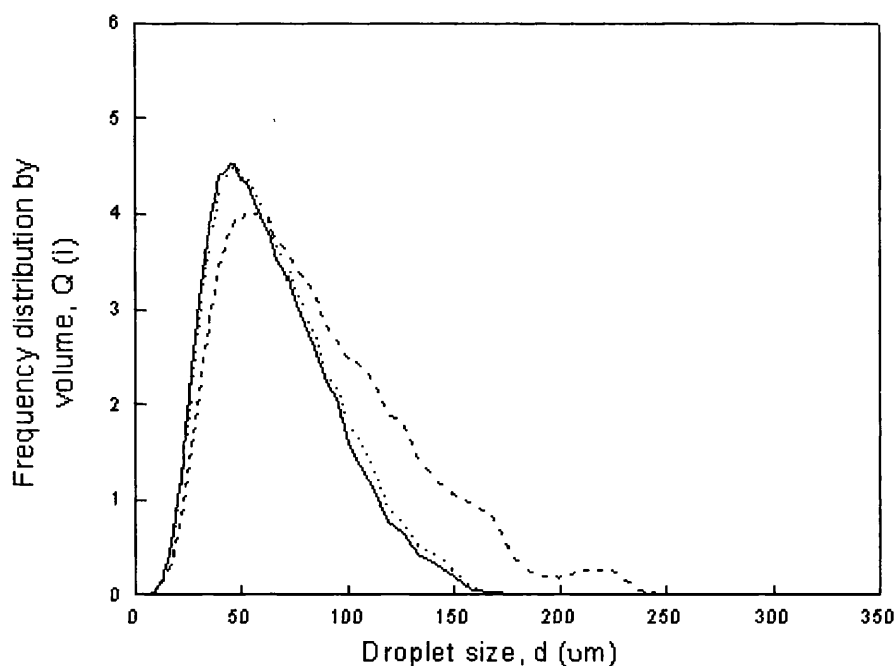


**Figure 6.8** Droplet size frequency distribution by volume for a 20 % v/v toluene-aqueous system in the absence of substrate or biomass: (—) 3 L reactor at 600 rpm; (....) 75 L reactor for scale-up using constant P/V at 305 rpm; (---) 75 L reactor with scale-up using constant tip speed criteria at 218 rpm. Droplet size measured as described in Section 2.6.2.5.

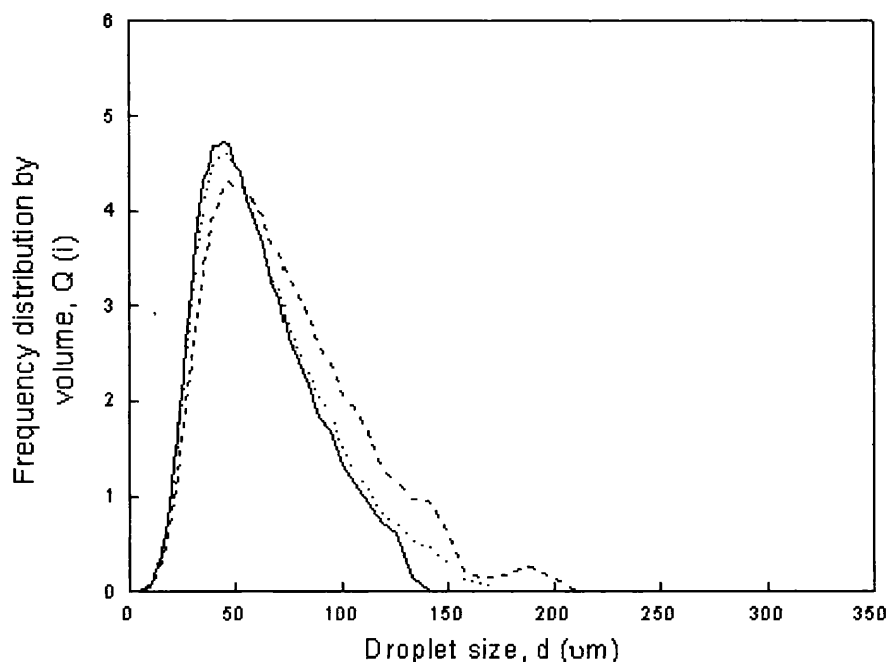


**Figure 6.9** Droplet size frequency distribution by volume for a 20 % v/v toluene-aqueous system in the absence of substrate or biomass: (—) 3 L reactor at 700 rpm; (....) 75 L reactor for scale-up using constant P/V at 357 rpm; (---) 75 L reactor with scale-up using constant tip speed criteria at 255 rpm. Droplet size measured as described in Section 2.6.2.5.

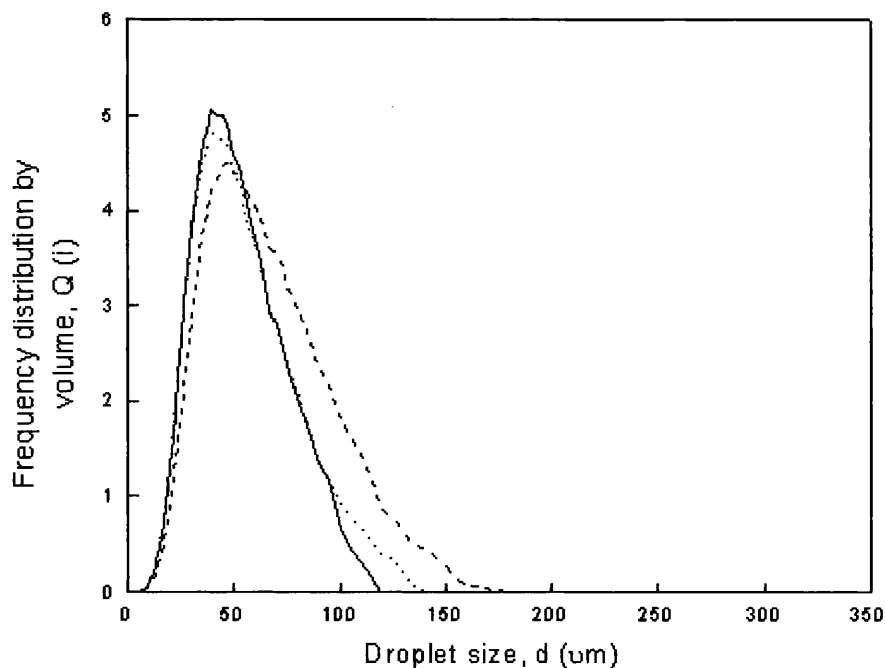


**Figure 6.10** Droplet size frequency distribution by volume for a 20 % v/v toluene-aqueous system in the absence of substrate or biomass: (—) 3 L reactor at 800 rpm; (---) 75 L reactor for scale-up using constant P/V at 408 rpm; (- -) 75 L reactor with scale-up using constant tip speed criteria at 291 rpm. Droplet size measured as described in Section 2.6.2.5.

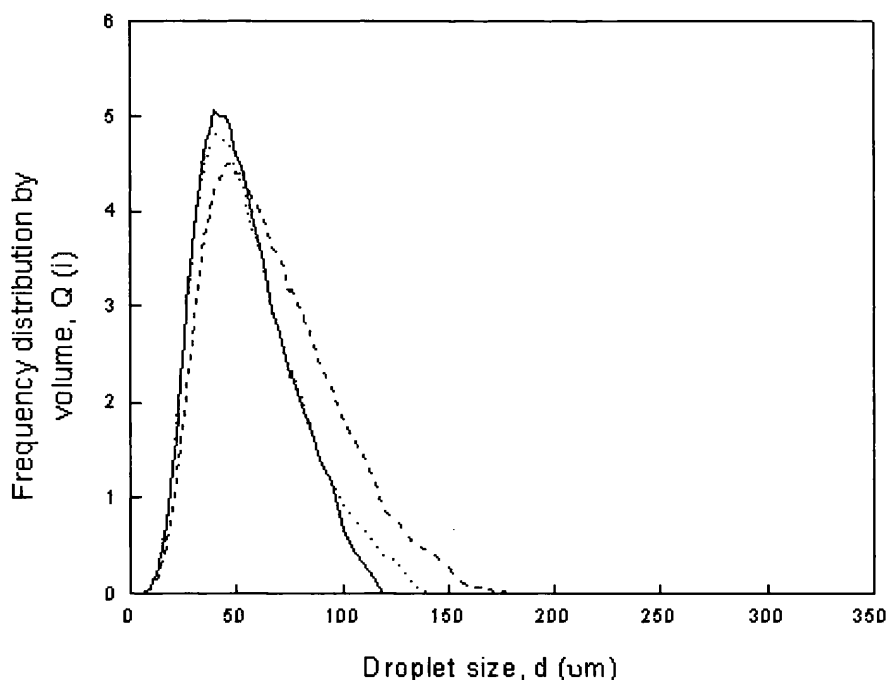


**Figure 6.11** Droplet size frequency distribution by volume for a 20 % v/v toluene-aqueous system in the absence of substrate or biomass: (—) 3 L reactor at 900 rpm; (---) 75 L reactor for scale-up using constant P/V at 459 rpm; (- -) 75 L reactor with scale-up using constant tip speed criteria at 328 rpm. Droplet size measured as described in Section 2.6.2.5.

Finally, Figure 6.12 shows the Sauter mean drop diameters determined from the drop size distribution data obtained in the 75 L reactor for both the ‘clean’ and biomass-containing phase systems. The trends are similar to those found at the 3 L scale (Figures 6.3-6.5) with  $d_{32}$  values decreasing with increasing impeller speed and the mean drop sizes obtained in the system with  $15 \text{ g}_{\text{ww}}\cdot\text{L}^{-1}$  of biomass present being around 25% smaller than those in the ‘clean’ phase system. Figure 6.12 also shows the predicted  $d_{32}$  values obtained using the various correlations described in Table 6.1 again adjusted to take account of the difference in power input as described in Section 6.3.3.1. As also found at the 3 L scale (Figure 6.6), the Chen and Middleman correlation (Chen and Middleman, 1967) was the most appropriate for the ‘clean’ phase system, over predicting  $d_{32}$  values by 25 – 118 %. The Godfrey and Grilc correlation (Godfrey and Grilc, 1977) was again the most appropriate for the system with biomass present, under predicting  $d_{32}$  values by 38 - 65%. Predictions from both correlations again show the closest agreement with the experimental values at the highest agitation rates used.

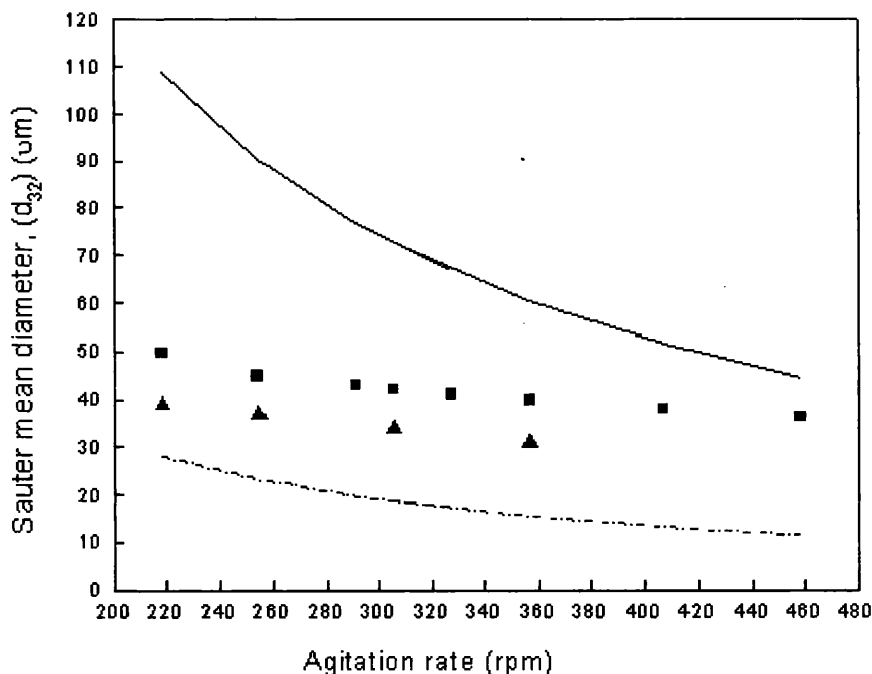


**Figure 6.12** Sauter mean diameter ( $d_{32}$ ) against agitation rate in 20% v/v toluene-aqueous systems in the 75 L reactor (■) without biomass present and (▲) with  $15 \text{ g}_{\text{ww}}\cdot\text{L}^{-1}$  biomass present. Lines show predicted  $d_{32}$  values using correlations from Table 1 corrected for increased power input: (solid line) Chen and Middleman predictions for the biomass-free system; (dashed line) Godfrey and Grilc predictions for the biomass-containing system. Droplet size measurements were performed as described in Section 2.6.2.5.

## 6.4 CONCLUSIONS

Maintenance of interfacial area is one of the key requirements for successful and reproducible scale-up of two-liquid phase biotransformation processes. This Chapter demonstrates that constant power input per unit volume appears to be the best basis for predictive scale-up using both 'clean' phase systems and ones containing resting whole cell biocatalysts. For both types of phase system Sauter mean drop diameters and drop size distributions were very similar for scale-up on this basis from 3 L to 75 L scale in geometrically similar reactors. In all cases the drop size distributions obtained were Log-normal and the Sauter mean droplet diameters could be adequately predicted by available literature correlations.

The results presented in this work were obtained in a particular bioreactor geometry for the defined bioreactor two-phase system (Chapter 4) comprising 20% v/v toluene dispersed in an aqueous buffer containing 15 g<sub>ww</sub>.L<sup>-1</sup> of a *Rhodococcus* R312 biocatalyst. While the general trends observed could be expected to apply to a range of bioconversion processes the actual magnitude of the Sauter mean drop diameters obtained, and hence the interfacial area available for solute mass transfer, will be system specific. In this respect the scale-down methodology demonstrated here would allow the rapid experimental evaluation of specific systems using the minimum quantity of substrate and biocatalyst with a 25-fold reduction in scale. In this way problems that might be encountered at the large scale, due to carry over of antifoam from the fermentation stage or the release of surface active cellular components due to cell lysis, could be rapidly and efficiently identified.

Having investigated the influence of scale-up on the measured hydrodynamics of the system and hence the interfacial area the next chapter will examine the actual biotransformation profiles at 3 L and 75 L scales using both P/V and tip speed as scale-up criteria.

# 7. SCALE-UP OF TWO-PHASE AROMATIC NITRILE HYDRATION

## 7.1 INTRODUCTION

Chapter 6 investigated the maintenance of constant interfacial area as a means to compare the criteria of power per unit volume and tip speed for the scale-up of the bioreactor hydrodynamics. In this chapter the implications of scale-up on the biotransformation in the 75 L bioreactor are investigated. As previously stated in the introduction (Section 1.7) there is currently very little literature available on the scale-up of two-phase bioreactors. This chapter will bring together the findings of Chapters 4 and 6, which covered optimal biotransformation conditions and the criteria for the maintenance of constant interfacial area. It will use these results to operate the two-phase 75 L bioreactor under the scale-up regimes of P/V and tip speed.

### 7.1.1 Objectives

This chapter will focus on scale-up of the two-phase biotransformation process described in Chapter 4 for constant power per unit volume and tip speed regimes on the kinetics of the biotransformation. The number of 75 L biotransformation experiments that could be performed were limited by the mass of biocatalyst that could be produced in one 450 L fermentation batch in order that all biotransformations were from the same batch of cells. Therefore initially biotransformation kinetics will be examined in the 3 L scale-down reactor described in Chapter 6. The selected conditions will then be scaled-up to 75 L on the basis of P/V and tip speed.

## 7.2 MATERIALS AND METHODS

### 7.2.1 Chemicals and microorganism

The organic solvents and biological agents used in this chapter are as described in Section 2.1.

### 7.2.2 Experimental methods

Production of the whole cell *Rhodococcus* biocatalyst using 7, 20 and 450 L fermenters is as described in Sections 2.3.2.1, 2.3.2.2 and 2.3.2.3 respectively. Cells were prepared for 3 L and 75 L two-phase biotransformation experiments as described in Sections 2.4.1 and 2.4.2. The vessels used for the 3 L and 75 L biotransformation studies are as described in Section 2.6.2.1. Biotransformation experiments in the 3 L and 75 L bioreactors were performed as described in 2.6.2.2 and 2.6.2.3 respectively.

## 7.3 RESULTS AND DISCUSSION

### 7.3.1 Selection of agitation rates for scale-up studies

Due to the limitation of fermentation capacity the amount of biomass available for the large scale biotransformation experiments was limited to the amount that could be produced in one batch fermentation performed in the 450 L fermenter. Further, the cost and time constraints of the project meant that only one 450 L batch of biocatalyst could be produced for these experiments. Assuming a biomass recovery of approximately  $10 \text{ g}_{\text{ww}} \cdot \text{L}^{-1}$  biomass and allowing for the 300 L working volume in the fermenter ensured that sufficient biomass would be produced for four 75 L biotransformations and corresponding 3 L biotransformations. Thus only two experiments in 3 L bioreactors had to be selected for scale-up assuming that both rates would be scaled on the basis of power per unit volume and tip speed.

The effect of agitation rate in the 3 L bioreactor was investigated in a series of initial two-phase biotransformations. Biotransformations were performed over a range of agitation rates from 600 to 900 rpm, as described in Section 2.6.2.2, corresponding to the agitation rates used in the drop size investigation in Chapter 6. Sufficient biomass for these four agitation rates was initially produced in the 20 L fermenter (Section 2.3.2.2) to allow for a fair comparison of the biotransformation results. The kinetic profiles for all the agitation rates showed a steady concentration of 1,3-DCB substrate in the aqueous phase of  $\sim 0.5 \text{ g.L}^{-1}$ . However, there was a noticeable difference in the rates of amide production as can be seen from Figure 7.1. Agitation rates of 600 to 700 rpm produced a slightly enhanced amide profile under optimised conditions. 600 and 700 rpm achieved initial rates of amide production of  $0.144 \text{ mM.min}^{-1}$  and  $0.1574 \text{ mM.min}^{-1}$  respectively compared to the previous shake flask experiments described in Chapter 4 (Fig 4.10) which produced amide at an initial rate of  $0.1 \text{ mM.min}^{-1}$ .

Thus modest agitation appears to have a beneficial effect on the biotransformation due to improved solute mass transfer. This is most likely due to a larger interfacial area in the agitated system. It is apparent however that the higher agitation rates had a damaging effect on the biocatalyst as can be seen in the decline in amide product concentration from 800 to 900 rpm. Thus at higher agitation rates the biotransformation kinetics are not improved by the enlarged interfacial area and improved mass transfer. This may possibly be due to shear effects on the biocatalyst or inhibition of the NHase enzyme due to the increased supply of substrate (The  $C_{\text{aq}}$  of 1,3-DCB in the agitated 3 L bioreactor was  $\sim 0.5\text{-}0.6 \text{ g.L}^{-1}$  compared to  $\sim 0.35 \text{ g.L}^{-1}$  in the optimised shake flask biotransformation shown in Figure 4.10). Although there was an obvious effect of agitation on the rate of amide production there was no apparent change in the kinetics of acid production and this is therefore not displayed.

Based on the results shown in Figure 7.1 agitation rates of 600 and 700 rpm were selected for scale-up biotransformation experiments since they showed similar or improved kinetics compared to chapter 4.

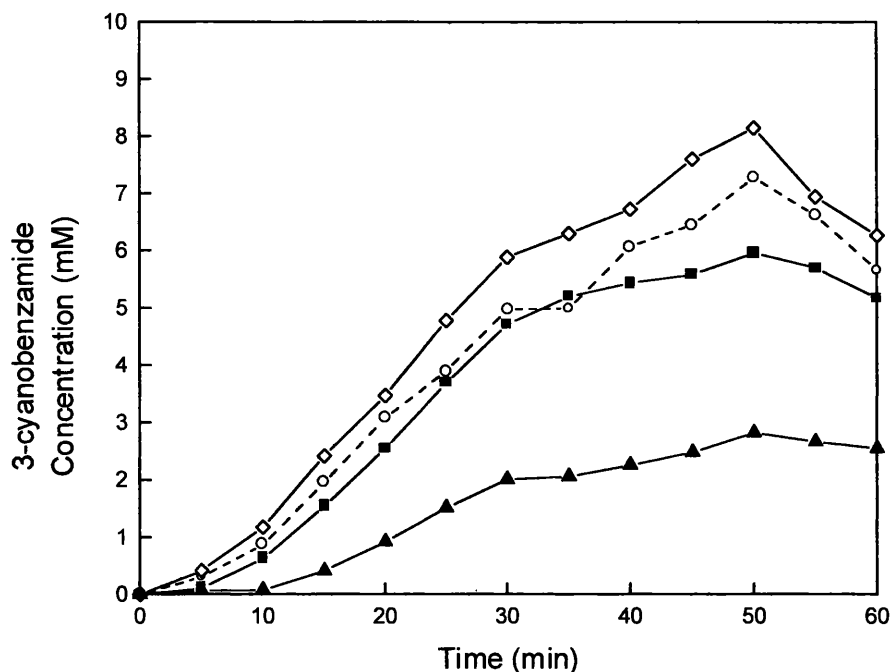


**Figure 7.1** Kinetics of 3-cyanobenzamide production over a range of agitation rates in the 3 L bioreactor; (○) 600 rpm, (◇) 700 rpm, (■) 800 rpm, (▲) 900 rpm. Cells produced as described in Section 2.3.2.3 and harvested at 31 hours. Biotransformations were performed as described in Section 2.6.2.2.

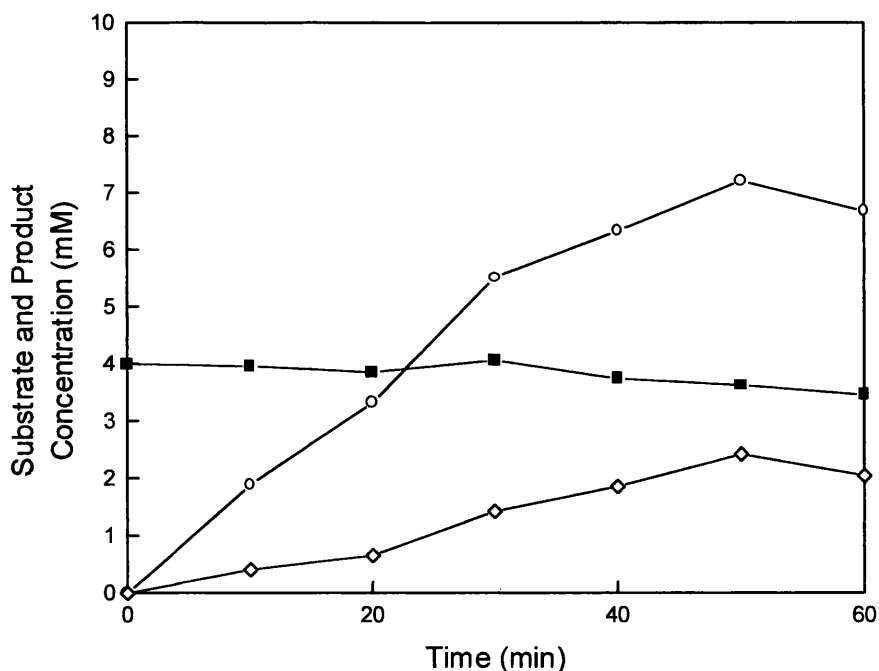


**Figure 7.2** Two-phase *Rhodococcus* R312 biotransformation kinetics at an agitation rate of 600 rpm in a 3 L bioreactor; (■) 1,3-DCB, (○) 3-CB, (◇) 3-CA. Cells produced as described in Section 2.3.2.3 and harvested at 16 hours. Biotransformation was performed as described in Section 2.6.2.2.

### 7.3.2 Biomass production and processing

The 450 L fermentation was performed as described in detail in Chapter 3. After processing the fermentation broth through a Carr powerfuge (Section 2.4.2) approximately 3.6 kg of solid biomass was recovered which was then stored in polythene bags at 4°C. Prior to use this equates to a total bioprocess production of ~12 g.L<sup>-1</sup> from the 300 L of fermentation broth. The amount of biomass produced was sufficient for four 75 L reactor biotransformation experiments and corresponding 3 L reactor experiments.

#### 7.3.3 3 L scale biotransformation experiments

The biotransformation experiments in the scaled down 3 L reactor at 600 and 700 rpm were performed using biomass from the 450 L fermentation as described in Section 2.6.3.8 resuspended in pH 7 phosphate buffer. As can be seen in Figures 7.2 and 7.3 the kinetic profiles of 1,3-DCB mass transfer to the aqueous phase and amide and acid production correspond closely to the profiles of the optimised shake flask experiments described in Section 4.3.3 (Figure 4.10). The maximum production of amide was improved by 20 % and 31 % at 600 and 700 rpm respectively. The kinetic profiles shown in Figure 7.2 and 7.3 will now be used to compare the performance of 75 L scale biotransformations scaled-up on the basis of either constant tip speed or constant P/V.

#### 7.3.4 75 L scale biotransformation experiments

The biomass for each 75 L biotransformation was prepared and stored as described in section 2.4.2. Sufficient biomass to achieve a concentration of 15 g.L<sup>-1</sup> in 50 L of potassium phosphate buffer pH 7 was removed from the fridge and resuspended in a mixing vessel using a paddle. After ensuring complete resuspension of the biocatalyst in the mixing vessel it was transported to the solvent suite. The biomass phase was then pumped into the bioreactor. The substrate containing toluene phase was then carefully pumped (to prevent mixing) into the reactor on top of the aqueous phase, the agitator was set to the required

speed and the ORM probe activated to monitor the drop size for the duration of the experiment as described in Section 2.6.2.3.

The reactor agitation rate used are as given previously in Table 6.3 for scale-up of the 3 L experiments at 600 and 700 rpm under constant P/V and tip speed regimes. Unfortunately the biomass during the first attempt at 255 rpm (700 rpm scaled-up under a tip speed regime) was not suspended sufficiently and a large biomass residue was recovered from the mixing vessel after the liquid had been pumped into the bioreactor. The biotransformation profile produced showed negligible production of amide and acid as a consequence of the low concentration of biocatalyst in the reactor (probably  $< 2 \text{ g}_{\text{ww}}\cdot\text{L}^{-1}$ ), the data is not shown. The three subsequent 75 L scale experiments at 218, 305 and 357 rpm were successful and the biotransformation profiles are shown in Figures 7.4, 7.5 and 7.6 respectively.

As can be seen from all three profiles the mass transfer of 1,3-DCB to the aqueous phase was similar in all cases. This can be explained on the basis of similar interfacial areas ( $d_{32} = 40\text{-}35 \mu\text{m}$ ) as shown in Figure 6.5. But the production of 3-cyanobenzamide was severely reduced in all three 75 L reactors compared to the 3 L reactor. Even compared to the non-impeller agitated optimised reaction (4.10) all three reactors under-produced 3-cyanobenzamide by 58 %, 52 % and 62 % (on the basis of aqueous 3-cyanobenzamide peak concentration) at 218, 305 and 357 rpm respectively. However, the reduction in 3-cyanobenzamide production did not effect the production of 3-cyanobenzioc acid. The production profile of 3-cyanobenzoic acid in the three 75 L reactors (7.4-7.6) was very similar to that of the two 3 L reactors (7.2 and 7.3). This suggests that the reduction phenomenon is limited to the NHase enzyme. This under performance may be due to increased shear rates in the larger reactor, zones of poor mixing in the reactor, different cell recovery from the 450 L fermentation or the duration and method of storage of the biomass.

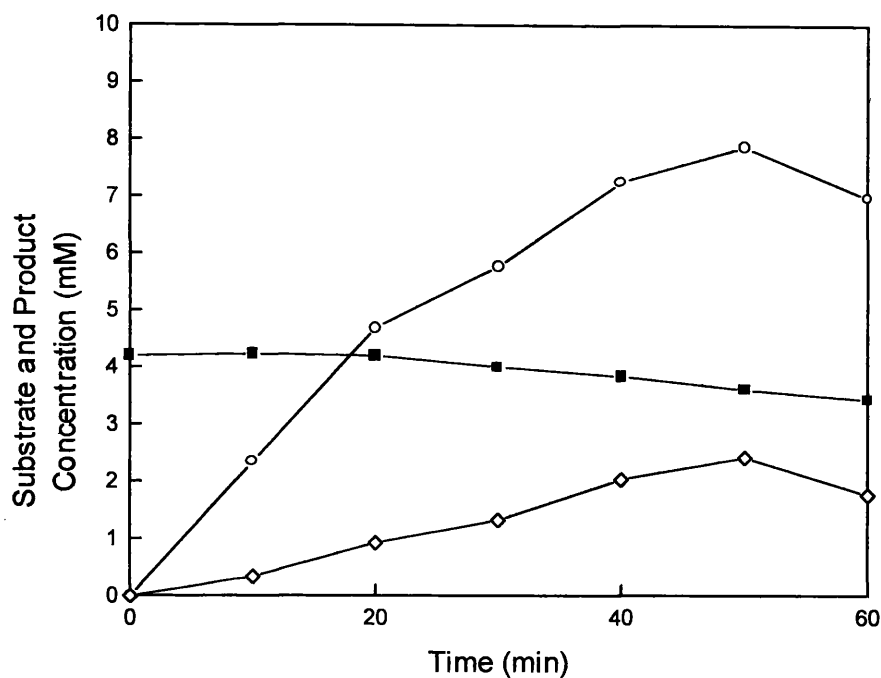


**Figure 7.3** Two-phase *Rhodococcus* R312 biotransformation kinetics at an agitation rate of 700 rpm in a 3 L bioreactor; (■) 1,3-DCB, (○) 3-CB, (◇) 3-CA. Cells produced as described in Section 2.3.2.3 and harvested at 16 hours. Biotransformation was performed as described in Section 2.6.6.2.

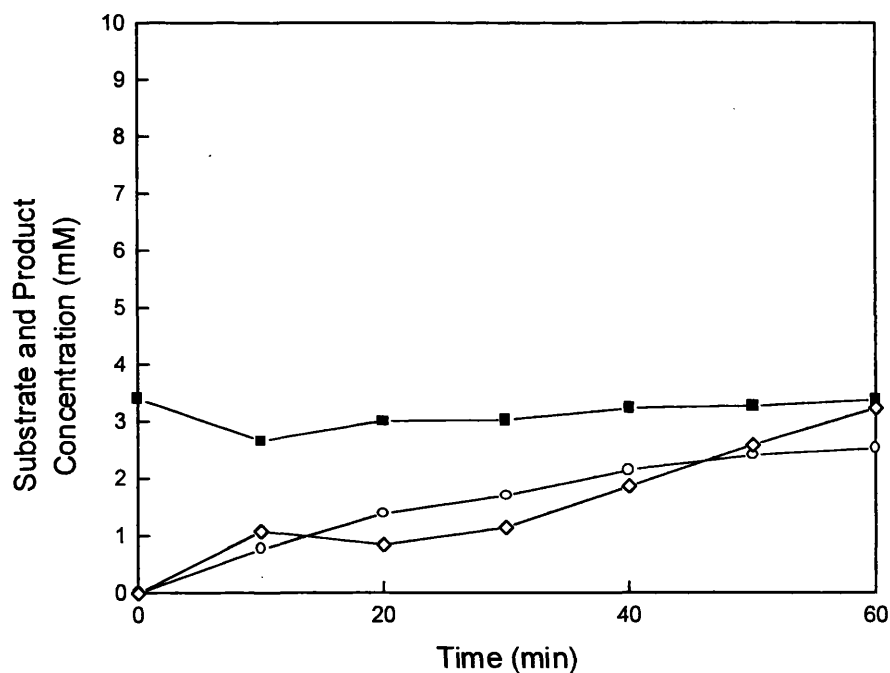


**Figure 7.4** Two-phase *Rhodococcus* R312 biotransformation kinetics at an agitation rate of 218 rpm in a 75 L bioreactor (equivalent to 600 rpm in the 3 L reactor scaled-up at constant tip speed); (■) 1,3-DCB, (○) 3-CB, (◇) 3-CA. Cells produced as described in Section 2.3.2.3 and harvested at 16 hours. Biotransformation was performed as described in Section 2.6.2.3.

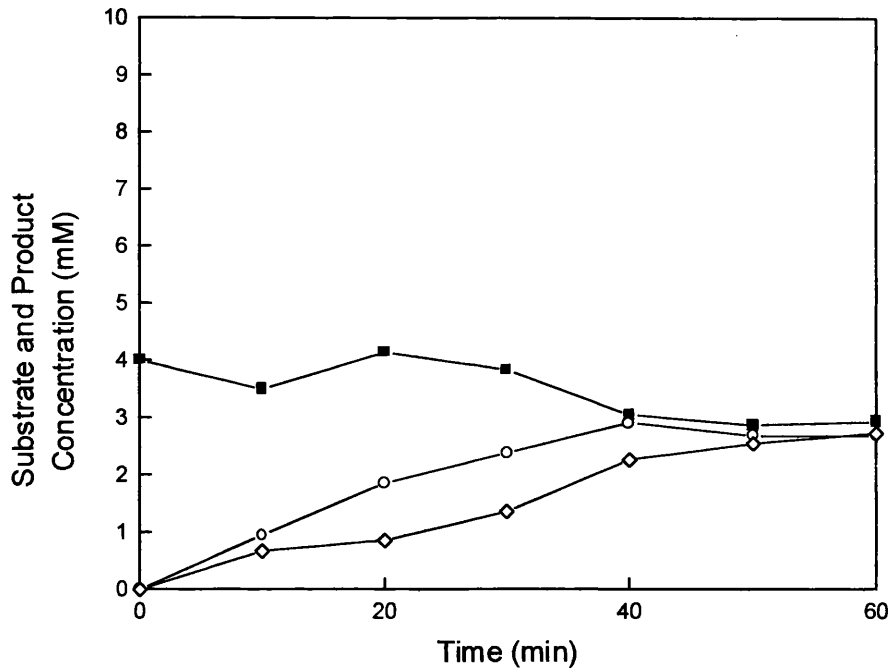


**Figure 7.5** Two-phase *Rhodococcus* R312 biotransformation kinetics at an agitation rate of 305 rpm in a 75 L bioreactor (equivalent to 600 rpm in the 3 L reactor scaled-up at constant P/V); (■) 1,3-DCB, (○) 3-CB, (◇) 3-CA. Cells produced as described in Section 2.3.2.3 and harvested at 16 hours. Biotransformation performed as described in Section 2.6.2.3.

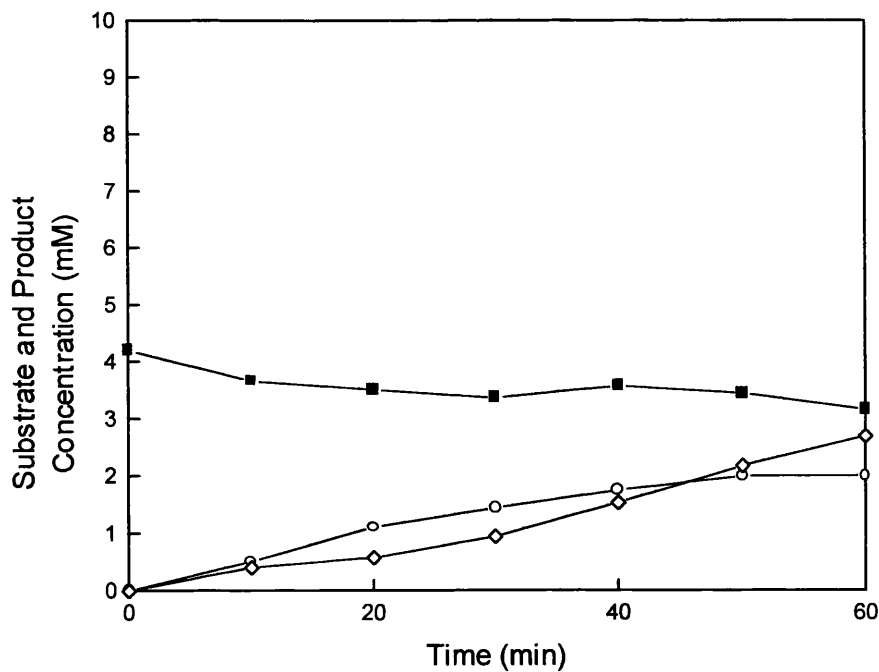


**Figure 7.6** Two-phase *Rhodococcus* R312 biotransformation kinetics at an agitation rate of 357 rpm in a 75 L bioreactor (equivalent to 700 rpm in the 3 L reactor scaled up at constant P/V); (■) 1,3-DCB, (○) 3-CB, (◇) 3-CA. Cells produced as described in Section 2.3.2.3 and harvested at 16 hours. Biotransformation performed as described in Section 2.6.2.3.

Comparing the initial rates of amide and acid production in the 75 L reactor shows that overall P/V scale-up results in a more rapid production of amide and acid. The initial rates for amide/acid production were 0.05/0.03 mM.min<sup>-1</sup>, 0.07/0.04 mM.min<sup>-1</sup> and 0.03/0.05 mM.min<sup>-1</sup> at 218, 305 and 357 rpm respectively. So in comparing the scale-up of 600 rpm the P/V initial rate 0.07/0.04 mM.min<sup>-1</sup> is higher than the tip speed initial rate 0.05/0.03 mM.min<sup>-1</sup>. The lower performance of tip speed scale-up may well be due to poor mixing, this can be seen in Figure 6.5 where the tip speed interfacial area is 39 μm and the P/V interfacial area is 35 μm. However, it appears that P/V scale-up at 700 rpm (357 rpm in 75 L) has started to reduce the initial rate of amide and acid production even though the interfacial area at 357 rpm is larger (34 μm) than the previous two speeds. This suggests shearing forces are a factor in enzyme efficacy at these agitation rates.

But scale-up on the basis of constant P/V produced the fastest initial rate of amide production. This is in agreement with the conclusion from Chapter 6 that power per unit volume is the better criterion for scale-up because it gives the most reproducible drop size distribution of the original scale.

## 7.4 CONCLUSIONS

This chapter has demonstrated that modest impeller agitation (600-700 rpm) in the 3 L bioreactor improves the production of 3-cyanobenzamide under the optimised biotransformation conditions for shake flask experiments described in chapter 4. Higher agitation rates above 700 rpm while shown to reduce mean drop size and hence increase the rate of substrate mass transfer have a detrimental effect on the biotransformation profile. Although the number of experiments was limited due to cost the scaled-up biotransformation experiments shown here would suggest that the conclusions of chapter 6 that the criterion of power per unit volume is the better method to use for this particular two-phase biotransformation is correct. However, why the production of 3-cyanobenzamide in the 75 L bioreactor is significantly reduced compared to the 3 L bioreactor is currently unknown and more experiments are required. This is examined in the discussion of the project that follows in the next chapter.

## 8. GENERAL DISCUSSION AND CONCLUSIONS

### 8.1 GENERAL DISCUSSION

This project has investigated the process design, optimisation and scale-up for the two-phase biotransformation of 1,3-DCB by *Rhodococcus* R312. This thesis has addressed all of the aims and objectives as defined Section 1.9 and has reported on novel findings in process design, the use of ionic liquids and two-phase hydrodynamics and scale-up. This final chapter will conclude the findings of this project and will also suggest areas for future work.

#### 8.1.1 BIOCATALYST PRODUCTION

Although there are number of examples of *Rhodococcus* R312 fermentations in the literature the production of the biocatalyst had to be investigated as part of the process design for this project as defined by objective A). Therefore it was necessary to define the media used and the production of biocatalyst. Due to the scale-up of the bioconversion it was also necessary to scale-up the production of biocatalyst.

The whole cell biocatalyst *Rhodococcus* R312 was selected for the project. The microorganism is known to have a regioselective NHase and no nitrilase and has been the subject of many investigations involving nitrile biotransformations (Yamada and Kobayashi, 1996; Cohen *et al.*, 1992; Beard *et al.*, 1993; Crosby *et al.*, 1994; Meth-Cohn and Wang, 1997b). A separate investigation (data not shown) demonstrated that the isolation of the NHase for process purposes would be impractical. Therefore a fermentation process had to be selected that would rapidly produce high volumes of active biomass. Initial fermentation experiments confirmed previous reports that the NHase was constitutive. In total three fermentation media were used. *Rhodococcus* 312 cultivated on the first, a specific

media (Kerridge, 1995) grew slowly and achieved low biomass production. An alternative was investigated and a rich growth medium (Nagasawa *et al.*, 1986) was used instead. This produced modest biomass growth in 48 hours of  $\sim 3\text{-}5 \text{ g}_{\text{ww}}\cdot\text{L}^{-1}$ , ( $\sim 1 \text{ g}_{\text{dcw}}\cdot\text{L}^{-1}$ ), which was used for the optimisation and ionic liquid experiments described in Chapters 4 and 5. However, to produce sufficient biomass for the 75 L biotransformations (chapters 6 and 7) another medium had to be used that would increase the biomass production within the fermenter. A rich proprietary medium Tryptic Soy Broth (TSB) was chosen and this produced much higher concentrations of biomass,  $\sim 25 \text{ g}_{\text{ww}}\cdot\text{L}^{-1}$ , ( $\sim 7 \text{ g}_{\text{dcw}}\cdot\text{L}^{-1}$ ).

Scale-up of the fermentation process was on the basis of constant tip speed to reduce any shearing effect on the biomass. Due to the time and cost constraints of the project only one 450 L fermentation could be attempted and this was successful as previously described in Section 3.4.

### 8.1.2 BIOCONVERSION PROCESS DESIGN AND OPTIMISATION

Project objectives A) covered the design of the investigation, optimisation and process design for the application of a second organic phase to increase the production of 3-cyanobenzamide. The production of 3-cyanobenzamide is of interest because no chemical process for its manufacture currently exists. Also, the biotransformation of poorly water soluble nitriles in general is of interest due to the number of processes being developed that incorporate the NHase enzyme (Yamada and Kobayashi, 1996; Eyal and Charles, 1990a; Eyal and Charles, 1990b). The process to produce this molecule is also of value because it provides an interesting case study into how process engineering can be used to overcome difficulties associated with competing enzyme activities. The bioprocess also provided a model system to study the scale-up of two-phase bioprocess in Chapters 6 and 7.

Initial experiments showed that the NHase had an optimal activity under mild conditions (20-30°C, pH 7-8). Whereas the amidase activity was favoured by a warmer temperature (40°C). Therefore the temperature and pH of the biotransformation were run under mild conditions to favour production of 3-

cyanobenzamide. After screening the literature and common solvents for biocompatibility and substrate solubility toluene was finally selected as the organic solvent for the process due its biocompatibility (Log P of 2.9) and substrate solubility of  $\sim 30 \text{ g.L}^{-1}$ . Although other solvents were more biocompatible or had higher substrate solubilities toluene had the best combination of these characteristics. Having selected the organic solvent the characteristics of the biotransformation were recorded in a process constraints table and the operating parameters of the two-phase biotransformation were defined. The three characteristics that had the greatest effect on the space-time yield of 3-cyanobenzamide were: biocatalyst concentration, substrate concentration and solvent phase volume ratio. These were optimised and combined into a window of operation (Woodley and Titchener-Hooker, 1996) as shown in Figure 4.9. This allowed the operational space to be rapidly determined. It was found that at near substrate saturation conditions ( $25 \text{ g.L}^{-1}$ ), at a phase volume ratio of 0.2 and at  $12.5 \text{ g}_{\text{ww}}.\text{L}^{-1}$  biocatalyst concentration that the greatest production of 3-cyanobenzamide was achieved. Although these conditions favour the production of 3-cyanobenzamide the conversion to 3-cyanobenzoic acid does occur due to the presence of an amidase. The only way to avoid this outcome would be to extract and isolate the NHase but this was attempted in a separate project and proved to be disappointing. Alternatively, an inhibitor molecule could be added to the biotransformation to inhibit the amidase. In this case urea was tried as an inhibitor but failed to cause any change in the biotransformation profile. This demonstrates the limitations of process engineering in this particular process. Optimising the reactor conditions could not completely eliminate the amidase activity. To improve the process a mutant would have to be developed by molecular biology methods. Such a mutant could either over-express its NHase or have its amidase gene switched off or deleted.

For potential future development of the project the constraints of the downstream processing should be considered. Figure 8.1 shows a second semi-quantitative operating window that has been constructed and on which constraints imposed by the subsequent downstream processing of the biotransformation mixture have been identified. The variable related to the concentration of 1,3-DCB in the toluene phase has been fixed by assuming the reactor will be operated under conditions

close to the saturation limit of the substrate (to ensure the highest space-time yield). There is a significant interaction between the reactor operating conditions and the ease of the phase separation step; operation at low dispersed phase volume fractions or high biomass concentration, which promote stable emulsion formation, will make the recovery of the dispersed phase considerably more difficult (Lye and Woodley, 2001).

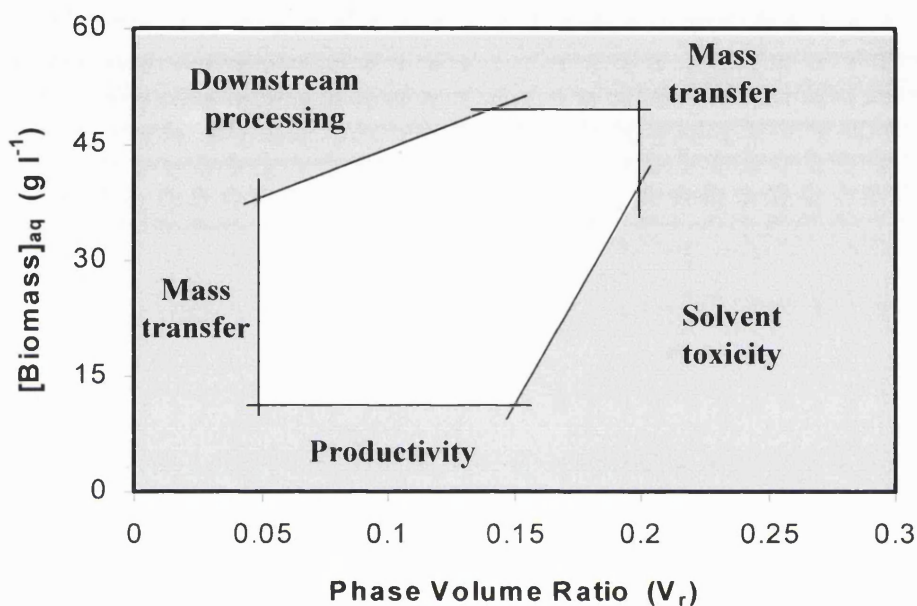


**Figure 8.1** Operating window for operation at  $[1,3\text{-DCB}]_{\text{org}} = 25 \text{ g.L}^{-1}$  showing further constraints imposed by downstream processing considerations.

### 8.1.3 USE OF IONIC LIQUIDS

Objective C) as stated in Section 1.9 was to investigate the application of ionic liquids as potential replacements for organic solvents that are currently used in two-phase bioprocesses. They have a number of advantages over organic solvents in that they are non-volatile, non-flammable and have a low toxicity. They may also be considered as 'designer solvents' due their tuneable physicochemical properties. Thus rather than screening organic solvents for use with substrates/products and biocatalysts, ionic liquids can potentially be designed to fit the specific needs of a process.

This project has shown for the first time that ionic liquids can be applied successfully to a two-phase bioprocess. In this instance the aqueous-toluene system and aqueous-[bmim][PF<sub>6</sub>] reaction profiles were very similar. The concentration of substrate in the aqueous phase in the aqueous-[bmim][PF<sub>6</sub>] system was lower than in the aqueous-toluene system due to the significantly higher viscosity of [bmim][PF<sub>6</sub>] ( $2.9 \times 10^{-1} \text{ Kg.m}^{-1}.\text{s}^{-1}$ ) compared to toluene ( $5.1 \times 10^{-4} \text{ Kg.m}^{-1}.\text{s}^{-1}$ ) which reduced the rate of substrate mass transfer. It is likely that by altering the chemistry of [bmim][PF<sub>6</sub>] the reduced rate of mass transfer can be overcome. Activity experiments demonstrated that the specific activity of the biocatalyst in the aqueous-[bmim][PF<sub>6</sub>] was an order of magnitude greater than the aqueous-toluene system which shows that when the properties of low toxicity and low solubility can be combined in a given ionic liquids will be excellent alternatives to organic solvents. However, ionic liquids still have to be shown to work with other biocatalysts and other substrates as well as be integrated into a full bioprocess to demonstrate their efficacy. They are also currently time consuming and costly to produce which is likely to remain a bottleneck for bioreactor investigations above lab scale.

Recently others have shown (Roberts and Lye, 2001) that the biocatalyst *Rhodococcus* R312 remains viable in both single phase and biphasic ionic liquid systems and that a number of isolated enzymes can function effectively in ionic liquids. Which indicates that the biocatalysts used with ionic liquids are recyclable.

#### 8.1.4 TWO-PHASE BIOREACTOR HYDRODYNAMICS

Chapter 6 addressed project objectives D). There is currently very little information on the phase behaviour and scale-up of two-phase biotransformations. Therefore the investigation in Chapter 6 was of interest because knowledge of drop size and drop distribution will provide an indication on the relative size of the interfacial area available for mass transfer and allow workers to further define and characterise a two-phase bioprocess. Thus knowledge of the hydrodynamics of the bioreactor can be used as in the case in Chapter 6 to assess the success of different scale-up criteria. In this case the two most common criteria were compared (tip

speed and P/V) and P/V was found to be the best criterion for this particular bioprocess. Scale-up on the basis of tip speed produces a reduced rate of agitation at 75 L compared to P/V scale-up. Whereas P/V scale-up produced conditions that were close to the original 3 L profile in terms of  $d_{32}$  and drop size distribution, tip speed agitated mixtures formed a greater number of large drop sizes which can be seen in Figure 6.8-6.11. This relationship was found to be the same for both a 'clean' aqueous-toluene system and systems containing up to  $15 \text{ g}_{\text{ww}}\cdot\text{L}^{-1}$  biocatalyst. However, the addition of biomass did cause a reduction in  $d_{32}$  compared to a clean system indicating that the surface properties of the biocatalyst caused a reduction in coalescence of drops in the dispersed phase.

A number of correlations exist in the literature for chemical processes that allow workers to predict the change in  $d_{32}$  in a reactor based on the systems physical characteristics and changes in agitation rate or scale. Currently there are no published correlation equations or protocols for prediction of  $d_{32}$  values in bioprocesses so the suitability of chemical system correlations was investigated. Correlations were selected from the literature on the basis of the similarity of the physical characteristics for the systems they were used in. Two equations were shown to predict  $d_{32}$  values close to those recorded with the ORM instrument as shown in Figure 6.6 (Chen and Middleman, 1967; Godfrey and Grilc, 1977). However, it is apparent that more accurate correlation equations need to be developed for bioprocesses that take into account the low interfacial tension values (in this case  $0.0013 \text{ Kg}\cdot\text{s}^{-2}$ ) caused by the presence of the biocatalyst.

### 8.1.5 TWO-PHASE BIOCONVERSION SCALE-UP

Finally, in Chapter 7 the effect of impeller agitation and the implication of scale-up on the biotransformation profile, objective E), were investigated. All three 75 L biotransformation profiles were significantly reduced compared to the 3 L reactor. This could be due to the effect of shearing in the bioreactor or possibly due to the processing of the biocatalyst. The biocatalyst was not washed twice with buffer after the 450 L fermentation unlike biomass produced using small shake flask fermentations. However, cells from the same batch were used to for the 3 L

agitated biotransformations (Figure 7.2 & 7.3) which gave exceptional profiles compared to a non-impeller agitated biotransformation. Therefore the reduced profiles in the 75 L reactors may well be due to shearing or duration of storage. But, the profiles observed in 7.4-7.6 are more complex than this. While 3-cyanobenzamide production is reduced 3-cyanobenzoic acid production proceeds as if the reaction were optimised. This suggests that whatever phenomenon is reducing 3-cyanobenzamide production may only be damaging the NHase.

## 8.2 CONCLUSIONS

1. The space-time production of amide product can be improved at least 90 fold by the application of an optimised two-phase bioprocess to the biotransformation of poorly water soluble nitriles compared to a single aqueous phase process. The process also increases the relative quantities of amide and acid production.
2. The two-phase bioprocess described in this project was successfully scaled-up from 3 L to 75 L on the basis of P/V and tip speed criteria. Hydrodynamic data demonstrated that scale-up under a P/V regime reproduced the drop size and distribution conditions of the 3 L reactor more accurately than tip speed.
3. Ionic liquids can be successfully substituted for organic solvents in two-phase bioprocesses. Their properties make them an ideal 'green' replacement for organic solvents in the increasingly environmentally conscious pharmaceutical and chemical manufacturing industries.
4. 75 L Scale-up of the biotransformation results in a significant decline in the space-time production of 3-cyanobenzamide but the production of 3-cyanobenzoic acid remains the same as in the 3 L bioreactor.

### 8.3 FUTURE WORK

The focus of this project was the optimisation and scale-up of a two-phase bioprocess. Therefore, the production of the catalyst used protocols currently described in the literature. To increase the biomass production of *Rhodococcus* R312 for the 75 L bioreactor the 450 L TSB fermentation needs to be optimised to produce the highest possible concentration of biomass for the bioprocess. This could be achieved by investigating the use of fed batch feeding strategies.

The process could be improved by creating a mutant *Rhodococcus* that either over-expresses NHase enzyme or has its amidase enzyme removed. Choosing another phase such as an ionic liquid may also improve the activity of the enzyme and increase space-time yield of 3-cyanobenzamide. However, the low toxicity of the ionic liquid would have to be combined with a low viscosity that would at least maintain the current mass transfer rate of substrate and ideally improve this characteristic.

The process could also be further characterised by the development and evaluation of mathematical models such as those developed by Chae and Yoo (1997) and Shin and Kim (1999). This would require Lewis cell experiments to determine the rate of mass transfer.

Ionic liquid biotransformations are still at an early stage of understanding and much more work is required. There are numerous important enzyme catalysed biotransformations still to be investigated with single phase and biphasic ionic liquids. Also the relationship between the state of the cell in the ionic liquid needs to be established. The impact of ionic liquid on cellular membranes also needs to be investigated as well as its interaction with micro-organisms with different physiology i.e. Gram positive and Gram negative bacteria. This could then lead to a suitable scale of toxicity such as Log P that is used for organic solvents.

Finally, a whole range of issues using ionic liquids in a commercial bioprocess needs to be investigated. These include engineering issues such mixing and phase

separation, diffusion and mass transfer, product recovery and the actual design and optimisation of an ionic liquid process. Also a number of industrial and regulatory issues need to be addressed such as the disposal of ionic liquids, their production and regulatory approval required by the pharmaceutical industry for their use.

Computer models and bioprocess specific correlations should also be developed that will allow the mixing and mass transfer of a bioprocess to be viewed and optimised before experimental work begins. This would reduce bioprocess development time and make bioprocesses development more competitive with chemical processes.

Although the experiments in chapter 7 indicate that scale-up on the basis of P/V produces the higher space-time production of 3-cyanobenzamide the results are limited and the interpretation is not fully understood. Further experimentation needs to be done at the 75 L scale both as replicates of the same agitation rates and also over a greater range of agitation rates to assess both scale-up criteria. Further experimentation will also see if higher or lower agitation rates will improve the space-time production of 3-cyanobenzamide to that of the agitated 3 L reactor. A set of experiments to investigate the role of shear in the biotransformation should also be conducted, such as assay for protein release, as shear rates may become significant under P/V scale-up.

## 9. REFERENCES

**Abdul-Sada, A.K., Ambler, P.W., Hodgson, P.K.G., Seddon, K.R. and Stewart, N.J.** (1995a.). Ionic liquids. *World patent*, WO95/21871.

**Abdul-Sada, A.K., Atkins, M.P. Ellis, B., Hodgson, P.K.G., Morgan, M.L.M. and Seddon, K.R.** (1995b.). Alkylation Process. *World patent*, WO95/21806.

**Adams, C.J., Earle, M.J. and Seddon, K.R.** (1999). Stereoselective hydrogenation reactions in chloroaluminate(III) ionic liquids: a new method for the reduction of aromatic compounds. *Chemical Communications*, **11**, 1043-1044.

**Ambler, P.W., Hodgson, P.K.G. and Stewart, N.J.** (1996). Butene polymers. *European patent application*, EP/0558187A0558181.

**Armenante, P.M. and Chang, G.M.** (1998). Power consumption in agitated vessels provided with multiple-disk turbines. *Industrial & Engineering Chemical Research*, **37**, 284-291.

**Asano, Y., Fujishiro, K., Tani, Y. and Yamada, H.** (1982). Aliphatic nitrile hydratase from *Arthrobacter* sp. J-1, purification and characterization. *Agricultural Biological Chemistry*, **46**, 1165-1174.

**Atkinson, B. and Mavituna, F.** (1991). Scale-up of processes. *Biochemical Engineering and Biotechnology Handbook*, 2<sup>nd</sup> edition, Macmillan, Basingstoke.

**Baldyga, J., Bourne, J.R., Pacek, A.W., Amanullah, A. and Nienow A.W.** (2001). Effects of agitation and scale-up on drop size in turbulent dispersions: allowance for intermittency. *Chemical Engineering Science*, **56**, 3377-3385.

**Ballesteros, A., Boross, L., Buchholz, K., Cabral, J.M.S. and Kasche, V.** (1994). Chapter 5: Biocatalyst Performance. *Applied Biocatalysis*, eds: Cabral,

J.M.S., Harwood Academic Publishers GmbH, Poststrasse 22, 7000 chur, Switzerland.

**Beard, T., Cohen, M.A., Parratt, J.S., Turner, N.J., Crosby, J. and Moilliet, J.** (1993). Stereoselective hydrolysis of nitriles and amides under mild conditions using a whole cell catalyst. *Tetrahedron: Asymmetry*, **4**, 1085-1104.

**Bengis-Garber, C. and Gutman, A.L.** (1989). Selective hydrolysis of dinitriles into cyano-carboxylic acids by *Rhodococcus rhodochrous* NCIB 11216. *Applied Microbiology and Biotechnology*, **32**, 11-16.

**Blakey, A.J., Colby, J., Williams, E. and O'Reilly, C.** (1995). Regio- and stereo-specific nitrile hydrolysis by the nitrile hydratase from *Rhodococcus* AJ270. *FEMS Microbiology Letters*, **129**, 57-62.

**Bonhôte, P., Dias, A.P., Papageorgiou, N., Kalyanasundaram, K. and Grätzel M.** (1996). Hydrophobic, highly conductive ambient-temperature molten-salts. *Inorganic Chemistry*, **35**, 1168-1178.

**Boye, A.M., Lo, M.-Y. A. and Shamlou, P.A.** (1996). The effect of two-liquid phase rheology on drop breakage in mechanically stirred vessels. *Chemical Engineering Communications*, **143**, 149-167.

**Brennan, B.A., Cummings, J.G., Chase, D.B., Turner, I.M. and Nelson, M.J.** (1996). Resonance raman spectroscopy of nitrile hydratase, a novel iron-sulphur enzyme. *Biochemistry*, **35**, 10068-10077.

**Brink, L.E.S. and Tramper, J.** (1985). Optimisation of organic solvent in multiphase biocatalysis. *Biotechnology and Bioengineering*, **27**, 1258-1269.

**Bruce, L.J. and Daugulis, A.J.** (1991). Solvent selection strategies for extractive biocatalysis. *Biotechnology Progress*, **7**, 116-124.

**Buckland, B.C., Dunnill, P. and Lilly, M.D.** (1975). The enzymatic

transformation of water- insoluble reactants in nonaqueous solvents. Conversion of cholesterol to cholest-4-ene-3-one by a *Nocardia* sp. *Biotechnology and Bioengineering*, **17**, 815-826.

**Bui, K., Fradet, H., Arnaud, A. and Galzy, P.** (1984a). A nitrile hydratase with a wide substrate spectrum produced by a *Brevibacterium* sp. *Journal of General Microbiology*, **130**, 89-93.

**Bui, K., Maestracci, M., Thiery, A., Arnaud, A. and Galzy, P.** (1984b). A note on the enzymic action and biosynthesis of a nitrile hydratase from a *Brevibacterium* sp. *Journal of Applied Bacteriology*, **57**, 183-190.

**Cabral, J.M.S., Aires-Barros, M.R., Pinheiro, H. and Prazeres, D.M.F.** (1997). Biotransformation in organic media by enzymes and whole cells. *Journal of Biotechnology*, **59**, 133-143.

**Carmichael, A.J., Earle, M.J., Holbrey, J.D., McCormac, P.B. and Seddon, K.R.** (1999). The Heck reaction in ionic liquids: A multiphasic catalyst system. *Organic Letters*, **1**, 997-1000.

**Carrea, G., Ottolina, G. and Riva, S.** (1995). Role of solvents in the control of enzyme selectivity in organic media. *Trends in Biotechnology*, **13**, 63-70.

**Chae, H.J. and Yoo, Y.J.** (1997). Mathematical analysis of an enzymatic reaction in an aqueous/organic two-phase system: Tyrosinase-catalysed hydroxylation of phenol. *Journal of Chemical Technology and Biotechnology*, **70**, 163-170.

**Chartrain, M., Jackey, B., Taylor, C., Sandford, S., Gbewonyo, K., Lister, L., Dimichele, L., Hirsch, C., Heimbuch, B., Maxwell, C., Pascoe, D., Buckland, B. and Greasham, R.** (1998). Bioconversion of Indene to *Cis* (1*S*, 2*R*) Indandiol and *trans* (1*R*,2*R*) Indandiol by *Rhodococcus* Species. *Journal of Fermentation and Bioengineering*, **86**, 550-558.

**Chauvin, Y. and Olivier-Bourbigou, H.** (1995). Nonaqueous ionic liquids as reaction solvents. *Chemtech*, **25**, 26-30.

**Chauvin, Y., Commereuc, D., Hirschauer, A., Hugues, F. and Saussine, L.** (1988). Process and catalyst for the dimerization or codimerization of olefins. *French Patent*, FR 2,611,700.

**Chauvin, Y., Mussmann, L. and Olivier, H.** (1996). A novel class of versatile solvents for two-phase catalysis: Hydrogenation, isomerization, and hydroformylation of alkenes catalyzed by rhodium complexes in liquid 1,3-dialkylimidazolium salts. *Angewandte Chemie-International Edition in English*, **34**, 2698-2700.

**Chauvin, Y.** (1996). Two-phase catalysis in nonaqueous ionic liquids. *Actualite chimique*, **V**, 44-46.

**Chen, H.S. and Middleman, S.** (1967) Drop size distribution in agitated liquid-liquid systems. *AIChEJ*, **13**, 989-995.

**Chesters, A.K.** (1991). The modelling of coalescence processes in fluid-liquid dispersions-A review of current understanding. *Chemical Engineering Research & Design*, **69**, 259-270.

**Cohen, M.A., Sawden, J. and Turner, N.J.** (1990). Selective hydrolysis of nitriles under mild conditions by an enzyme. *Tetrahedron Letters*, **31**, 7223-7226.

**Cohen, M.A., Parratt, J.S. and Turner, N.J.** (1992). Enantioselective hydrolysis of nitriles and amides using an immobilised whole cell system. *Tetrahedron: Asymmetry*, **3**, 1543-1546.

**Collins, A.M. and Woodley, J.M.** (1993). The scale-up of two-liquid phase microbially catalysed aromatic oxidations. *Proceedings of the 1993 IChemE Research Event*, IChemE, Rugby, 179-181.

**Collins, A.M., Woodley, J.M. and Liddell, J.M.** (1995). Determination of reactor operation for the microbial hydroxylation of toluene in a two-liquid phase process. *Journal of Industrial Microbiology*, **14**, 382-388.

**Cramp, R., Gilmour, M. and Cowan, D.A.** (1997). Novel thermophilic bacteria producing nitrile-degrading enzymes. *Microbiology-UK*, **143**, 2313-2320.

**Cremonesi, P., Carrea, G., Ferrara, L. and Antonini, E.** (1975). Enzymatic preparation of 20 $\beta$ -hydroxysteroids in a two-phase system. *Biotechnology and Engineering*, **17**, 1101-1108.

**Crosby, J., Moilliet, J., Parratt, J.S. and Turner, N.J.** (1994). Regioselective hydrolysis of aromatic dinitriles using a whole cell catalyst. *Journal of the Chemical Society, Perkins Transactions 1*, **13**, 1679-1687.

**Crosby, J.A., Parratt, J.S. and Turner, N.J.** (1992). Enzymic hydrolysis of prochiral dinitriles. *Tetrahedron: Asymmetry*, **3**, 1547-1550.

**Cull, S.G., Vargas-Mora, V., Lye, G.J., Holbrey, J.D. and Seddon, K.R.** (2000). Room temperature ionic liquids as replacements for organic solvents in multiphase bioprocess operations. *Biotechnology and Bioengineering*, **69**, 227-233.

**Cull, S.G., Woodley, J.M., and Lye, G.J.** (2001). Process selection and characterisation for the biocatalytic hydration of poorly water soluble aromatic dinitriles. *Biocatalysis and Biotransformations*, **19**, 131-154.

**de Bont, J.A.M.** (1998). Solvent-tolerant bacteria in biocatalysis. *Trends in Biotechnology*, **16**, 493-499.

**Diaz, A. and Acevedo, F.** (1999). Scale-up strategy for bioreactors with newtonian and non-newtonian broths. *Bioprocess Engineering*, **21**, 21-23.

**Doig, S.D., Boam, A.T., Leak, D.J., Livingston, A.G. and Stuckey, D.C.** (1998). A membrane bioreactor for biotransformations of hydrophobic molecules. *Biotechnology and Bioengineering*, **6**, 587-594.

**Doran, P.M.** (1997). *Bioprocess Engineering Principles*, Academic Press Limited, London.

**Doulah, M.S.** (1975) An effect of hold-up on drop sizes in liquid-liquid dispersions. *Industrial and Engineering Chemistry Fundamentals*, **14**, 137-138.

**Duran, R., Chion, C.K.N.C.K., Bigey, F., Arnaud, A. and Galzy, P.** (1992). The N-terminal amino acid sequences of *Brevibacterium* sp. R312 nitrile hydratase. *Journal of Basic Microbiology*, **32**, 13-19.

**Earle, M.J., McCormac, P.B. and Seddon, K.R.** (1998). Regioselective alkylation in ionic liquids. *Chemical Communications*, **20**, 2245-2246.

**Earle, M.J., McCormac, P.B. and Seddon, K.R.** (1999). Diels-Alder reactions in ionic liquids. *Green Chemistry*, **1**, 23-25.

**Eggers, D.K., Blanch, H.W. and Prausnitz, J.M.** (1989). Extractive catalysis: solvent effects on equilibria of enzymatic reactions in two-phase systems. *Enzyme Microbial Technology*, **11**, 84-89.

**El-Hamouz, A.M. and Stewart, A.C.** (1996) On-line drop size distribution measurement of oil-water dispersion using a Par-Tec M300 laser backscatter instrument. *SPE International*, **36672**, 1-14.

**Endo, I., Nojiri, M., Tsujimura, M., Nakasako, M., Nagashima, S., Yohda, M. and Odaka, M.** (2001). Fe-type nitrile hydratase. *Journal of Inorganic Biochemistry*, **83**, 247-253.

**Erbeldinger, M., Mesiano, A.J. and Russel, A.J.** (2000). Enzymatic catalysis of formation formation of Z-aspartame in ionic liquids – An alternative to enzymatic catalysis in organic solvents. *Biotechnology Progress*, **16**, 1129-1131.

**Eyal, J. and Charles, M.** (1990a). Hydration of 3-cyanopyridine to nicotinamide by crude extract nitrile hydratase. *Journal of Industrial Microbiology*, **5**, 71-78.

**Eyal, J. and Charles, M.** (1990b). Hydration of cyanopyridine to nicotinamide by whole cell nitrile hydratase. *Journal of Industrial Microbiology*, **6**, 185-190.

**Faber, K.** (1997a). *Biotransformations in organic chemistry*. Eds: Faber, K. Springer-Verlag, Berlin Heidelberg publishers.

**Faber, K.** (1997b). Biotransformations of non-natural compounds: State of the art and future development. *Pure & Applied Chemistry*, **69**, 1613-1632.

**Fernandes, P., Cabral, J.M.S., Pinheiro, H.M.** (1995). Bioconversion of a hydrocortisone derivative in an organic-aqueous two-liquid phase system. *Enzyme and Microbial Technology*, **17**, 163-167.

**Finnegan, I., Toerien, S., Smit, F. and Raubenheimer, H.** (1992). Commercial application of microbial enzymes with nitrile degrading activity. *South African Journal of Science*, **88**, 188-189.

**Fournaud, D., Bigey, F. and Arnaud, A.** (1998). Acyl transfer activity of an amidase from *Rhodococcus* sp. strain R312: Formation of a wide range of hydroxamic acids. *Applied and Environmental Microbiology*, **64**, 2844-2852.

**Freemantle M.** (1998). Designer solvents - Ionic liquids may boost clean technology development. *Chemical Engineering News*, **76**, 32-37.

**Galindo, E., Pacek, A.W. and Nienow A.W.** (2000) Study of drop and bubble sizes in a simulated mycelial fermentation broth of up to four phases. *Biotechnology and Bioengineering*, **69**, 213-221.

**Godfrey, J.C. and Grilc, V.** (1977) Drop size and drop size distributions for liquid-liquid dispersions in agitated tanks of square cross-section. *Proceedings 2<sup>nd</sup> European Conference on Mixing, BHRA Fluid Engineering: Cranfield, 1977, C1:* 1-20.

**Gordon, C.M., Holbrey, J.D., Kennedy, A. and Seddon, K.R.** (1998). Ionic liquid crystals: hexafluorophosphate salts. *Journal of Material Chemistry*, **8**, 2627-2636.

**Gradley, M.L., Deverson, C.J.F. and Knowles, C.J.** (1994a). Asymmetric hydrolysis of R(-), S(+)-2-methylbutyronitrile by *Rhodococcus rhodochrous* NCIMB 11216. *Archives of Microbiology*, **161**, 246-251.

**Gradley, M.L. and Knowles, C.J.** (1994b). Asymmetric hydrolysis of chiral nitriles by *Rhodococcus rhodochrous* NCIMB 11216 nitrilase. *Biotechnology Letters*, **16**, 41-46.

**Guilinger, T.R., Grislingas, A.K. and Erga, O.** (1988). Phase inversion behavior of water-kerosene dispersions. *Industrial and Engineering Chemistry Research*, **27**, 978-982.

**Halling, P. and Kvittingen, L.** (1999) Why did biocatalysis in organic media not take off in the 1930s? *Trends in Biotechnology*, **17**, 343-344.

**Heath, C.M., Imrie, R.C., Jones, J.J., Rees, M.J., Robins, K.G. and Verrall, M.S.** (1997). Whole cell biotransformation of 5-(4-(2-(2-Pyridyl)methylamino)ethoxy)benzylidene-thiazolidine-2,4,-dione to its benzyl derivative using a yeast reductase. *Journal of Chemical Technology and Biotechnology*, **68**, 324-330.

**Hempel, D.C.** (1988) Fundamentals of scale-up for biotechnological process in stirred fermentors. *Biotechnology Focus 1*, editors Finn, R.K. and Prave, P., Hanser publishers, Vienna, New York.

**Herrmann, W.A. and Bohm, V.P.W.** (1999). Heck reaction catalyzed by phosphá-palladacycles in non-aqueous ionic liquids. *Journal of Organometallic Chemistry*, **572**, 141.

**Hinze, J.O.** (1955). Fundamentals of the hydrodynamic mechanism of splitting in dispersion processes. *AIChEJ*, **1**, 289-295.

**Hobbel, E.F., Davies, R., Rennie, F.W., Allen, T., Butler, L.E., Waters, E.R., Smith, J.T and Sylvester, R.W.** (1991). Modern methods of on-line size analysis for particulate process streams. *Particle & Particle Systems Characterization*, **8**, 29-34.

**Holbrey, J.D. and Seddon, K.R.** (1999a). The phase behaviour of 1-alkyl-3-methylimidazolium tetrafluoroborates. *Journal of the Chemical Society-Dalton Transactions*, **13**, 2133-2139.

**Holbrey, J.D. and Seddon, K.R.** (1999b). Ionic liquids. *Clean Products and Processes*, **1**, 223-236.

**Huang, W., Jia, J., Cummings, J., Nelson, M., Schneider, G. and Lindqvist, Y.** (1997). Crystal structure of nitrile hydratase reveals a novel iron centre in a novel fold. *Structure*, **5**, 691-699.

**Jaeger, D.A. and Tucker, C.E.** (1989). Diels-Alder reactions in ethylammonium nitrate, a low- melting fused salt. *Tetrahedron Letters*, **30**, 1785-1788.

**Jakoby, W.B. and Fredericks, J.** (1964). Reactions catalyzed by amidases. *Journal of Biological Chemistry*, **239**, 1978-1982.

**Jallageas JC, Arnaud A, and Galzy P.** (1980). Bioconversion of nitriles and there applications. *Advances in Biochemical Engineering*, **14**, 1-32.

**Tramper, J.** (1996). Chemical versus biochemical conversion: When and how to use biocatalysts. *Biotechnology and Bioengineering*, **52**, 290-295.

**Ju L.K. and Chase G.G.** (1992). Improved scale-up strategies of bioreactors. *Bioprocess Engineering*, **8**, 49-53.

**Kerridge, A.** (1995). The Microbial Biotransformation of Nitrile Compounds. *PhD Thesis. University of Exeter.*

**Klibanov, A.M., Samokhin, G.P., Martinek, K. and Berezin, I.** (1975). A new approach to preparative enzymatic synthesis. *Biotechnology and Bioengineering*, **19**, 1351-1361.

**Kobayashi, M. and Shimizu, S.** (2000). Nitrile hydrolases. *Current Opinion in Chemical Biology*, **4**, 95-102.

**Kobayashi, M. and Shimizu, S.** (1998). Metalloenzyme nitrile hydratase: Structure, regulation, and application to biotechnology. *Nature Biotechnology*, **16**, 733-736.

**Kollmer, A., Schmid, A., Rudolf von Rohr, Ph. and Sonnleitner, B.** (1999) On liquid-liquid mass transfer in two-liquid-phase fermentations. *Bioprocess Engineering*, **20**, 441-448.

**Kumar, S., Ganvir, V., Satyanand, C., Kumar, R. and Gandhi K.S.** (1998). Alternative mechanisms of drop breakup in stirred vessels. *Chemical Engineering Science*, **53**, 3269-3280.

**Laane, C., Boeren, S., Vos, K. and Veeger, C.** (1987). Rules for optimization of biocatalysis in organic solvents. *Biotechnology and Bioengineering*, **30**, 81-87. (Check use in text.).

**Laane, C., Boeren, S., Hilhorst, R. and Veeger, C.** (1987). Optimization of biocatalysis in organic media. In: *Biocatalysis in organic media*, p.65-84, eds., Laane, C., Tramper, J. and Lilly, M.D., Elsevier Science Publishers, Amsterdam.

**Laane, C., Boeren, S. and Vos, K.** (1985). On optimizing organic solvents in multi-liquid-phase biocatalysis. *Trends in Biotechnology*, **3**, 251-252.

**Lau, R.M., Van Rantwijk, F., Seddon, K.R. and Sheldon, R.A.** (2000). Lipase-catalysed reactions in ionic liquids. *Organic Letters*, **26**, 4189-4191.

**Layh, N. and Willetts, A.** (1998). Enzymatic nitrile hydrolysis in low water systems. *Biotechnology Letters*, **20**, 329-331.

**León, R., Fernandes, P., Pinheiro, H.M. and Cabral, J.M.S.** (1998) Whole-cell biocatalysis in organic media. *Enzyme and Microbial Technology*, **23**, 483-500.

**Li, W.Z., Zhang, Y.Q. and Yang H.F.** (1992). Formation and purification of nitrile hydratase from *Corynebacterium-pseudodiphtheriticum* ZBB-41. *Applied Biochemistry and Biotechnology*, **36**, 171-181.

**Lilly, M.D., Woodley, J.M.** (1985). Biocatalytic reactions involving water-insoluble organic compounds. In: *Biocatalysts in Organic Syntheses*, p.179-192, eds., Tramper, J., Van der Plas, H.C., and Linko, P., Elsevier Science Publishers, Amsterdam.

**Lopez, J.L. and Matson, S.L.** (1997). A multiphase/extractive enzyme membrane reactor for production of diltiazem chiral intermediate. *Journal of Membrane Science*, **125**, 189-211.

**Lye, G.J. and Woodley, J.M.** (2001). Advances in the selection and design of two-liquid phase biocatalytic reactors. In: *Principles of Multiphase Bioreactor Design*, eds., Cabral, J.M.S., Mota, M. and Tramper, J., Harwood Academic Publishers, Reading, in press.

**Maddrell, S.J., Turner, N.J., Kerridge, A., Willetts, A.J. and Crosby, J.** (1996). Nitrile hydratase enzymes in organic synthesis: enantioselective synthesis of the lactone moiety of the mevinic acids. *Tetrahedron Letters*, **37**, 6001-6004.

**Maestracci, M., Thiery, A., Arnaud, A. and Galzy, P.** (1988). Inhibition kinetics of nitrile-hydratase in *Brevibacterium* sp. R312 strain. *Indian Journal of Microbiology*, **28**, 34-37.

**Margaritis, A. and Zajic, J.E.** (1978). Mixing, mass transfer, and scale-up of polysaccharide fermentations. *Biotechnology and Bioengineering*, **20**, 939-1001.

**Martínková, L., Olšovský, P., Prepechalová, I. and Kren, V.** (1995). Biotransformations of aromatic dinitriles using *Rhodococcus equi* cells. *Biotechnology Letters*, **17**, 1219-1222.

**Mathys, R.G., Schmid, A. and Witholt, B.** (1999). Integrated two-liquid phase bioconversion and product-recovery processes for the oxidation of alkanes: Process design and economic evaluation. *Biotechnology and Bioengineering*, **64**, 459-477.

**Mayaux, J.F., Cerbelaud, E., Soubrier, F., Yeh, P., Blanche, F. and Petre, D.** (1991). Purification, cloning, and primary structure of a new enantiomer-selective amidase from a *Rhodococcus* strain: Structural evidence for a conserved genetic coupling with nitrile hydratase. *Journal of Bacteriology*, **173**, 6694-6704.

**Meth-Cohn, O. and Wang, M.X.** (1995). A powerful new nitrile hydratase for organic synthesis - aromatic and heteroaromatic nitrile hydrolyses - a rationalisation. *Tetrahedron Letters*, **36**, 9561-9564.

**Meth-Cohn, O. and Wang, M.X.** (1997a). An in-depth study of the biotransformation of nitriles into amides and/or acids using *Rhodococcus rhodochrous* AJ270. *Journal of the Chemical Society, Perkin Transactions 1*, 1099-1104.

**Meth-Cohn, O. and Wang, M.X.** (1997b) Regioselective biotransformations of dinitriles using *Rhodococcus* sp. AJ270. *Journal of the Chemical Society, Perkin Transactions 1*, 3197-3204.

**Miller, J.M. and Knowles, C.J.** (1984). The cellular location of nitrilase and amidase enzymes of *Brevibacterium* R312. *FEMS Microbiology Letters*, **21**, 147-151.

**Nagamune, T., Honda, J., Cho, W., Kamiya, N., Teratani, Y., Hirata, A., Sasabe, H. and Endo, I.** (1991). Crystallization of a photosensitive nitrile hydratase from *Rhodococcus* sp. N-771. *Journal of Molecular Biology*, **220**, 221-222.

**Nagamune, T., Kurata, H., Hirata, M., Honda, J., Koike, H., Ikeuchi, M., Inoue, Y., Endo, I.** (1990). Purification of inactivated photoresponsive nitrile hydratase. *Biochemical and Biophysical Research Communication*, **168**, 437-442.

**Nagasawa, T., Ryuno, K. and Yamada, H.** (1986). Nitrile hydratase of *brevibacterium* R312. *Biochemical and Biophysical Research Communication*, **139**, 1305-1312.

**Nawaz, M., Heinze, T. and Cerniglia, C.** (1992). Metabolism of benzonitrile and butyronitrile by *Klebsiella-pneumoniae*. *Applied and Environmental Microbiology*, **58**, 27-31.

**Okufi, S., Perez de Ortiz, E.S., Sawitowski.** (1990). Scale-up of liquid-liquid dispersions in stirred tanks. *Canadian Journal of Chemical Engineering*, **68**, 400-406.

**Osborne, S.J., Leaver, J., Turner, M.K. and Dunnill, P.** (1990) Correlation of biocatalytic activity in an organic-aqueous two-liquid phase system with solvent concentration in the cell membrane. *Enzyme Microbial Technology*, **12**, 281-291.

- Osprian, I., Jarret, C., Strauss, U., Kroutil, W., Orru, R.V.A., Felfer, U., Willetts, A.J. and Faber, K.** (1999). Large-scale preparation of a nitrile-hydrolysing biocatalyst: *Rhodococcus* R312 (CBS 717.73). *Journal of Molecular Catalysis B: Enzymatic*, **6**, 555-560.
- Pacek, A.W., Man, C.C. and Nienow, A.W.** (1998) On the Sauter mean diameter and size distributions in turbulent liquid/liquid dispersions in a stirred vessel. *Chemical Engineering Science*, **53**, 2005-2011.
- Payne, M.S., Wu, S., Fallon, R.D., Tudor, G., Stieglitz, B., Turner, I.M., Nelson, M.J.** (1997). A Stereoselective cobalt-containing nitrile hydratase. *Biochemistry*, **36**, 5447-5454.
- Podgorska, W. and Baldyga, J.** (2001). Scale-up on the drop size distribution of liquid-liquid dispersions in agitated vessels. *Chemical Engineering Science*, **56**, 741-746.
- Rimpler, S. and Daniels R.** (1996). In situ particle sizing in highly concentrated oil-in-water emulsions. *Pharmaceutical Technology in Europe*, 72-80.
- Roberts, N.J. and Lye, G.J.** (2001). Application of Room Temperature Ionic Liquids in Biocatalysis: Opportunities and Challenges. (In submission)
- Sangster, J.** (1989), Octanol-Water Partition Coefficients of Simple Organic Compounds. *Journal of Chemical Reference Data*, **12**, 1111-1229.
- Schluter, V, Deckwer, W.D.** (1993). Power input, mixing and mass transfer in bioreactors with single and multiple stirrers. In: *3<sup>rd</sup> International Conference on Bioreactors and Bioprocess Fluid Dynamics*, Mechanical Engineering Publications Limited, London.
- Schmid, A., Kollmer, A. and Witholt, B.** (1998) Effects of biosurfactant and emulsification on two-liquid phase *Pseudomonas oleovorans* cultures and cell-free emulsions containing n-decane. *Enzyme and Microbial Technology*, **22**, 487-493.

**Schroën, C.G.P.H. and Woodley, J.M.** (1997). Membrane separation for downstream processing of aqueous-organic bioconversions. *Biotechnology Progress*, **13**, 276-283.

**Schofer, S.H., Kaftzik, N. Wasserscheid, P. and Kragl, U.**(2001) Enzyme catalysis in ionic liquids: lipase catalysed kinetic resolution of 1-phenylethanol with improved enantioselectivity. *Chemical Communications*, **7**, 425-426.

**Seddon, K.R.** (1997). Ionic liquids for clean technology. *Journal of Chemical Technology and Biotechnology*, **68**, 351-356.

**Shin, J.S. and Kim, B.G.** (1999). Modelling of the kinetic resolution of  $\alpha$ -methylbenzylamine with  $\omega$ -transaminase in a two-liquid-phase system. *Enzyme and Microbial Technology*, **25**, 426-432.

**Simmons, M.J.H., Zaidi, S.H. and Azzopardi B.J.** (2000). Comparison of laser-based drop-size measurement techniques and their application to dispersed liquid-liquid pipe flow. *Optical Engineering*, **39**, 505-509.

**Smith, J.L and Dell, J.** (1990). Capability of selective media to detect heat-injured *Shigella flexneri*. *Journal of Food Protection*, **53**, 141-144.

**Sugiura, Y., Kuwahara, J., Nagasawa, T. and Yamada, H.** (1987). Nitrile hydratase: the first non-heme iron enzyme with a typical low-spin Fe(III)-active centre. *Journal of the American Chemical Society*, **109**, 5848-5850.

**Tourneix, D., Thiery, A., Maestracci, M., Arnaud, A. and Galzy, P.** (1986). Regulation of nitrile-hydratase synthesis in a *Brevibacterium* species. *Antonie van Leeuwenhoek*, **52**, 173-182.

**Van Sonsbeek, H.M., Beftink, H.H. and Tramper, J.** (1993). Two-liquid-phase bioreactors. *Enzyme and Microbial Technology*, **15**, 722-729.

**Vermuë, M., Sikkema, J., Verheul, A., Bakker, R. and Tramper, J.** (1993). Toxicity of homologous series of organic solvents for the gram-positive bacteria *Arthrobacter* and *Nocardia* sp. And the gram-negative bacteria *Acinetobacter* and *Pseudomonas* sp. *Biotechnology and Bioengineering*, **42**, 747-758.

**Warhurst, A. and Fewson, C.** (1994). Biotransformations catalyzed by the genus *Rhodococcus*. *Critical Reviews in Biotechnology*, **14**, 29-73.

**Wernersson, E.S. and Trägårdh C.** (1999). Scale-up of rushton turbine-agitated tanks. *Chemical Engineering Science*, **54**, 4245-4256.

**Westcott, C.R. and Klibanov, A.M.** (1994). The solvent dependence of enzyme specificity. *Biochimica et Biophysica Acta*, **1206**, 1-9.

**Westgate, S., Bell, G. and Halling, P.J.** (1995). Kinetics of uptake of organic liquid substrates by microbial cells: A method to distinguish interfacial contact and mass-transfer mechanisms. *Biotechnology Letters*, **17**, 1013-1018.

**Wilkes, J.S. and Zaworotko, M.J.** (1992). Air and water stable 1-ethyl-3-methylimidazolium based ionic liquids. *Journal of the Chemistry Society, Chemical Communications*, **13**, 965-967.

**Woodley, J.M. and Titchener-Hooker, N.J.** (1996). The use of windows of operation as a bioprocess design tool. *Bioprocess Engineering*, **14**, 263-268.

**Woodley, J.M. and Lilly, M.D.** (1992). Process engineering of two-liquid phase biocatalysts. In: *Biocatalysis in Non-Conventional Media*, p.147-154, Eds., Tramper, J., Vermue, M.H., Beefink, H.H. and von Stockar, U., Elsevier Science Publishers, Amsterdam.

**Woodley, J.M., Brazier, A.J. and Lilly, M.D.** (1991). Lewis cell studies to determine reactor design data for two-liquid-phase bacterial and enzymatic reactions. *Biotechnology and Bioengineering*, **37**, 133-140.

**Woodley, J.M., Harrop, A.J. and Lilly, M.D.** (1990). The impact of biocatalyst selection on the design of aqueous-organic biphasic biocatalytic processes. *Enzyme Engineering*, **10**, 191-199, Annals of the New York Academy of Sciences.

**Woodley, J.M. and Lilly, M.D.** (1990). Extractive biocatalysis: the use of two liquid phase biocatalytic reactors to assist product recovery. *Chemical Engineering Science*, **43**, 2391-2396.

**Woodley, J.M.** (1990). Stirred tank power input for the scale-up of two-liquid phase biotransformations. In: *Opportunities in Biotransformations*, p. 63-66., Eds., Copping, L.G., Martin, R.E., Pickett, J.A., Bucks, C. and Bunch, A.W. Elsevier Science Publishers, London and New York.

**Yamada, H. and Kobayashi, M.** (1996). Nitrile hydratase and its application to industrial production of acrylamide. *Bioscience, Biotechnology and Biochemistry*, **60**, 1391-1400.

**Zhou G. and Kresta S.M.** (1998). Correlation of mean drop size and minimum drop size with the turbulence energy dissipation and the flow in an agitated tank. *Chemical Engineering Science*, **53**, 2063-2079.

# APPENDIX 1: 75 L REACTOR GUIDE

## SOP

Note: Due to the hazards associated with working with large volumes of toluene workers must wear lab coats, safety glasses, rubber gloves, rubber shoes and a visor at all times.

### **A1.1. Operating procedure for toluene/aqueous mixing studies in the 75 L reactor**

1. Check that all inlet/outlet valves coming off the vessel are closed.
2. Fill side tank with 50 L of toluene.
3. Fit the probe to head plate port and test seal integrity at 1 bar pressure overnight. Open exit gas valves.
4. Remove probe and fill vessel with 48 L pH 7 0.1 M phosphate buffer.
5. Maintain vessel at 30 °C using reactor temperature control system.
6. Connect side tank from 2 to main vessel and pump in 12 L toluene through addition port.
7. Replace probe in head plate port and sparge the vessel with nitrogen to remove dissolved oxygen, validate by observing dissolved oxygen measurement.
8. Maintain positive pressure of nitrogen in headspace of vessel at all times during mixing experiments.
9. Set the reactor impeller to the required agitation rate using vessel control panel. Start timer.
10. Monitor drop size and take measurements for the duration of the experiment.
11. At the end of the experimental period stop the impeller and temperature control.
12. Open the harvest port and using nitrogen gas force the liquid mix out of the vessel into an electrically insulated 250 L storage drum.
13. Repeatedly wash and rinse vessel with RO water using internal spray ball. Collect liquid in storage drum. After thorough rinsing vent vessel until smell of toluene is no longer present.

**A1.2. Operating procedure for toluene/aqueous biotransformation and mixing studies in the 75 L reactor**

1. Check that all inlet/outlet valves coming of the vessel are closed.
2. Fill side tank with 50 L of toluene containing 25 g.L<sup>-1</sup> 1,3-DCB.
3. Fit the probe to head plate port and test seal integrity at 1 bar pressure overnight. Open exit gas valves.
4. Remove probe and fill vessel with 48 L pH 7 0.1 M phosphate buffer containing 15 g.L<sup>-1</sup> *Rhodococcus* R312 biocatalyst.
5. Replace probe in head plate port and sparge the vessel with nitrogen to remove dissolved oxygen, validate by observing dissolve oxygen measurement.
6. Maintain vessel at 30 °C using reactor temperature control system.
7. Connect side tank from 2 to main vessel and add 12 L toluene containing 25 g.L<sup>-1</sup>.
8. Maintain positive pressure of nitrogen in headspace of vessel at all times during mixing experiments.
9. Set the reactor impeller to the required agitation rate using vessel control panel. Start timer.
10. Monitor drop size and take measurements for the duration of the experiment.
11. Take regular 10 mL samples from the sample port and quench the reaction immediately with 4 M HCl<sub>(aq)</sub>.
12. At the end of the experimental period stop the impeller and temperature control.
13. Open the harvest port and using nitrogen gas force the liquid mix out of the vessel into an electrically insulated 250 L storage drum.
14. Repeatedly wash and rinse vessel with RO water using internal spray ball. Collect liquid in storage drum. After thorough rinsing vent vessel until smell of toluene is no longer present.

## APPENDIX 2: CALCULATION OF MODIFIED WEBER NUMBER

The following calculation derives the power number correction equation (A2.11) used in this work from the literature Weber equation (A2.1) (Zou and Kresta, 1998).

$$We = \frac{c\rho_c \varepsilon^{2/3} d_{\max}^{5/3}}{\sigma} \quad (\text{A2.1})$$

$$\varepsilon = \frac{P_o \rho N^3 D^{3^2}}{\Delta\rho} = P_o N^3 D^2 \quad (\text{A2.2})$$

$$We = \frac{c\rho_c^{2/3} N^2 D^{4/3} d_{\max}^{5/3}}{\sigma} \quad (\text{A2.3})$$

$$\frac{d_{\max}^{5/3}}{D^{5/3}} = \frac{We \sigma}{c\rho_c^{2/3} N^2 D^3} = \frac{We}{cP_o^{2/3}} \cdot \frac{\sigma}{\rho_c N^2 D^3} \quad (\text{A2.4})$$

$$\frac{d_{\max}}{D} = \left( \frac{We}{c\rho_c^{2/3}} \right)^{3/5} \cdot \left( \frac{\sigma}{\rho_c N^2 D^3} \right)^{3/5} \quad (\text{A2.5})$$

$$\frac{d_{\max}}{D} = c \left( \frac{\rho_c N^2 D^3}{\sigma} \right)^{-0.6} = c We_T^{-0.6} \quad (\text{A2.6})$$

$$\text{lit. } \frac{d_{\max}}{D} = c_{\text{lit}} We_T^{-0.6}, \quad c_{\text{lit}} = \left( \frac{We}{cP_{o_{\text{lit}}}^{2/3}} \right)^{3/5} \quad (\text{A2.7})$$

$$\text{ex. } \frac{d_{\max}}{D} = c_{\text{ex}} We_T^{-0.6}, \quad c_{\text{ex}} = \left( \frac{We}{cP_{o_{\text{ex}}}^{2/3}} \right)^{3/5} \quad (\text{A2.8})$$

$$c_{lit} = \left( \frac{We^{3/5}}{c^{3/5} P_{o_{lit}}^{2/3}} \right)^{3/5} \Rightarrow P_{lit}^{2/5} = \frac{We^{3/5}}{c^{3/5}} \quad (A2.9)$$

$$c_{ex} = \left( \frac{We^{3/5}}{c^{3/5} P_{o_{ex}}^{2/3}} \right)^{3/5} \Rightarrow P_{ex}^{2/5} = \frac{We^{3/5}}{c^{3/5}} \quad (A2.10)$$

$$c_{lit} P_{o_{lit}}^{2/5} = c_{ex} P_{ex}^{2/5} \Rightarrow c_{ex} = c_{lit} \left( \frac{P_{o_{lit}}}{P_{o_{ex}}} \right)^{2/5} \quad (A2.11)$$